SWITCHING FREQUENCY EFFECTS ON TRACTION DRIVE SYSTEM EFFICIENCY

William L. Cornwell

Thesis submitted to the faculty of the Virginia Polytechnic Institute and State University in partial fulfillment of the requirements for the degree of

MASTER OF SCIENCE

In

Electrical Engineering

Approved:

_____

Dr. Jason Lai, Chair

_____ _____

Dr. Doug Nelson Dr. Charles Konrad

September 6, 2002

Blacksburg, VA

Keywords: Voltage Source Inverter (VSI), Induction Motor, Traction Drive, Electric Vehicle

Switching Frequency Effects on Traction Drive System Efficiency

William L Cornwell

(Abstract)

Energy demands are steadily increasing as the world's population continues to grow. Automobiles are primary transportation means in a large portion of the world. The combination of fuel consumption by automobiles along with the shrinking fossil fuel reserves makes the development of new more energy efficient technologies crucial. Electric vehicle technologies have been studied and are still being studied today as a means of improving fuel efficiency. To that end, this work studies the effect of switching frequency on the efficiency of a hybrid electric vehicle traction drive, which contains both an internal combustion engine as well as an electric motor. Therefore improving the efficiency of the electric motor and its drive will help improve the viability of alternative vehicle technologies. Automobiles spend the majority of their operational time in the lower speed, lower torque region. This work focuses on efficiency improvements in that region. To estimate the efficiency trend, the system is modeled and then tested both electrically and thermally. The efficiency is shown to increase at lower switching frequencies. The experimental results show that there are some exceptions, but the basic trend is the same.

Acknowledgments

I would like to first thank my advisor Dr. Jason Lai for his guidance in the area of power electronics and for sparking my interest while doing my undergraduate work. I would also like to thank him for giving me the opportunity to work in the CPES lab. I believe that CPES is the best lab I have had the opportunity to work in.

I would also like to thank my committee members Dr. Charles Konrad and Dr. Doug Nelson. Dr. Konrad has given me the opportunity to work on his VPT projects where I have gained a great deal of practical experience. With his years of industry experience, he gave me a better understanding into research outside of the academic environment. Dr. Nelson for agreeing to be on my committee at the last minute.

Dr. Boroyevich's undergraduate and graduate classes where by far some of the most enjoyable classes I had the pleasure of taking. His knowledge as well as his ability to convey it to his students is truly amazing. I would also like to thank my entire committee along with Dr. Boroyevich and Carlos Alicea for their help and contributions to this thesis research.

I would like to thank Bob Martin, Gary Kerr, Trish Rose, Elizabeth Tranter, and the remaining CPES staff. Their contributions make the research in CPES possible.

I would also like to thank all of my friends and colleagues in the lab; Jeremy Ferrell, Troy Nergaard, Len Leslie, Elton Pepa, Jerry Francis, Carl Tinsley, Cory Papenfuss, and Chris Smith. Their help as well as their presence in the lab definitely made life in CPES more enjoyable.

Finally, I would like to thank my mother and grandmother. Without their support and assistance throughout my entire college career this work would not be possible.

Thank you to Virginia Power Technologies (VPT) and the Department of Energy (DOE) for providing equipment and resources for this work.

Table of Contents

List of Figures

List of Tables

1. Introduction

1.1. Motivation

The motivation for this work stems from the need for reduced energy consumption. The demand for energy increases almost yearly. The worldwide energy consumption is expected to rise from 382 quadrillion BTUs in 1999 to 612 quadrillion BTUs in 2020. Figure 1 shows the worldwide projected energy demand up to the year 2020. [1]

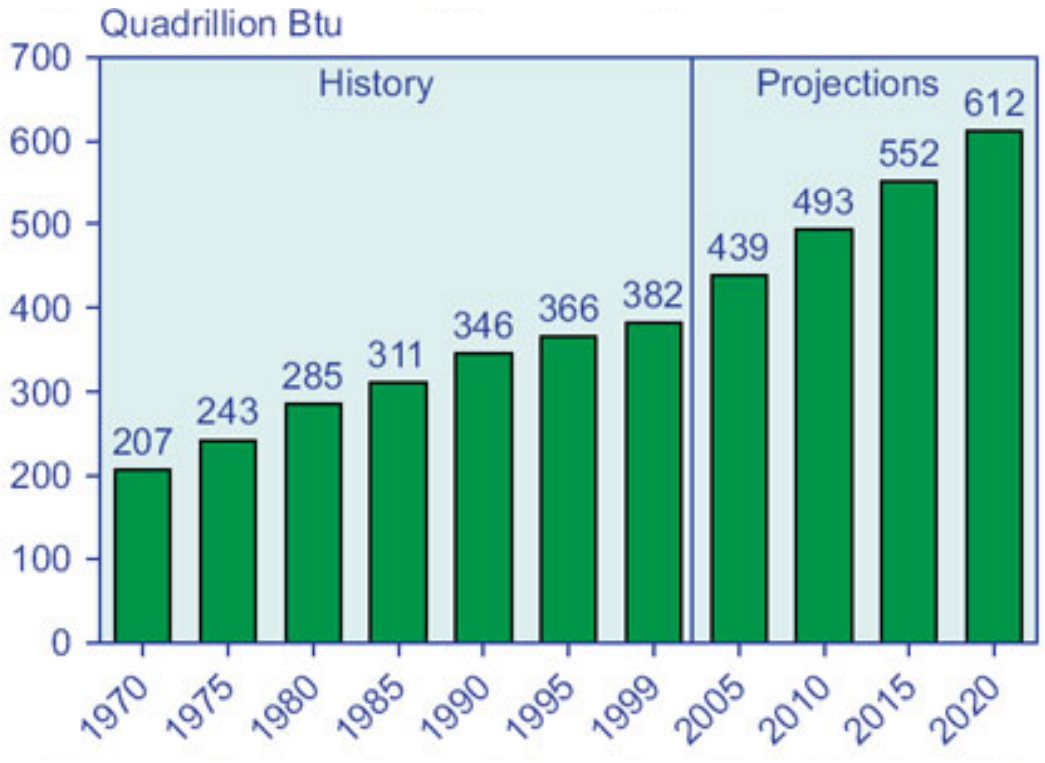

Figure 1 Projected Energy Demand

Escalating tensions in the Middle East combined with the Organization of Petroleum Exporting Countries (OPEC) reduction of oil exports makes the need for energy conservation that much more important. Therefore, advantages from improving energy consumption would be very beneficial and include the following:

- Lower energy cost
- Reduced pollution
- Conservation of resources

With these benefits as well as others, the motivation for this work becomes apparent.

Another more precise benefit of improving energy consumption is the improvement in alternative energy systems. Improving alternative energy technology makes its application more practical in everyday use. For example, electric vehicles are not being pursued as much because of their impracticality. With their restricted range and limited charging opportunities, hybrid technology has become a more popular alternative. Hybrid technology, in itself, is not perfect though. There are problems with limited benefits with respect to power versus fuel economy. This work addresses the power-fuel economy trade-off through the improvement of a hybrid electric traction drive.

1.1.1. Possible Solutions

Currently, there exists a number of ways to conserve and use energy more wisely. As stated previously, this work focuses on efficiency improvements of an existing technology; hybrid vehicle traction drives. There are other ways of conserving and producing energy as well. The simplest would be to drive less and keep your thermostat lowered.

Alternate energy generation, such as fuel cells, is being researched extensively for automotive applications as well as stand-alone power generation. However, as with any technology, they are far from perfect. Other technologies include solar, wind, and even

tidal energy production. While the energy production is relatively clean, the ability to produce large quantities is the major problem. Therefore, increasing the efficiency of an existing technology is a more immediate solution.

1.2. Previous Work

Induction motors are commonly used in some traction drives as well as a large percentage of industrial drives. There has been some previous work in the area of traction drive efficiency improvements. Below, there are several studies that support the work in this thesis. They are expanded on below.

Previous work has shown noticeable improvements in both inverter and motor efficiency with varying switching frequency although not in the same direction [3]. The test setup was a typical dynamometer setup with microprocessor speed control. The input and output power of both the motor and inverter were recorded. The scope of Khomfoi et al not only involved switching frequency but also modulation index and modulation scheme.

The findings from Khomfoi et al show several interesting results. The most important result as it relates to this work is the effect on inverter and motor losses as switching frequency is reduced. The inverter losses are decreased substantially as the switching frequency is lowered; where the motor core losses increase as the switching frequency is decreased. Figure 2 below shows the results of motor losses from [3].

Other interesting results include the effect of modulation index on core losses in the motor and the effect of the modulation scheme. The work found that the higher the modulations index the lower the core losses. Khomfoi et al recommends that the use of higher modulation index be used with a lower DC bus voltage. This is important because for a traction drive system for an automotive application the battery unit will have higher bus voltage that is not adjustable. Modulation scheme is also interesting. The use of SPWM and some forms of SVM are found to have some effects on losses.

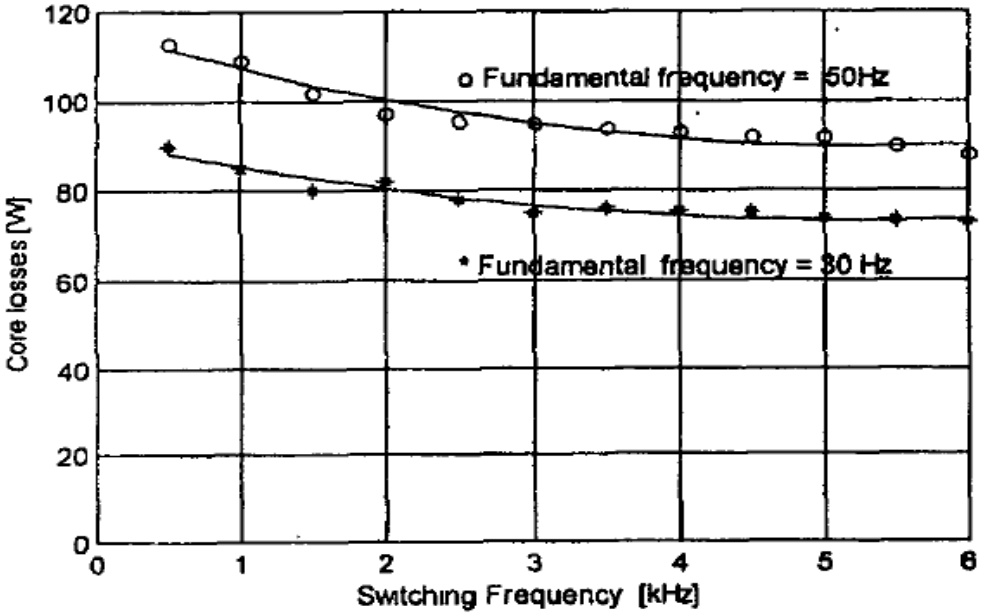

Figure 2 Previous Work [3] on Core Loss vs. Switching Frequency

Other work in Boroyevich et al shows some of the same findings as Khomfoi et al. The research examines switching frequency effects on the inverter as well as the motor, but also investigates soft switching. Although soft switching is not the focus of this work, the hard switching results of the paper offer some relevant results.

Figure 3 and Figure 4 below show the motor efficiency and inverter losses as a function of switching losses. Examining the graphs demonstrates that the findings are the same as in [3]. As switching frequency is decreases the motor efficiency decreases as well; while the inverter efficiency increases with the reduced switching frequency. It should be noted that this paper Boroyevich et al has only simulation results for the motor where as Khomfoi et al has only experimental.

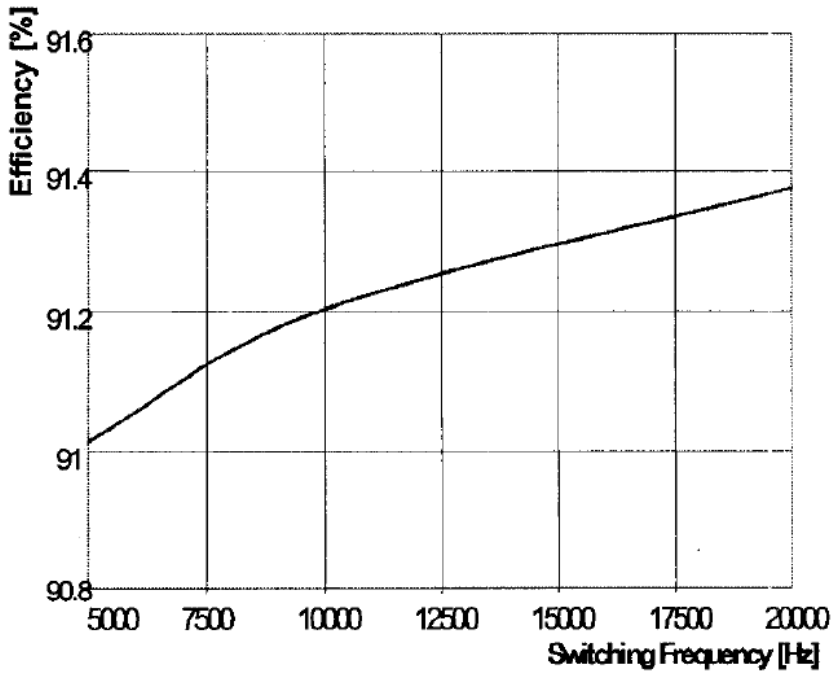

Figure 3 Previous Work [4] Motor Efficiency vs. Switching Frequency

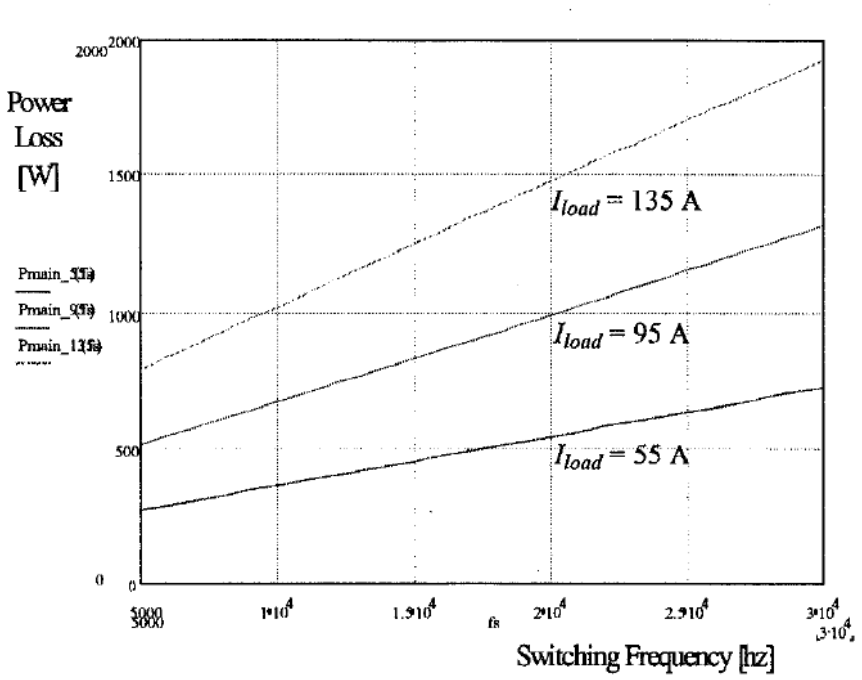

Figure 4 Previous Work [4] Inverter Power Loss vs. Switching Frequency

The motor losses were calculated with the widely used induction motor model, Figure 5. This model is used to first calculate the ripple current into the motor. The parameters in this model are defined as slip s, stator resistance R_s, stator inductance L_s, magnetizing inductance L_m, rotor inductance L_r, and rotor resistance R_r.

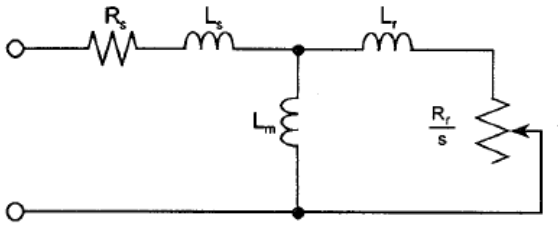

Figure 5 Single Phase Induction Motor Model

An FFT is then run to calculate the harmonic content of the current. The harmonic content is used to calculate the harmonic losses. The harmonic loss equations in Boroyevich et al are used to calculate the losses. The results in the paper show that at lower switching frequency more ripple and thus more harmonic losses are evident.

The inverter's losses are calculated by estimating the IGBT turn on and turn off losses as well as the IGBT and diode on-state voltage drop [4]. These values are related to the characteristics of the device. The modulation scheme is also examined as it has an effect on the losses, but more precisely, the zero vector selection of the SVM modulation.

1.3. Objective

This work focuses on improving efficiency of a hybrid automotive traction motor drive. Previous studies have shown that automobiles spend a large percentage of their operating time in the low torque region [2]. This would equate into cruising speeds where the needed power is low. For this reason as well as other limitations this work primarily takes place in this operating range.

Although this work focuses on the low torque region, the primary objective is to prove the hypothesis that by changing the switching frequency of a three-phase voltage source inverter, there will be trend toward higher system efficiency.

The motor and inverter are first modeled in section two: Analytical Model. This allows an efficiency trend to be observed. Next, the analytical model trends are tested and presented in section three Experimental Results section. Section four compares the analytical and experimental results for verification: Analytical and Experimental Comparison. Finally, the conclusions are given in section five.

2. Analytical Model

Three-phase induction motor traction drives are not uncommon in today's hybrid and electric vehicle applications. For this reason the need to model the system is important, but has not been done to observe the impact of varying the switching frequency. Therefore the system used in this work is modeled in MathCAD with switching frequency as the independent variable. The model used is made up of two parts: the motor and inverter. The motor is modeled with the commonly accepted per phase equivalent circuit model. The inverter model is a combination of work in [5] and [6].

As stated before, this work focuses on the effects of switching frequency on efficiency. The test points for both the analytical model as well as experimental testing were obtained from slight variations of work in [2]. Therefore, this analytical model is used to approximate the efficiency trend as switching frequency is changed. In order to prove the trends shown with the model, experimental validation is provided for the same test conditions.

2.1. Inverter Model Derivation

The inverter model is made up of several variables: conduction losses, switching losses, bus capacitor losses, and miscellaneous losses [5]. The basic IGBT device model is developed in [6]. A 2nd order model is used which allows for more accurate modeling at lighter loads where this work primarily takes place.

2.1.1. Copper Conduction Losses

To account for space vector modulation (SVM), as opposed to sinusoidal pulse width modulation (SPWM), the copper losses are separated into three regions for both the diode and IGBT [5]. The following equations (2.1-2.3) show the conduction losses for the IGBT switches.

$$\text{PcswA} := \frac{1}{2\cdot\pi}\cdot\int_{0}^{\frac{\pi}{3}} \left[0.427 + \sqrt{2}\cdot\text{Is}\cdot\sin(x)\cdot 0.0237 - 7.3\cdot 10^{-5}\cdot\left(\sqrt{2}\cdot\text{Is}\cdot\sin(x)\right)^{2}\right]\cdot\sqrt{2}\cdot\text{Is}\cdot\sin(x)\cdot\left(\frac{1}{2}+\frac{1}{2}\cdot\text{M}\cdot\sin\left(x+\theta\right)\right) dx \quad (2.1)$$

$$\text{PcswB} := \frac{1}{2\cdot\pi}\cdot\int_{\frac{\pi}{3}}^{\frac{2\cdot\pi}{3}} \left[0.427 + \sqrt{2}\cdot\text{Is}\cdot\sin(x)\cdot 0.0237 - 7.3\cdot 10^{-5}\cdot\left(\sqrt{2}\cdot\text{Is}\cdot\sin(x)\right)^{2}\right]\cdot\sqrt{2}\cdot\text{Is}\cdot\sin(x)\, dx \quad (2.2)$$

$$\text{PcswC} := \frac{1}{2\cdot\pi}\cdot\int_{\frac{2\cdot\pi}{3}}^{\pi} \left[0.427 + \sqrt{2}\cdot\text{Is}\cdot\sin(x)\cdot 0.0237 - 7.3\cdot 10^{-5}\cdot\left(\sqrt{2}\cdot\text{Is}\cdot\sin(x)\right)^{2}\right]\cdot\sqrt{2}\cdot\text{Is}\cdot\sin(x)\cdot\left(\frac{1}{2}+\frac{1}{2}\cdot\text{M}\cdot\sin\left(x+\theta\right)\right) dx \quad (2.3)$$

The parameters listed in the switch equations as well as the diode equations below include stator current I_s, Modulation index M, and power factor angle θ. The total switch conduction losses are then:

$$Pcsw := PcswA + PcswB + PcswC \tag{2.4}$$

These equations show that for this model, the conduction losses are not a function of switching frequency. The equations for the diode conduction losses, equations (2.5-2.7), are very similar to the switches.

$$PcdA := \frac{1}{2\cdot\pi}\cdot\int_{0}^{\frac{\pi}{3}} \left[0.4256 + \sqrt{2}\cdot Is\cdot\sin(x)\cdot.0212 - .000062\left(\sqrt{2}\cdot Is\cdot\sin(x)\right)^2\right]\cdot\sqrt{2}\cdot Is\cdot\sin(x)\cdot\left(\frac{1}{2} - \frac{1}{2}\cdot M\cdot\sin(x+\theta)\right)dx \tag{2.5}$$

$$PcdB := \frac{1}{2\cdot\pi}\cdot\int_{\frac{\pi}{3}}^{\frac{2\cdot\pi}{3}} \left[0.4256 + \sqrt{2}\cdot Is\cdot\sin(x)\cdot.0212 - .000062\left(\sqrt{2}\cdot Is\cdot\sin(x)\right)^2\right]\cdot\sqrt{2}\cdot Is\cdot\sin(x)\,dx \tag{2.6}$$

$$PcdC := \frac{1}{2\cdot\pi}\cdot\int_{\frac{2\cdot\pi}{3}}^{\pi} \left[0.4256 + \sqrt{2}\cdot Is\cdot\sin(x)\cdot.0212 - .000062\left(\sqrt{2}\cdot Is\cdot\sin(x)\right)^2\right]\cdot\sqrt{2}\cdot Is\cdot\sin(x)\cdot\left(\frac{1}{2} - \frac{1}{2}\cdot M\cdot\sin(x+\theta)\right)dx \tag{2.7}$$

The total diode conduction losses are then,

$$Pcd := PcdA + PcdB + PcdC \tag{2.8}$$

Therefore, the total conduction losses are given in equation (2.9). The previous equations are for a single switch or diode. Therefore, they must be multiplied by six to account for all six switches and diodes.

$$Pc := 6\cdot(Pcsw + Pcd) \tag{2.9}$$

The variable definitions in these equations are relatively straightforward. M is the modulation index, θ is the motor displacement factor angle, and I_s is the peak stator current.

2.1.2. Switching Losses

The switching losses are comprised of turn on energy, turn off energy, and reverse recovery energy. Multiplying the switching energies and integrating over one line cycle gives the average turn on and turn off power loss [5].

$$Pswon := \frac{1}{2\cdot\sqrt{\pi}}\cdot fs\cdot\frac{k}{\sqrt{3}}\cdot\left(Is\cdot\sqrt{2}\right)^{h}\cdot kgon\frac{Vdc}{Vtest}\cdot\frac{\Gamma\left(\frac{h+1}{2}\right)}{\Gamma\left(\frac{h}{2}+1\right)} \tag{2.10}$$

$$Pswoff := \frac{1}{2\cdot\sqrt{\pi}}\cdot fs\cdot\frac{m}{\sqrt{3}}\cdot\left(Is\cdot\sqrt{2}\right)^{n}\cdot kgoff\frac{Vdc}{Vtest}\cdot\frac{\Gamma\left(\frac{n+1}{2}\right)}{\Gamma\left(\frac{n}{2}+1\right)} \tag{2.11}$$

The parameters in equations 2.10 and 2.11 are derived in [6]. The parameters used in this work are given in Table 1. (k, h, m, and n) are the actual parameters modeling the IGBT, and are derived from least squared fitting of experimental data at 80% of the device rating [6]. V_{test} is the actual test condition of the device from the data sheet test conditions. V_{dc} is the DC bus voltage and I_s is the stator current. k_{gon} and k_{goff} are related to the gate drive stiffness [5]. Finally f_s is defined as the switching frequency.

Table 1 Inverter Model Parameters

R_{ce}	0.0033	k	$109e^{-4}$
V_{cesat}	1	h	1.0506
R_{ak}	0.00125	m	$6.175e^{-4}$
V_f	1.1	n	0.7198
t_{rr}	$50e^{-9}$	k_{gon}	2
t_r	$80e^{-9}$	k_{goff}	1
V_{test}	600	*ripple*	0.2
R_{esr}	0.1		

The parameters reverse recovery time t_{rr} and rise time t_r are included in the reverse recovery loss equation (2.12).

$$Prr := \frac{Is \cdot \sqrt{2} \cdot Vdc}{8 \cdot \pi} \cdot \frac{trr^2}{tr - trr} \cdot fs \tag{2.12}$$

The three losses P_{swon}, P_{swoff}, and P_{rr} are added to get the total losses for one switch/diode pair. Therefore, to calculate the total losses the sum is multiplied by six. The total losses for all six devices is then,

$$Psw := 6 \cdot (Pswon + Pswoff + Prr) \tag{2.13}$$

2.1.3. Capacitor Losses

The bus capacitor losses are related to ripple as shown in (2.14).

$$Pcap := (Is \cdot ripple)^2 \cdot (Resr) \tag{2.14}$$

The parameter R_{esr} is obtained from the data sheets. The ripple variable is an approximation, and for this work is assumed the same as in [5].

2.1.4. Total Losses

For this work the miscellaneous losses are ignored. This is related to the fact that this model was only used to show a trend, and therefore didn't need to be as precise. Therefore, the total inverter losses are given by:

$$Plossinv := Pc + \frac{Psw}{2} + Pcap \tag{2.15}$$

The efficiency equation is also given by:

$$\eta inv1 := \frac{Pin}{Pin + Plossinv} \tag{2.16}$$

The input power for the inverter is simply the power supplied from the DC supply.

2.2. Induction Motor Model

The induction motor model used in this work is the generally accepted equivalent per phase circuit model. This model as opposed to Figure 5 includes the parameter Rc to estimate the core losses of the motor. The circuit model is given in Figure 6.

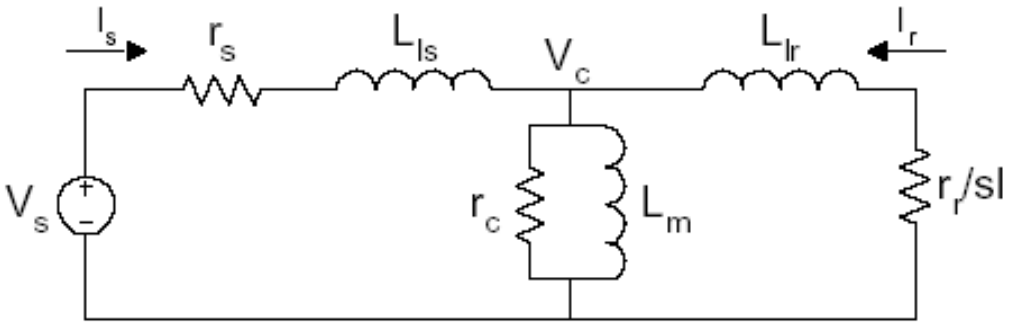

Figure 6 Induction Motor Models

The losses for the motor can be made up of the core losses, copper losses, and any stray losses. The stray losses can include the windage and friction as well as others. This area of induction motor modeling is still not understood very clearly. The motor parameters, explained in section 1.2, which were recorded at 60 Hz, are given below in Table 2.

Table 2 Induction Motor Parameters at 60 Hz

Rc (Ω)	Rs (Ω)	Rr (Ω)	Llr (μH)	Lls (μH)	Lm (mH)
14.4	0.012	0.0125	41	39.5	2.7

To begin, the motor calculations for the copper losses are given. (2.17) Below, shows the copper loss equation.

$$Pcu := 3\cdot\left(Is^2\cdot rs + Ir^2\cdot rr\right) \tag{2.17}$$

The core losses are then given in equation (2.18).

$$Pcore := 3\cdot\left(\frac{Vc^2}{rc}\right) \tag{2.18}$$

The parameters for the copper losses include the stator current I_s, stator resistance rs, rotor current I_r, and rotor resistance rr. The rotor current is calculated, equation (2.19), with the output torque Te, the synchronous speed ωe, and slip sl.

$$Ir := \sqrt{\frac{2}{3 \cdot p} \cdot Te \cdot \omega e \cdot \frac{sl}{rr}} \tag{2.19}$$

Rotor current along with the magnetizing branch current is then used in the calculation of stator current. Equation (2.20) shows the magnetizing current.

$$Im := \frac{Vs \cdot \sqrt{rc^2 + (\omega e \cdot Lm)^2}}{\omega e \cdot rc \cdot Lm} \tag{2.20}$$

The stator current equation is then given below.

$$Is := \frac{Ir \cdot \sqrt{\left(\frac{rc \cdot rr}{sl} - \omega e^2 \cdot Llr \cdot Lm\right)^2 + \left[\omega e \cdot \left(Lm \cdot rc + \frac{rr}{sl} \cdot Lm + rc \cdot Llr\right)\right]^2}}{rc \cdot \omega e \cdot Lm} \tag{2.21}$$

The remaining parameters in the stator current equation are rotor and magnetizing inductance L_{lr} and L_m respectively. The core loss equation (2.18) has the variables, air gap voltage, Vc, and core resistance, rc.

The remaining model calculation is of stator voltage (2.22). This is used in this work to calculate the input power to the motor.

$$Vs := \sqrt{\frac{2}{3 \cdot p} \cdot Te \cdot \omega e \cdot \frac{sl}{rr} \cdot \left[\left(rs + \frac{rr}{sl}\right)^2 + \omega e^2 \cdot (Lls + Llr)^2\right]} \tag{2.22}$$

To calculate input power, the displacement factor also needs to be calculated. The calculation involves the following impedances: magnetizing, stator, and rotor impedance.

$$Zm := \frac{rc \cdot \omega e \cdot Lmi}{rc + \omega e \cdot Lmi} \tag{2.23}$$

$$Zs := rs + \omega e \cdot Llsi \tag{2.24}$$

$$Zr := \frac{rr}{sl} + \omega e \cdot Llri \tag{2.25}$$

The equivalent impedance is then calculated in equation (2.26).

$$Zeq := Zs + \frac{Zm \cdot Zr}{Zm + Zr} \tag{2.26}$$

The displacement factor is then shown in equation (2.27). The "arg" function in MathCAD returns the displacement factor angle.

$$DF := \cos(\arg(Zeq)) \tag{2.27}$$

The input power for the motor can then be calculated as follows:

$$Pin := 3Vs \cdot Is \cdot DF \tag{2.28}$$

The output power is calculated with the output torque and speed.

$$Pout := Te \cdot \omega r \tag{2.29}$$

The motor efficiency can then be calculated with the input power and output power.

$$\eta mot := \frac{Pout}{Pin} \tag{2.30}$$

2.3. Analytical Results

The results for the overall system efficiency are given below. The system efficiency is defined as the output shaft power of the motor over the input power from the DC power supply. The overall system efficiency is simulated for three speeds 1000, 2000, and 3000 RPM. Each speed is a separate MathCAD file and attached in Appendix II. While each speed has results for three load torques of 60, 120, and 180 in-lb.

2.3.1. 1000 RPM Data

Figure 7 below, gives the system efficiency as a function of switching frequency at 1000 RPM. ηsys1, ηsys2, and ηsys3 is the efficiency at 60, 120, and 180 in-lb torque respectively.

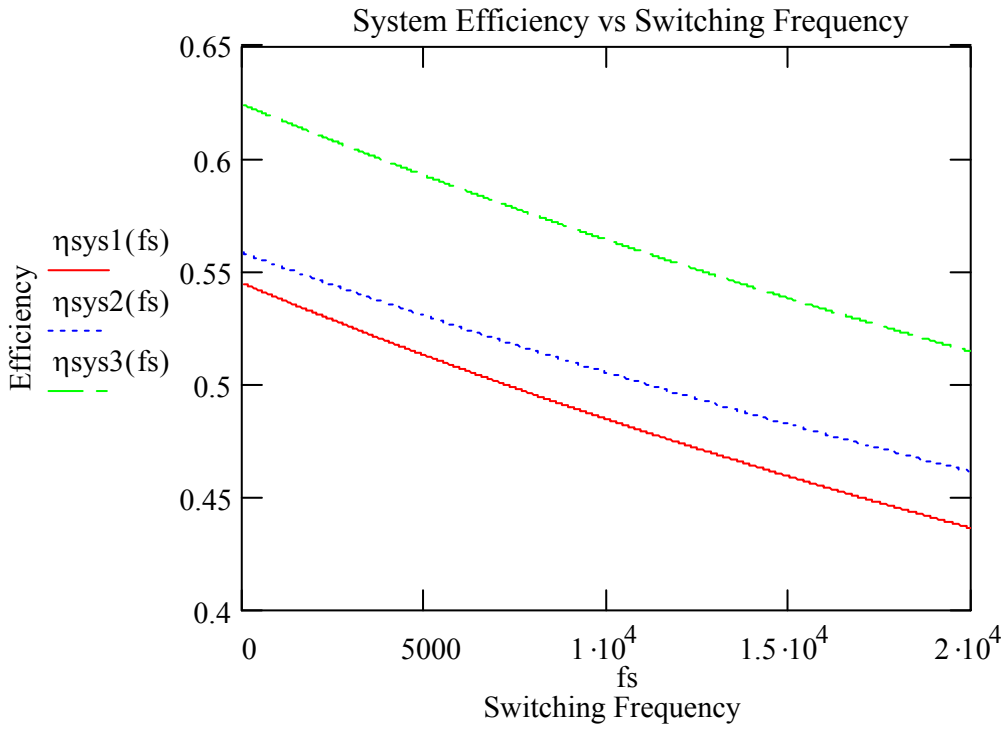

Figure 7 Efficiency vs. Switching Frequency at 1000 RPM

Examining the plots shows that the efficiency tends to improve at lower switching frequencies. The efficiency also improves as the load is increased.

2.3.2. 2000 RPM Data

Figure 8 shows the results at 2000 RPM. The legend is the same as in the 1000 RPM section. The same trend can be seen in these plots with some added results.

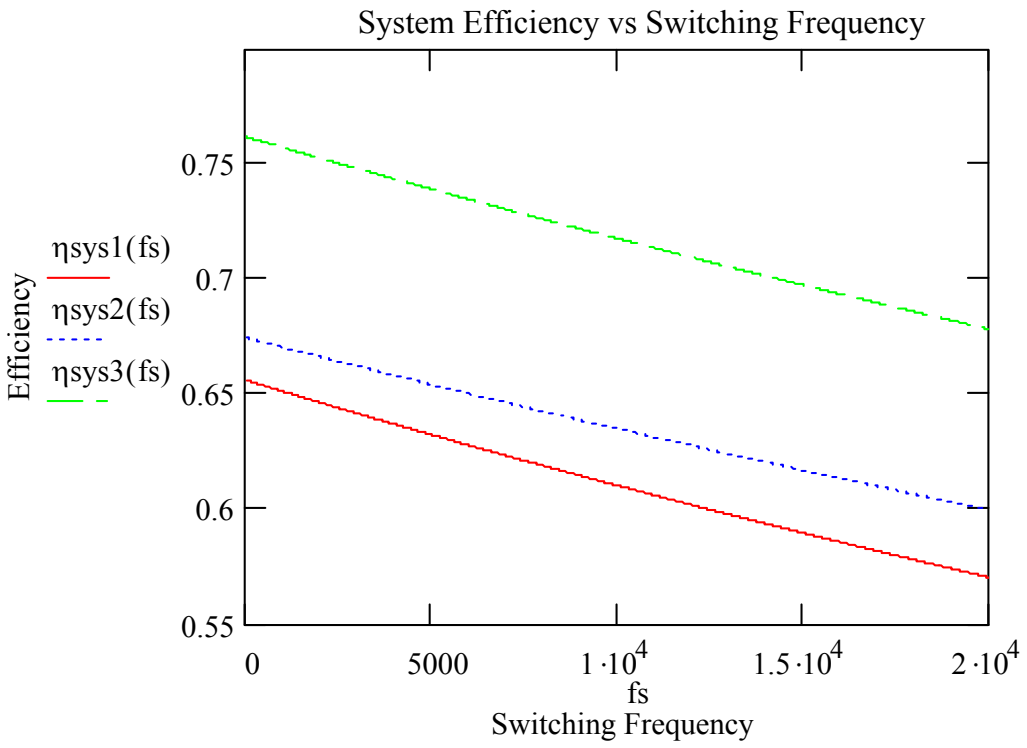

Figure 8 Efficiency vs. Switching Frequency at 2000 RPM

Again, the efficiency trend increases with the lower switching frequency, and overall efficiency improves with the increased load. Another result is the fact that the overall efficiency for all 2000 RPM cases is improved over the 1000 RPM case.

2.3.3. 3000 RPM Data

Figure 9 below shows the results for 2000 RPM with the same conditions as before.

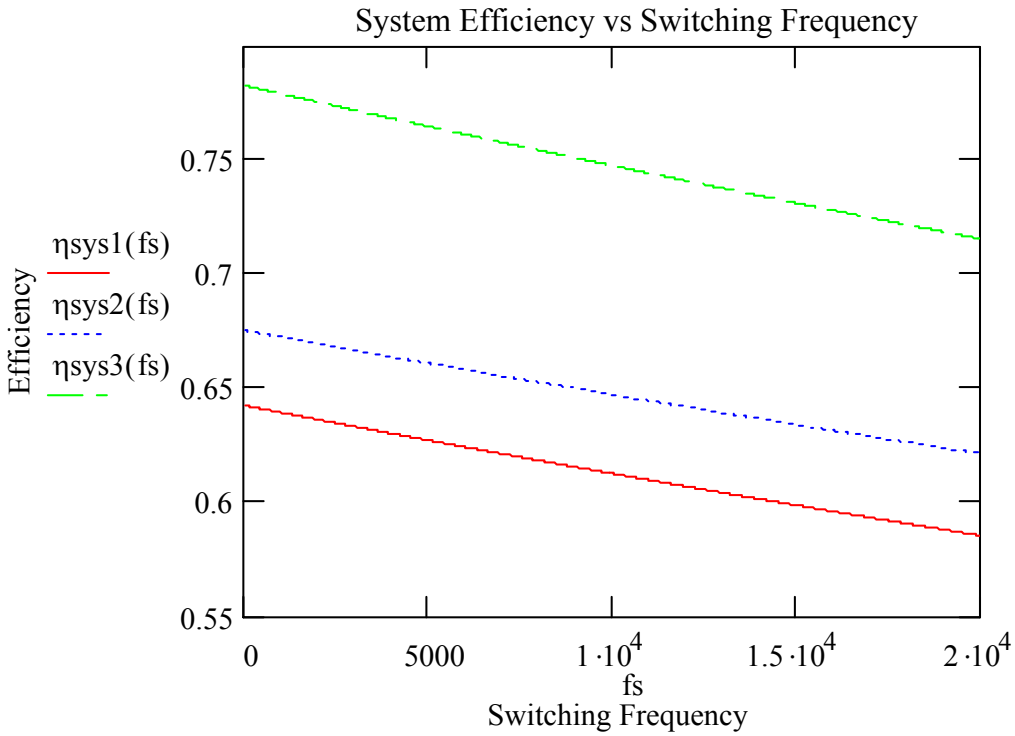

Figure 9 Efficiency vs. Switching Frequency at 3000RPM

The same trends as with 2000 RPM can be seen with the switching frequency. The difference being that the efficiency does not improve as much with the lowered switching frequency.

3. Experimental Results

3.1. Measurements and Testing

The test setup for this work incorporates the custom designed three-phase voltage source inverter and induction motor. Both were designed for electric vehicle traction drive

applications. The units were tested on an in-house dynamometer consisting of a Yaskawa Verispeed 626VM3 drive along with a Himmelstein 28003TNS torque sensor. The dynamometer is rated at 22 kW and 6000 RPM, and uses closed loop speed for its control algorithm. Figure 10 shows the motor setup for testing.

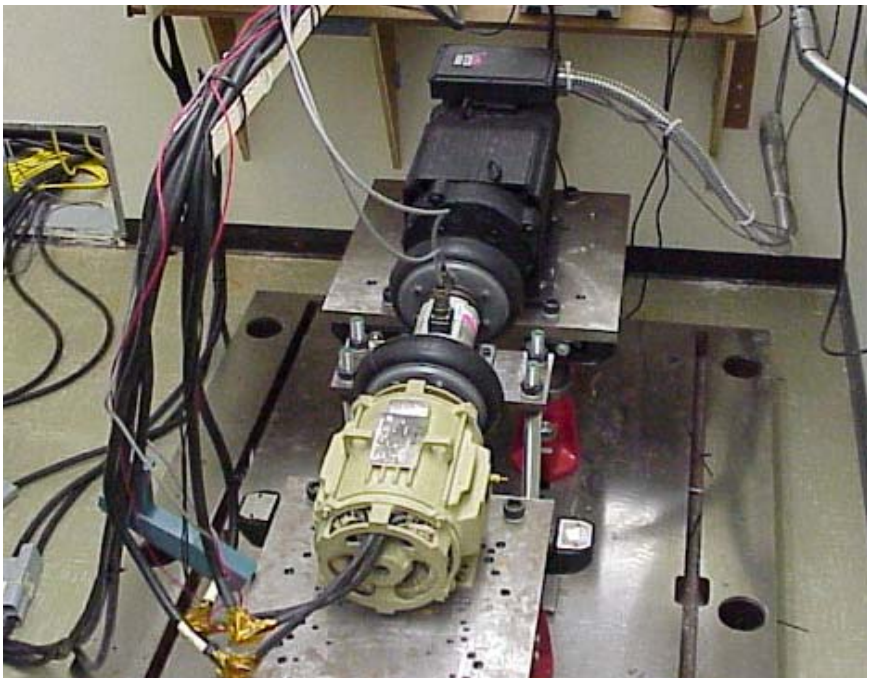

Figure 10 Motor Dynamometer Setup

To measure all the necessary data for this study, several pieces of laboratory equipment where used. The equipment list as well as a basic overview of the equipment, Figure 11, is given below.

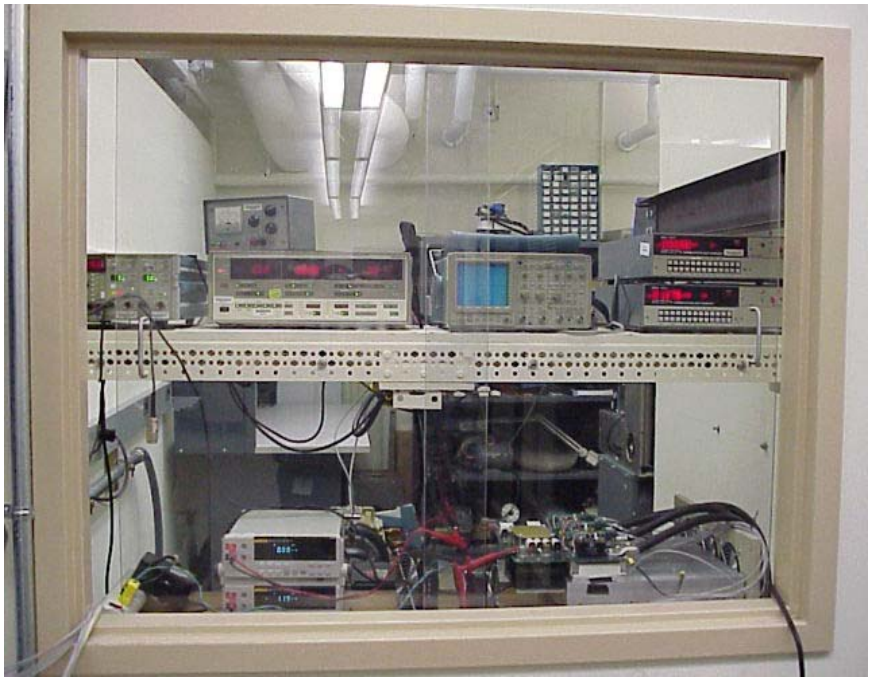

Figure 11 Measurement Equipment Setup

Along with the dynamometer listed above, the equipment used in this testing include the following:

- Tektronix TDS7054 Oscilloscope
- Yokogawa 2533EAC Power Meter
- Himmelstein 66032 Dynamometer
- 2 HP E3631A Power Supplies
- Tektronix A6304XL Current Probe
- Tektronix AM503B Probe Amplifier
- 2 Fluke 45 Digital Multimeters
- 3 Tektronix P5205 HV Differential Probes
- Analog Devices ADMC401 DSP

The instrument applications in the setup are typical. The digital multimeters were used for measuring DC bus voltage and DC bus current through a current shunt. The two differential probes and the current probe were used for measuring voltage and current waveforms for oscilloscope FFT calculations. The remaining equipment use is clear.

Temperature measurements were handled with the use of two J-type thermocouples. The inverter was mounted on a standard aluminum heat sink with three fans placed at one end to provide the cooling. The thermocouple was placed next to the IGBT that was furthest away from the cooling fans. Figure 12 below illustrates the position of both the fan and thermocouple placement. This placement gave a good approximation of the worst-case condition with respect to cooling and maximum temperature.

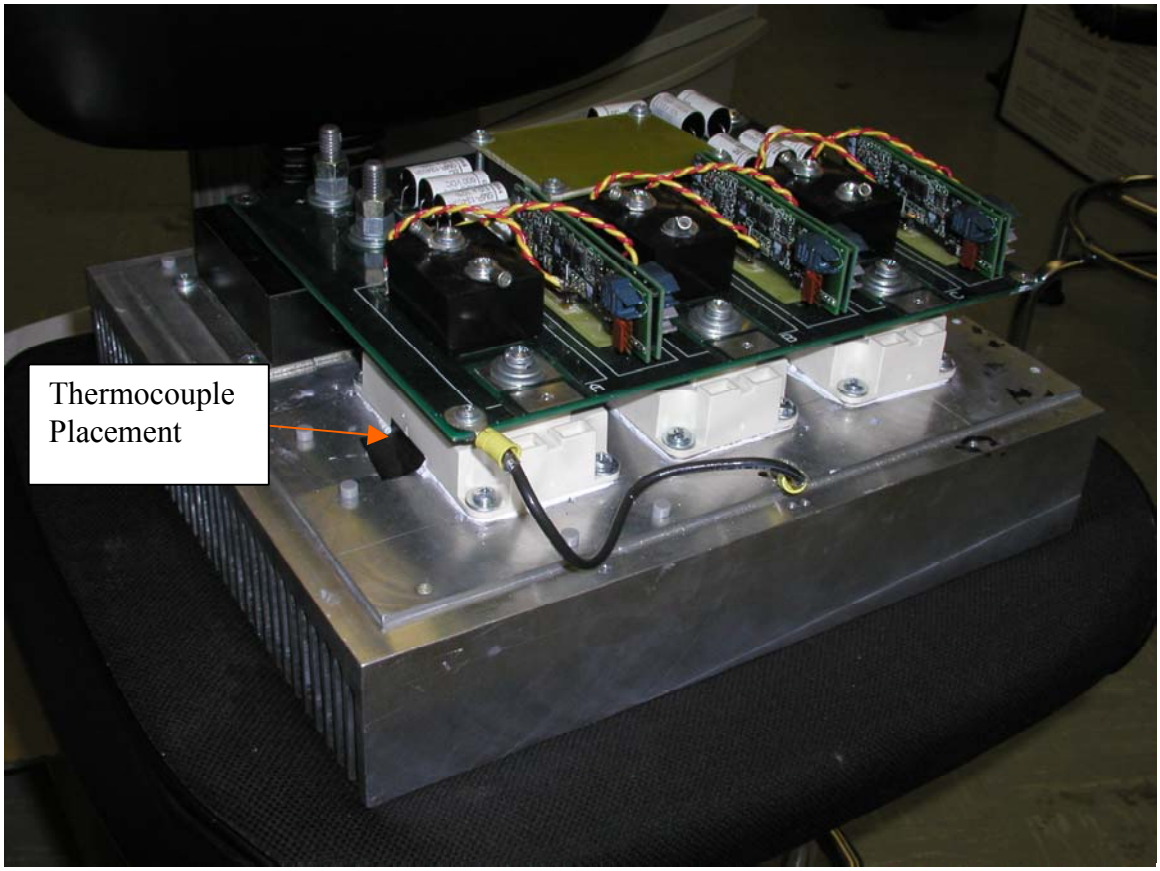

Figure 12 Inverter Thermocouple Placements

The motor proved to be much more difficult to cool than the inverter. The GE standard industrial housing is not specifically designed for forced convection cooling. The ideal cooling would be the use of circulated oil in a sealed housing. To help alleviate this problem, a large blower with ducting was placed directly behind the motor. The use of the blower gave much better airflow around the stator as well as through the air-gap of

the motor. All in all, this allowed for better cooling, but was still not sufficient enough for heavier load testing.

To track the motor temperature, a thermocouple was placed on the opposing end of the motor to the blower on the stator windings. Similar to the inverter, the end away from the blower was the most probable hot spot. Another benefit to placing the thermocouple in this position is the fact that the stator end turn windings are not touching the motor housing, which can act as a heat sink. Therefore, the most probable hot spot is monitored. Figure 13 below shows the thermocouple placement on the motor.

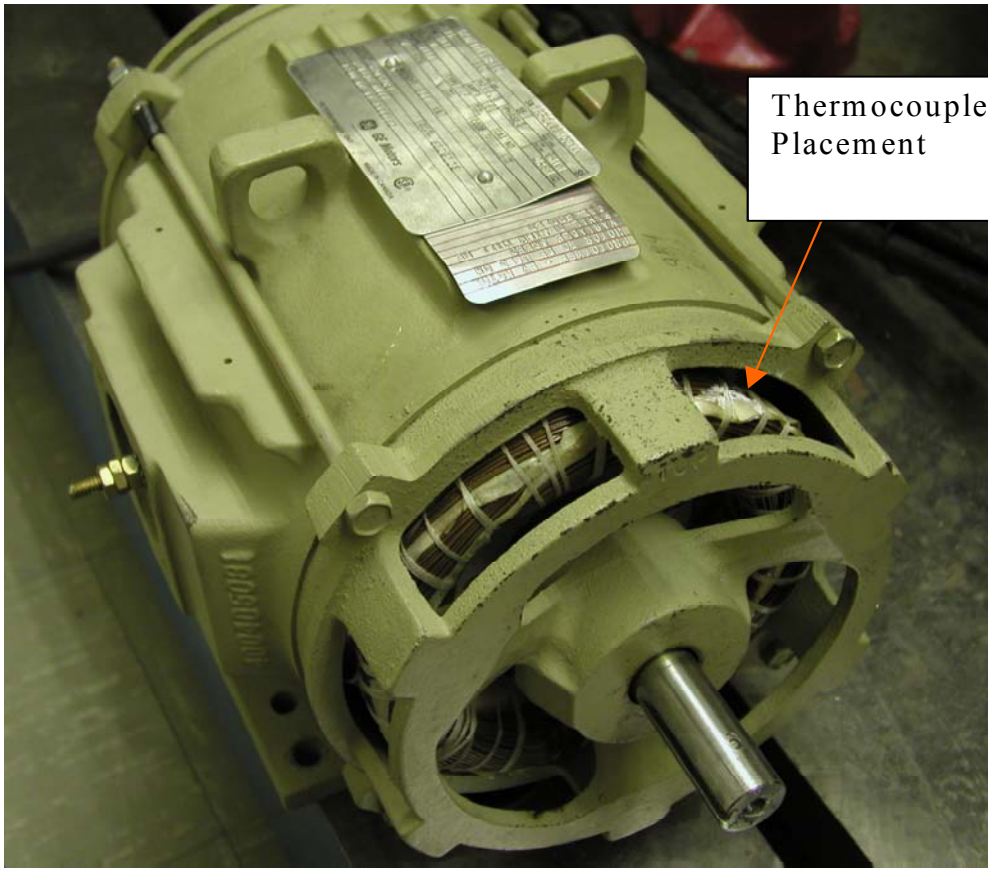

Figure 13 Motor Thermocouple Placements

3.2. Inverter Overview

The inverter was developed in house [2] with a large amount of integration. It consists of three phases with three half-bridge IGBT modules as the switching devices. Figure 14 shows the basic schematic of the three-phase inverter.

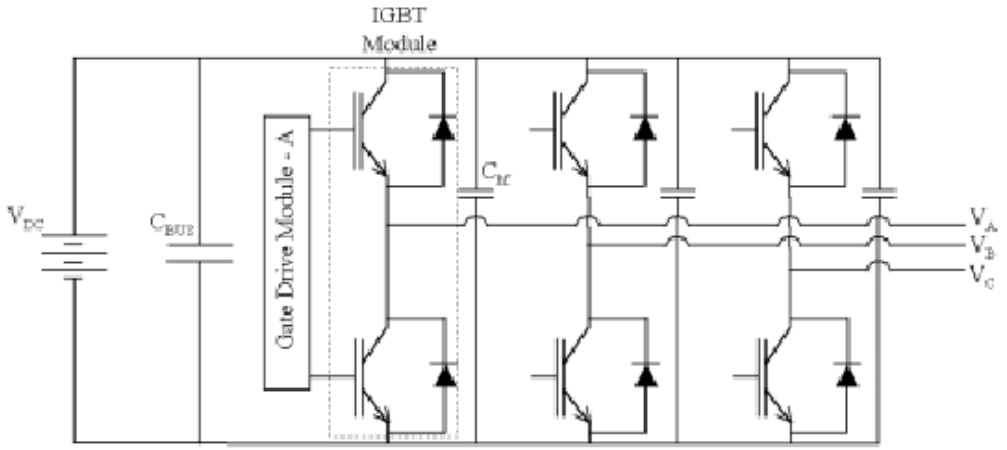

Figure 14 Basic Voltage Source Inverter Schematic [2]

For this work, SKM 300 GB 063D IGBTs were used. Separate laminated bus bars were replaced by integrating them into a PC board design. The PCB consists of heavy 14-ounce copper for the DC bus with four layers. The top layer is the positive DC bus, and the bottom layer the negative DC bus. The middle layers are used for the IGBT's gate signals. The manufacturing was handled by UPE, Inc. The PCB also consists of an integrated common mode choke. The inductor is a one turn E and I core set clamped through the board, and the Y-capacitors are standard Electronic Concepts stock. The fully assembled inverter is shown in Figure 16.

The ratings for the inverter were designed for up to 400 VDC bus voltage, and 300 A capability. The voltage rating is based on a typical battery pack for an electric traction drive. The current rating also explains the need for the heavy copper bus bars.

Another feature of the inverter is the use of fiber optic isolation. The gate drive boards, shown in Figure 15, use optical transmitters and receivers for the gate signals

from the DSP as well as the fault signals from the gate drive circuits. There are fault signals for each drive circuit, but for each set of boards they are combined into a single signal that is then sent back to the control board.

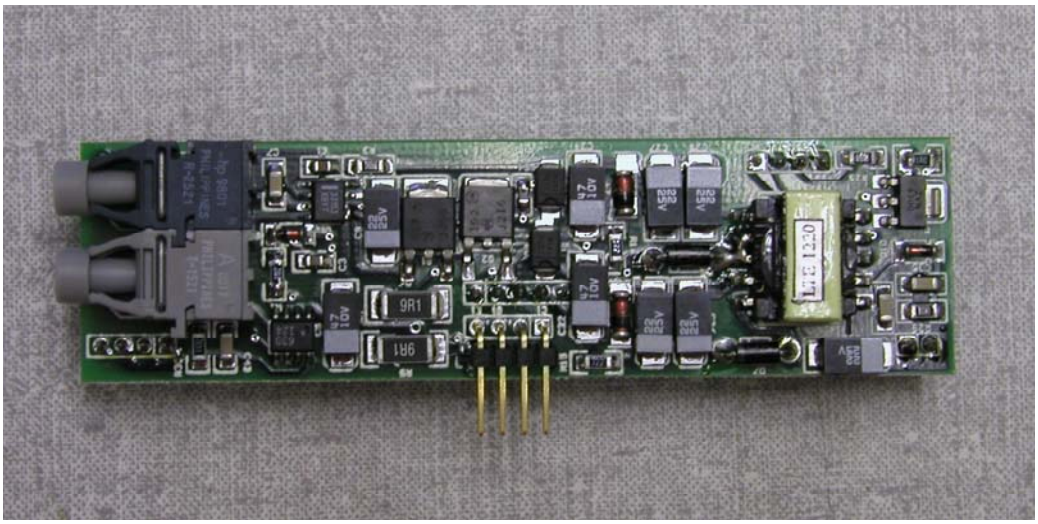

Figure 15 Gate Drive Board

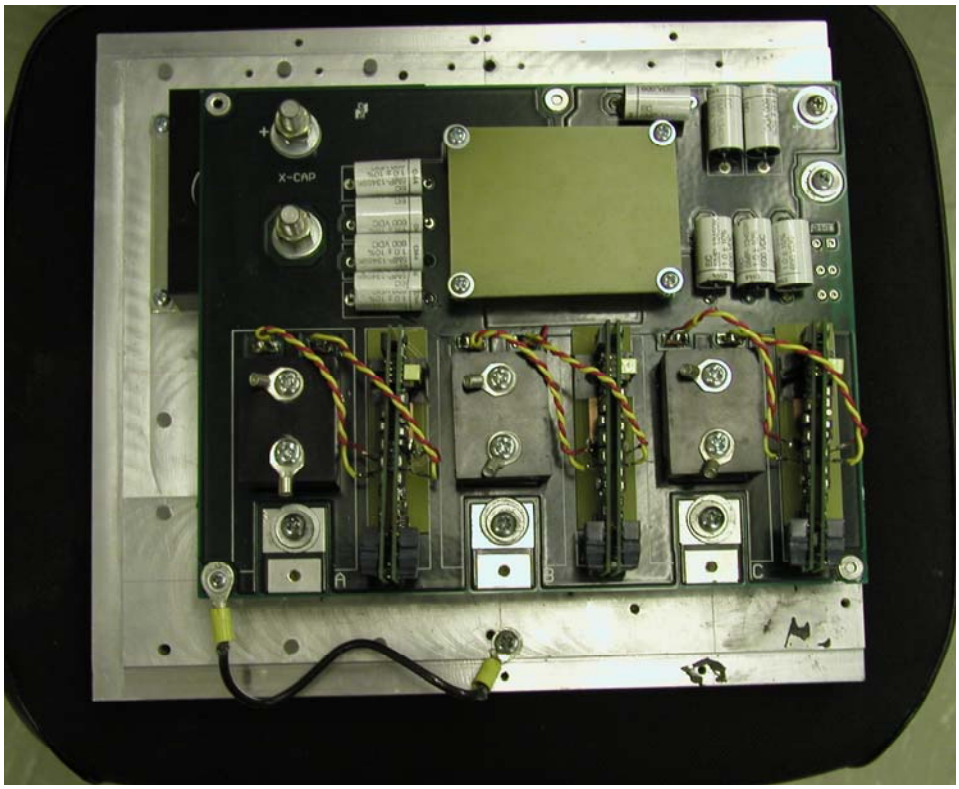

Figure 16 Inverter

Another unique design feature in the inverter is the use of an Electronic Concepts film capacitor for the DC bus. The capacitor is custom designed, has a slim profile, and takes the place of a larger electrolytic capacitor with a high current rating. Overall, this allows the inverter to be much slimmer without giving up DC capacitor performance. There are also small Electronic Concept capacitors across each half-bridge device, but according to previous work, these are not necessary [2].

3.3. Induction Motor Overview

As mentioned above, the motor used in this work is a high frequency three-phase two-pole squirrel-cage induction motor. This type of motor is very robust, and widely used in industrial applications. The motor was designed by Virginia Power Technologies (VPT) and built by General Electric (GE). The motor, shown in Figure 17, uses a standard GE 180-frame industrial housing.

Figure 17 VPT Induction Motor

The motor, which was designed for automotive traction drive applications, needs to have a high power density or power to weight ratio. This is the main difference between this motor and a typical industrial induction motor. Therefore, it was designed as a smaller high-speed 20,000 RPM motor. This allows for reduced weight and size as well as lower rotor inertia. The lower inertia benefits the need for quick acceleration and deceleration. Acceleration is a common automotive requirement, but in this case, with such a high-speed motor and the use of a transmission, the need for the motor to accelerate and decelerate quickly is even more important. The torque production does suffer because of the motor's smaller size, but with the use of the previously mentioned transmission, the torque is recovered.

3.4. Testing Methodology

For this type of testing, with multiple measurement equipment, a reasonable amount of accuracy is required. In this case, the inverter is run with open loop control of the line frequency and modulation index. Both were controlled via a potentiometer feeding a voltage signal into the DSP A/D converter, and scaled internally to the appropriate value. Changing the switching frequency was accomplished by changing the value directly in the DSP code. While this allowed for a reasonable amount of control over the testing, it also posed the problem that the resolution is limited on all three variables. The switching frequency resolution was limited because of the original coding of the DSP. The code was not intended for use with a variable switching frequency. Therefore, the program would only accept increments of 1000 Hz. This was not as much of a problem with accuracy in that it just limited the number of experimental data points. The potentiometer controlled variables, line frequency and modulation index, where limited in resolution by the onboard A/D.

While the above resolution problems offered some challenges, the larger problem came from the way the DSP code was originally written with respect to the line and switching frequency. As stated before, the code was not intended for use in variable switching frequency applications. Therefore, the problem arises in that for a given line frequency and switching frequency, the program calculates the total number of switchings in one line cycle. This would not be as much a problem except for the fact that the program has limited resolution. Thus, for a given test condition, the actual line frequency can vary slightly with the change in switching frequency, and because line frequency is directly related to slip of the induction motor, the loading could also change slightly. Therefore, the data points taken for each test are not shown to be linear, but there is a visible trend in the data. To show that the data trends make sense, temperature was also recorded for each individual test on the inverter and motor. The testing was all run at a steady state temperature. In recording the temperatures, the expected trends were confirmed. The testing routine is given below.

The first step was to set both the line frequency of the inverter and the speed of the dynamometer. To begin both speeds were set close to 1000, 2000, and 3000 RPM

depending on the test. After the speed was achieved, the DC bus voltage is applied and set to approximately 300 V. This voltage approximates the use of a battery pack in an electric vehicle. Next, the speed of the dynamometer is lowered to produce the desired slip. The actual value of slip was not as important as keeping it the same throughout the testing because this work is focusing on general efficiency improvements.

When the desired slip is reached the modulation index is increased or decreased depending on what load is being run. By adjusting the modulation index up or down, the line-to-line voltage on the motor is changed. Ideally the DC bus voltage would not change, but as discussed before the code's precision is not as high as desired. Therefore, the DC bus voltage would be adjusted slightly to set the load precisely.

Once the conditions above are met, the temperature is monitored. During the thermal transient the modulation index or DC bus voltage will have to be adjusted to account for the thermal losses. As the temperature rises, the conduction losses increase causing the load to drop. Once thermal steady state is reached the measurement data can be recorded. The data recorded would be for a particular switching frequency. Thus, once the data has been recorded the power supply is turned off, and the DSP code is changed to the next switching frequency. Once the code has been loaded into the DSP the power supply can be brought back on-line. From here, the temperature must reach steady state again before any measurements are taken. It is worthwhile to note that because there is a large thermal mass to both the induction motor and inverter, the time to steady state is reduced quite a bit. The above procedure is repeated for all switching frequencies at that particular load. For the next load, the slip is adjusted and the process is repeated.

3.5. Results

Once the test plan and test setup were complete, the testing was run at three speeds and at each of those speeds, three loads. These data points where chosen to get an approximate data trend. The raw data collected for all test results are located in Appendix I. The speeds selected for all the testing are: 1000, 2000, and 3000 RPM. Then, for each speed,

the following load-torques were run: 60.5, 120.3, and 180 in-lb. Since the main scope of this work is the effect of switching frequency on the motor and inverter, the switching frequency is varied from 5 kHz to 10 kHz in 1000 Hz increments.

3.5.1. 1000 RPM Operation

The first tests run were at 1000 RPM with the three different load torques and switching frequencies. Below, Figure 18 shows the overall efficiency of the system for the three separate loads. A quick look at the data points in Figure 18 show the DSP resolution problem. The data jumps around as the switching frequency is changed. Later, the temperature plots will show a much more linear trend. A side note to the problem is that at 7 kHz the before mentioned DSP precision error was so bad that for all tests this data point was excluded.

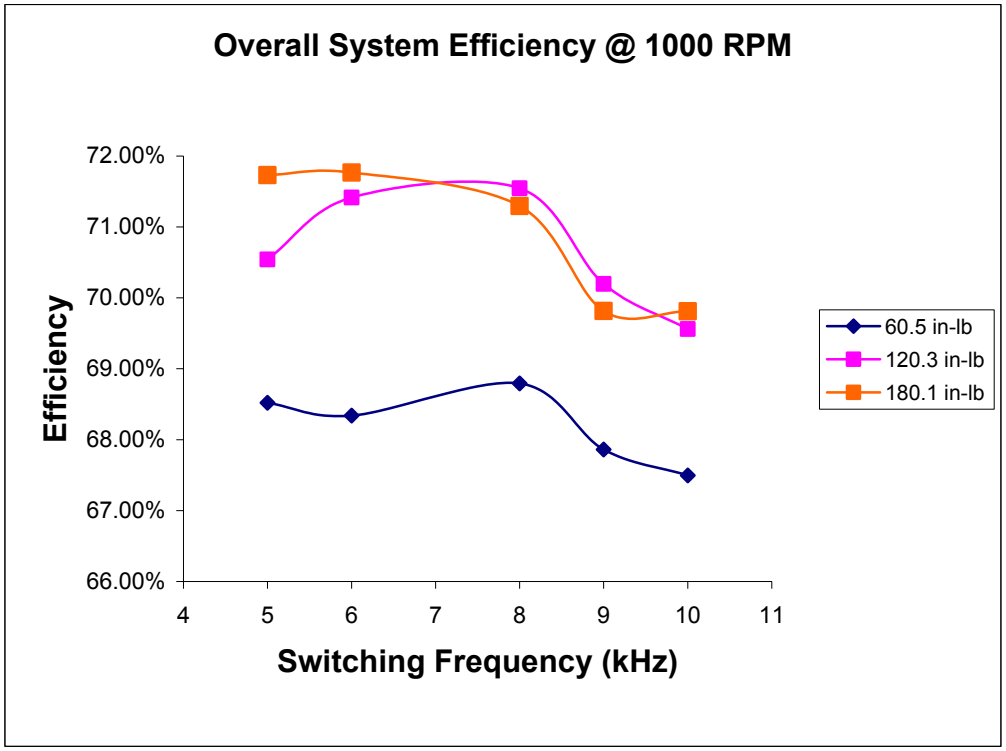

Figure 18 Overall System Efficiency at 1000 RPM

Examining the data further shows a trend where as the switching frequency is decreased the overall system efficiency increases. To support this trend, the temperature was also recorded at each data point.

As stated in the procedure, the data was recorded when the temperature had reached steady state. Figure 19 and Figure 20 below show the steady state temperatures of both the inverter and motor respectively. The results support the efficiency trend illustrated in Figure 18. Comparing the temperature plot of the inverter to that of the motor shows that the inverter temperature decreases at a faster rate than the motor temperature increases as the switching frequency is reduced.

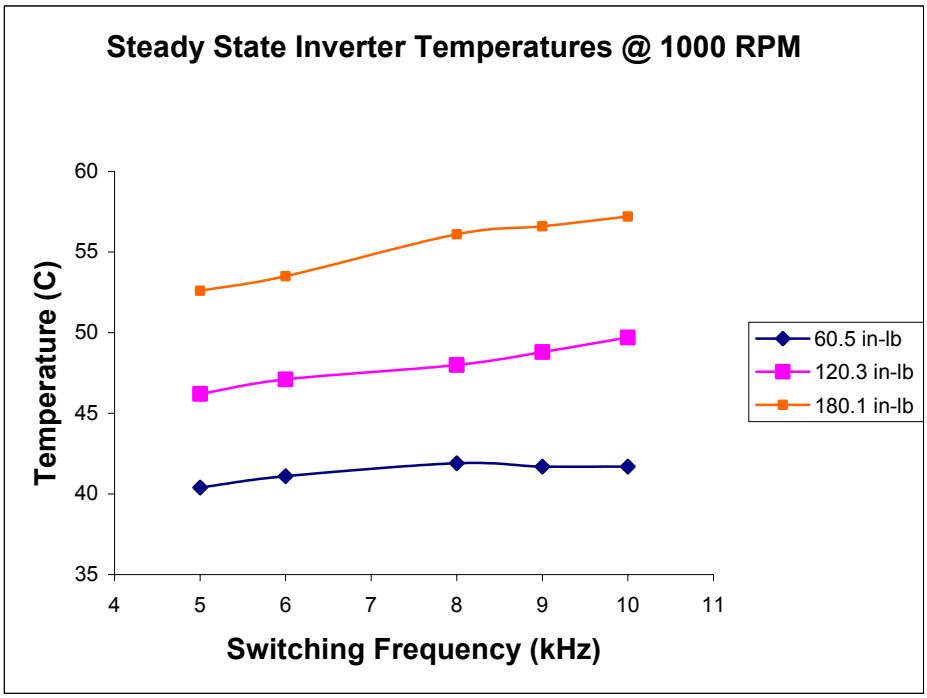

Figure 19 Steady State Inverter Temperatures for 1000 RPM

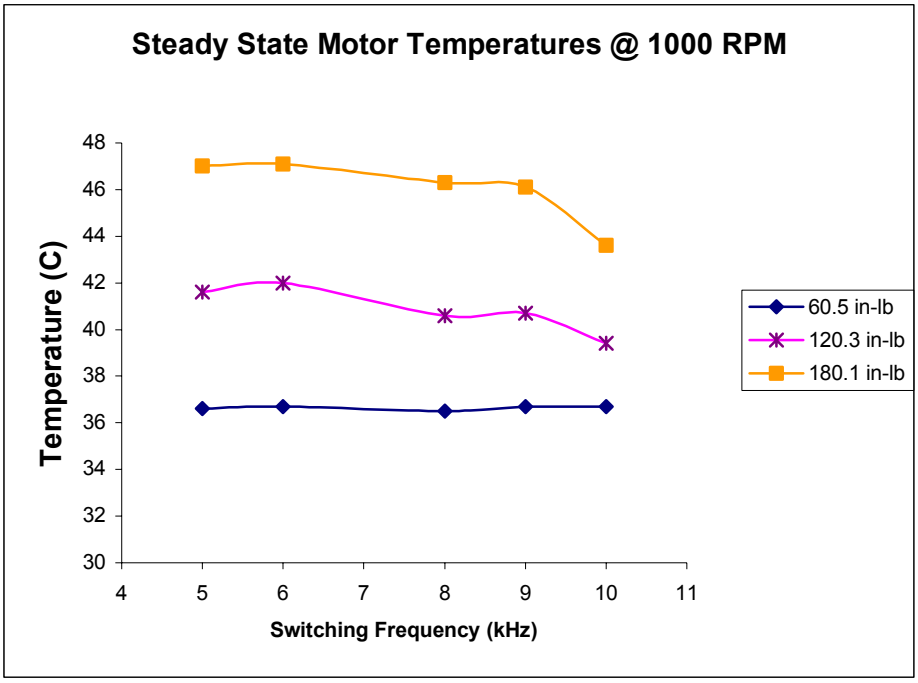

Figure 20 Steady State Motor Temperatures for 1000 RPM

The power loss plots for both the motor and inverter are shown in Figure 21 and Figure 22 respectively. These also illustrate the trends shown in the efficiency and temperature graphs. As in the case of temperature, the inverter power loss decreases more than the motor losses increase with the reduced switching frequency.

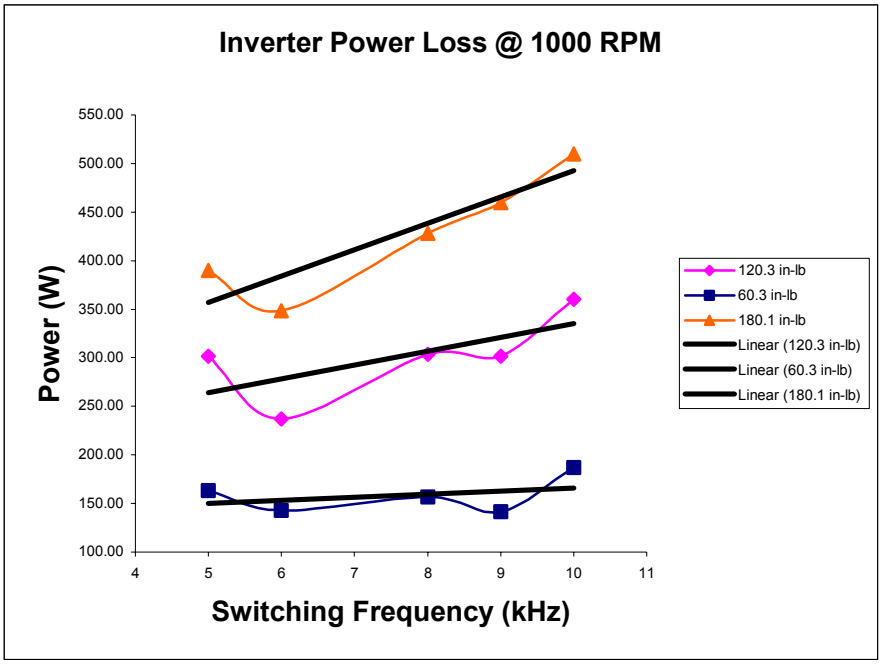

Figure 21 Inverter Power Losses for 1000 RPM

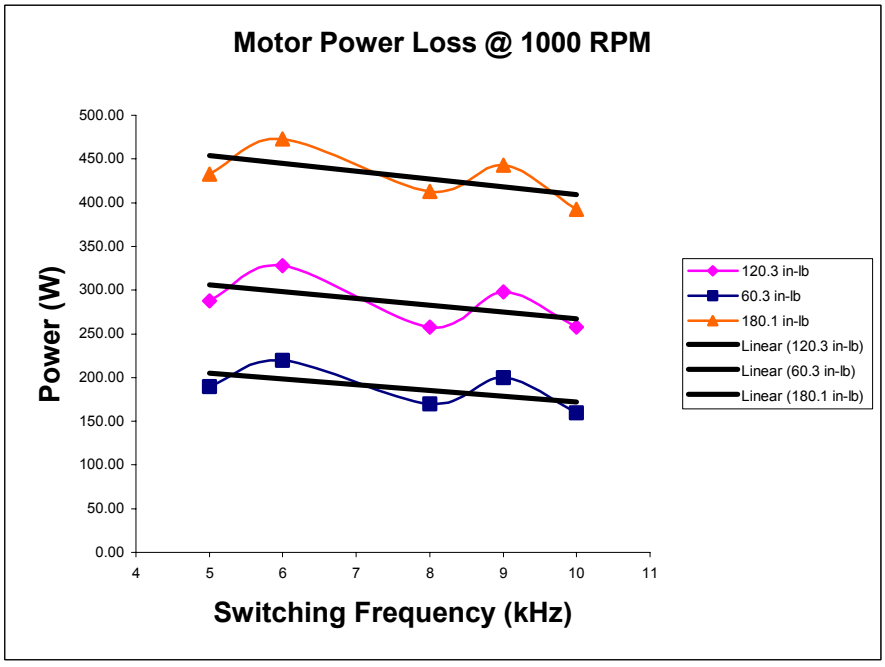

Figure 22 Motor Power Losses for 1000 RPM

Another interesting result of lowering the switching frequency is the fact that the improvements increase as the load increases. Basically, the slope of a trend line for the

inverter temperature and power loss increases as the load is increased while the motor slopes are essentially the same. As a result, the overall system efficiency improves with the reduced switching frequency. This is also the case for all three load torque conditions.

3.5.1.1.Harmonic Content

Since the results shown in the previous section show an improvement in overall efficiency, the frequency spectrum is examined for some explanation of the improvements. To accomplish this, a FFT was run on the line-to-line motor voltage as well as the motor phase current using the Tektronix oscilloscope. Since the results show a somewhat linear trend, the FFT was run at 5 kHz and 10 kHz switching frequencies for each load. This should then give the largest differential in harmonic content.

Figure 23 and Figure 24 below show the difference between the line-to-line motor voltage frequency spectrums at the 60.5 in-lb load. Since both plots are on the same scale, the difference is easily discerned. The lines placed on the plots also show the difference. For this case, the 10 kHz operating condition shows a larger magnitude for the switching frequency harmonic as well as multiples of the switching frequency.

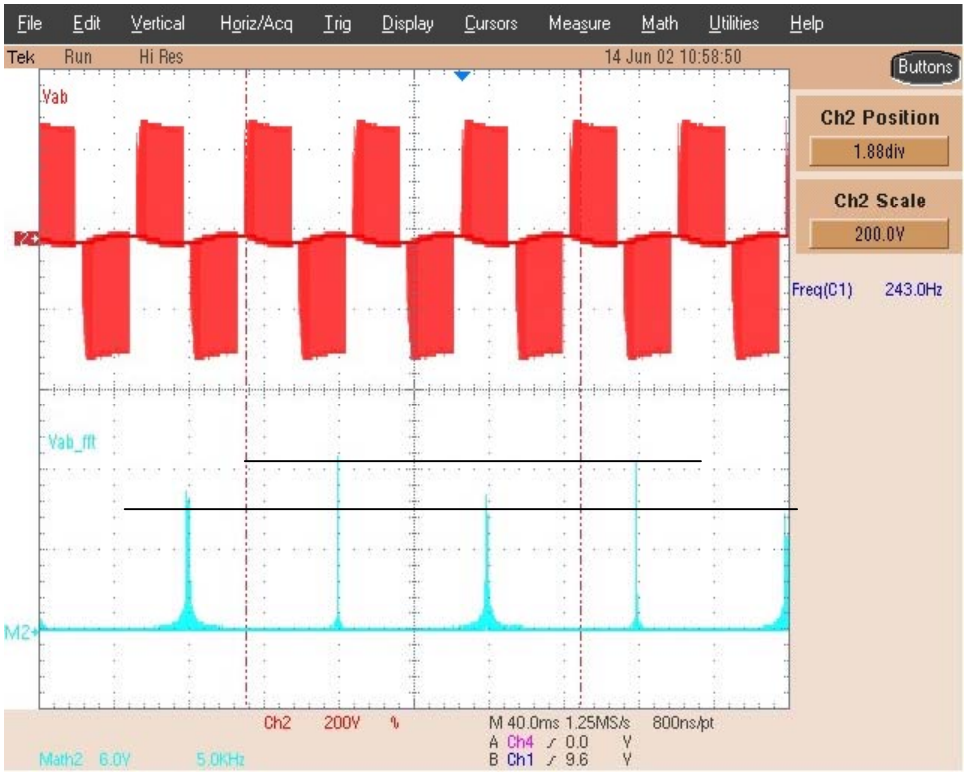

Figure 23 Voltage FFT for 60.5 in-lb, 1000 RPM, and 10 kHz Switching

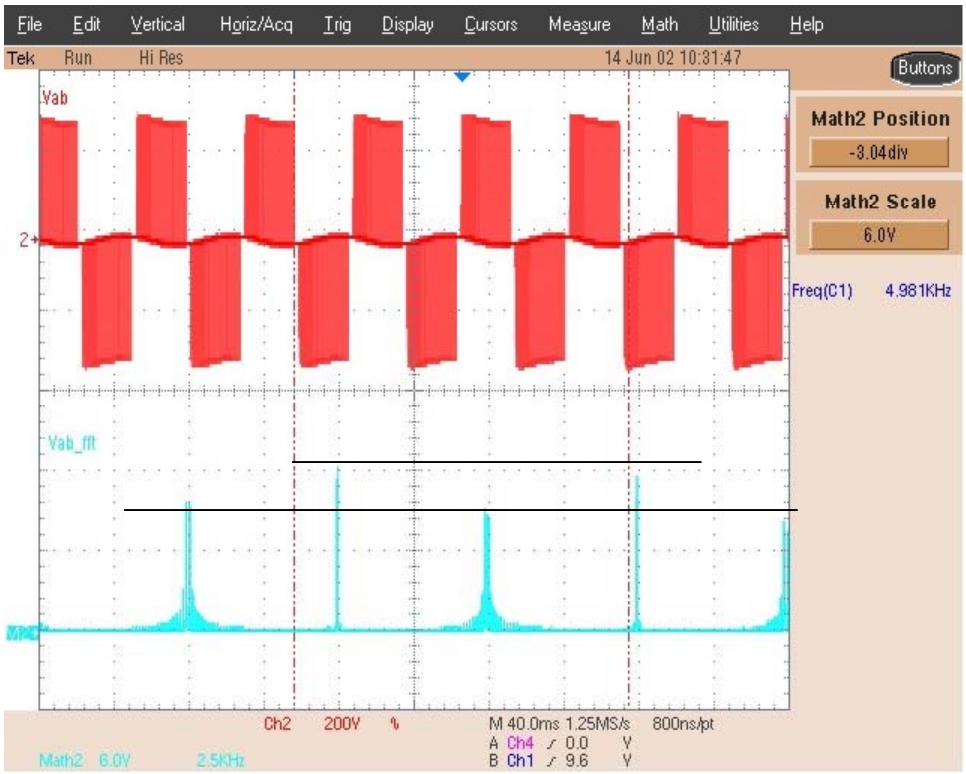

Figure 24 Voltage FFT for 60.5 in-lb, 1000 RPM, and 5 kHz Switching

Next, the current frequency spectrum needs to be examined. Figure 25 and Figure 26 show the current spectrum at the same load of 60.5 in-lb. Looking closely at the spectrum shows that the sidebands, marked with the oval, of the fundamental have increased with the lower switching frequency. This can be expected because of the increased ripple current introduced into the motor by essentially leaving the IGBTs on and off longer causing larger peaks or ripple. These differences on voltage and current can help explain the improvements shown before because of an improved distortion factor, which is directly related to THD (3.1). The current distortion factor would appear to worsen as the voltage distortion factor improves.

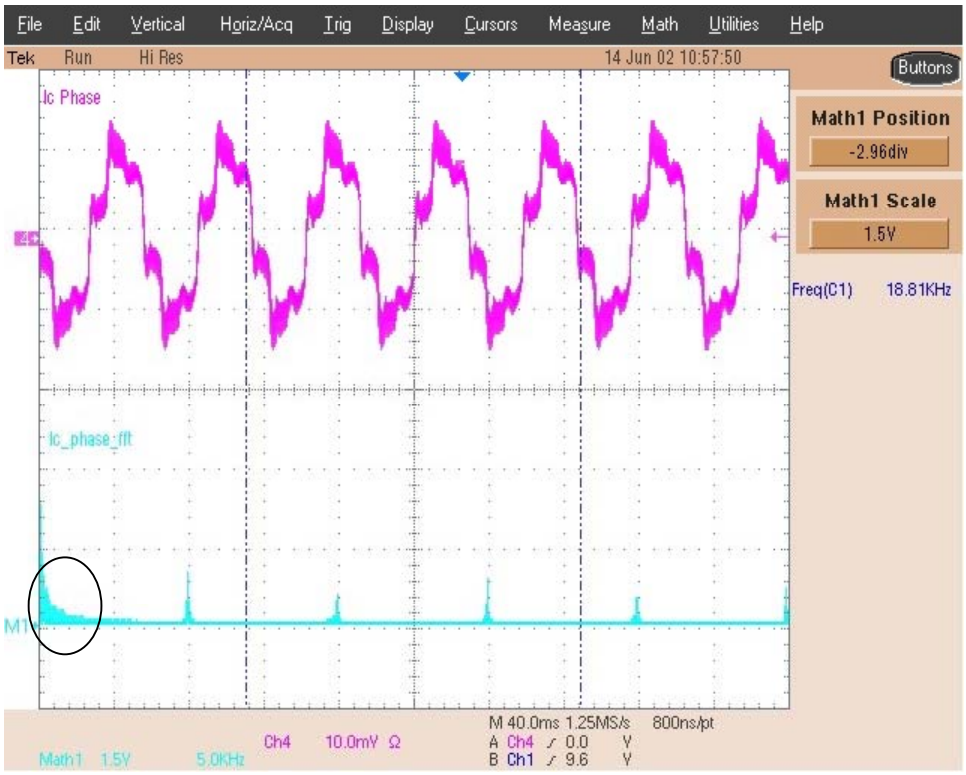

Figure 25 Current FFT for 60.5 in-lb, 1000 RPM, and 10 kHz Switching

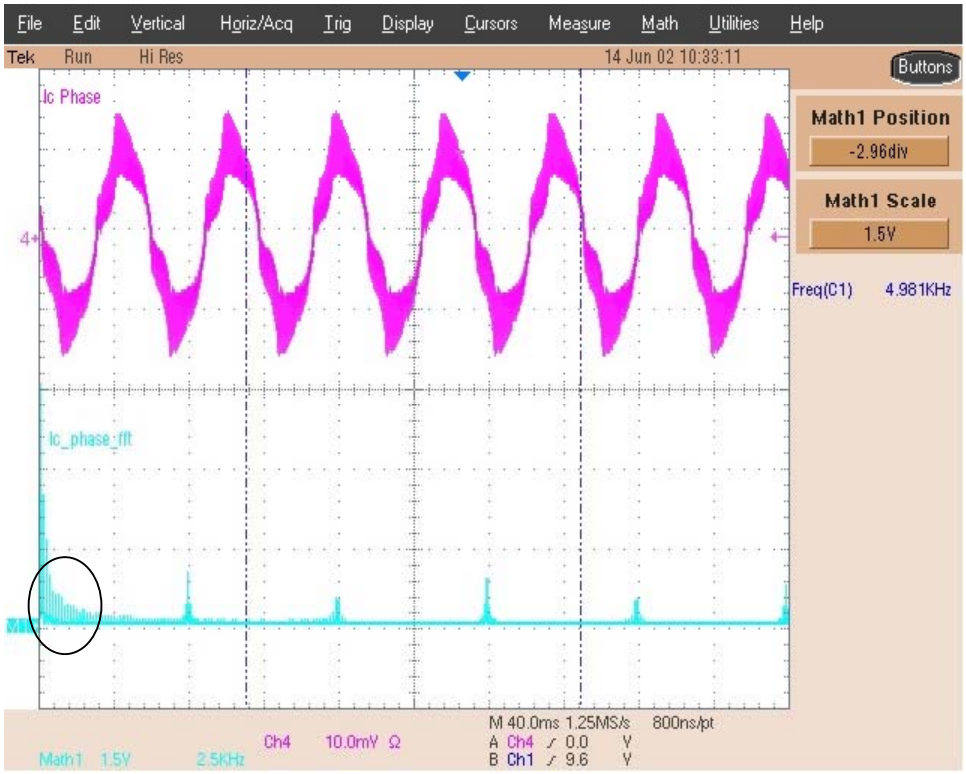

Figure 26 Current FFT for 60.5 in-lb, 1000 RPM, and 5 kHz Switching

The results for the 120.3 in-lb loads are given below. Figure 27 and Figure 28 show the voltage spectrum and Figure 29 and Figure 30 show the current spectrums. Examining these results also show the same results as the lighter 60.5 in-lb load. The voltage switching frequency harmonics are higher at higher switching frequency while the fundamental frequency side bands of current are worse at lower switching frequency.

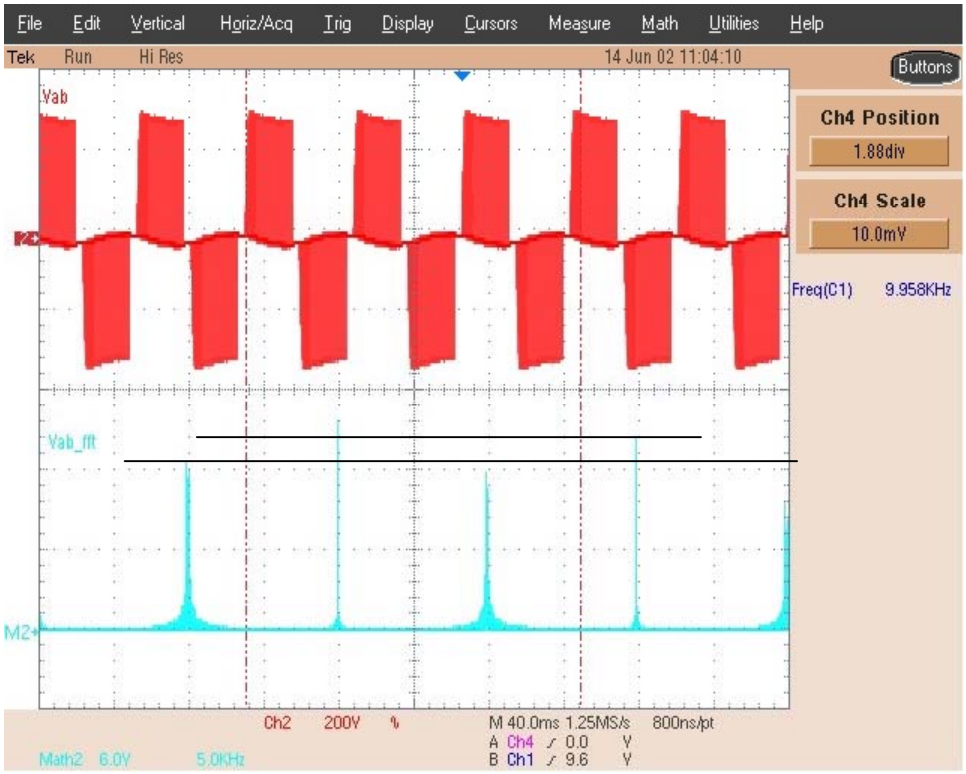

Figure 27 Voltage FFT for 120.3 in-lb, 1000 RPM, and 10 kHz Switching

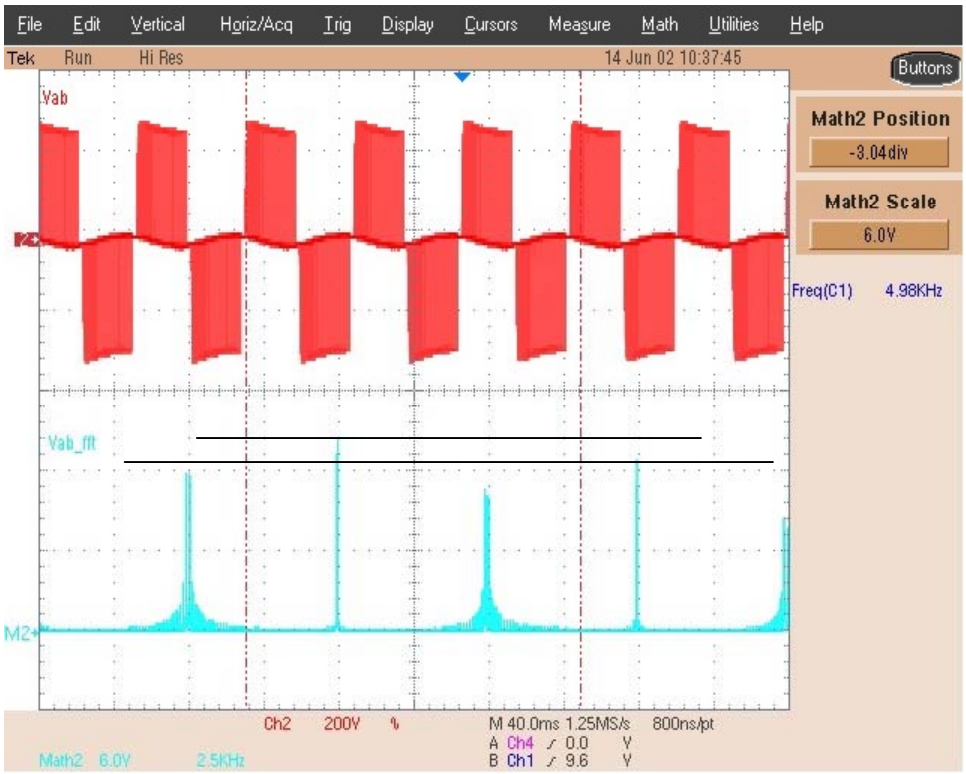

Figure 28 Voltage FFT for 120.3 in-lb, 1000 RPM, and 5 kHz Switching

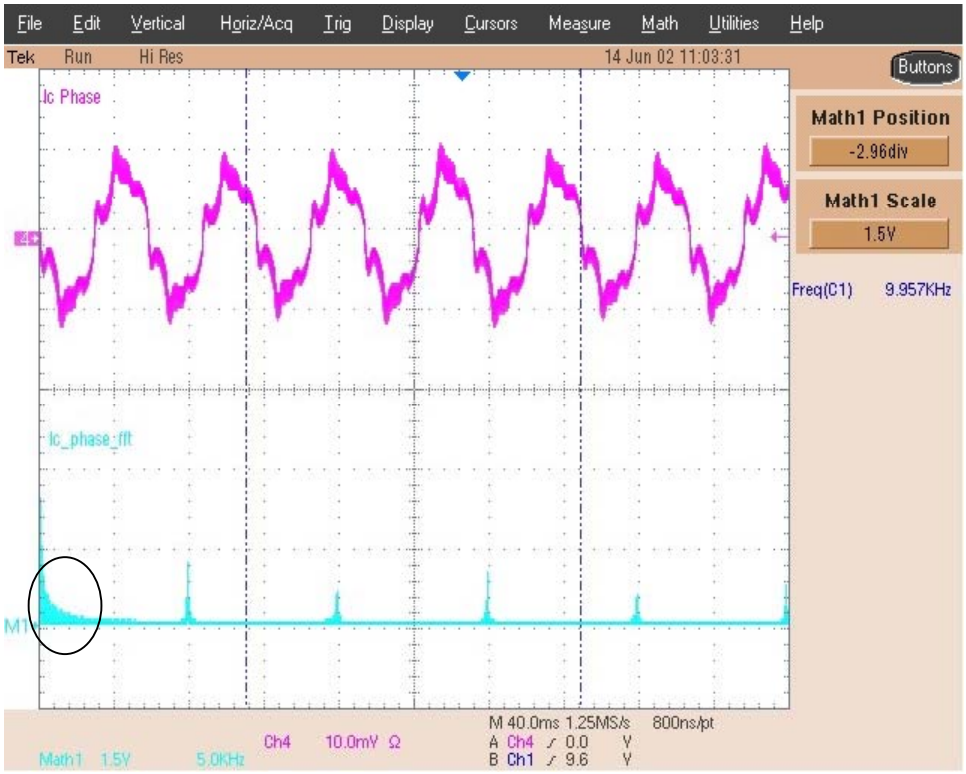

Figure 29 Current FFT for 120.3 in-lb, 1000 RPM, and 10 kHz Switching

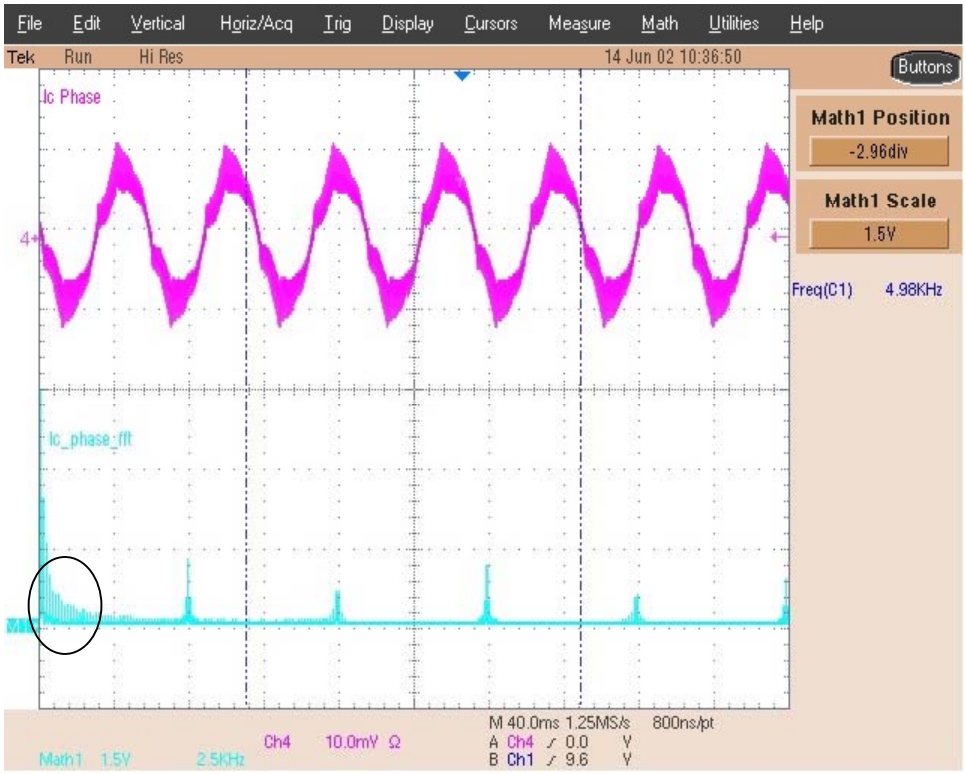

Figure 30 Current FFT for 120.3 in-lb, 1000 RPM, and 5 kHz Switching

As mentioned before, the improvements in efficiency are greater as the load is increased. Therefore, by examining the data closer, there is a more noticeable difference in the harmonic content for both voltage and current for the increased load. This same trend can also be seen in the heaviest load condition. The results for the 180 in-lb. load are given in Figure 31 and Figure 32 for voltage, and Figure 33 and Figure 34 for current. These results again show the same trends as in the two previous load conditions.

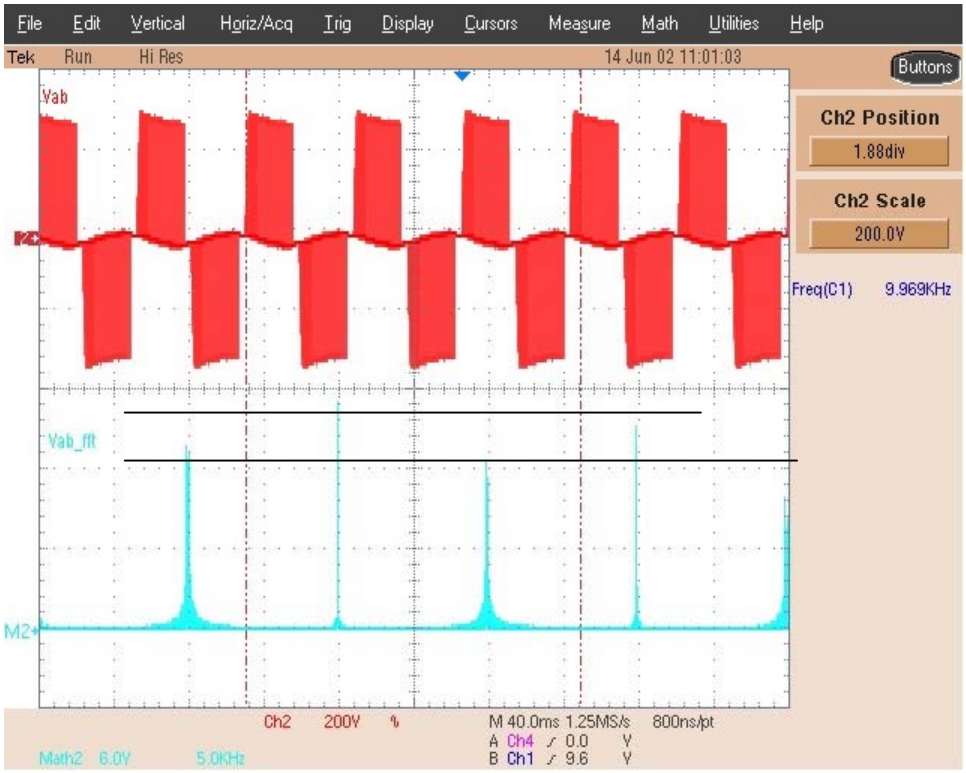

Figure 31 Voltage FFT for 180.0 in-lb, 1000 RPM, and 10 kHz Switching

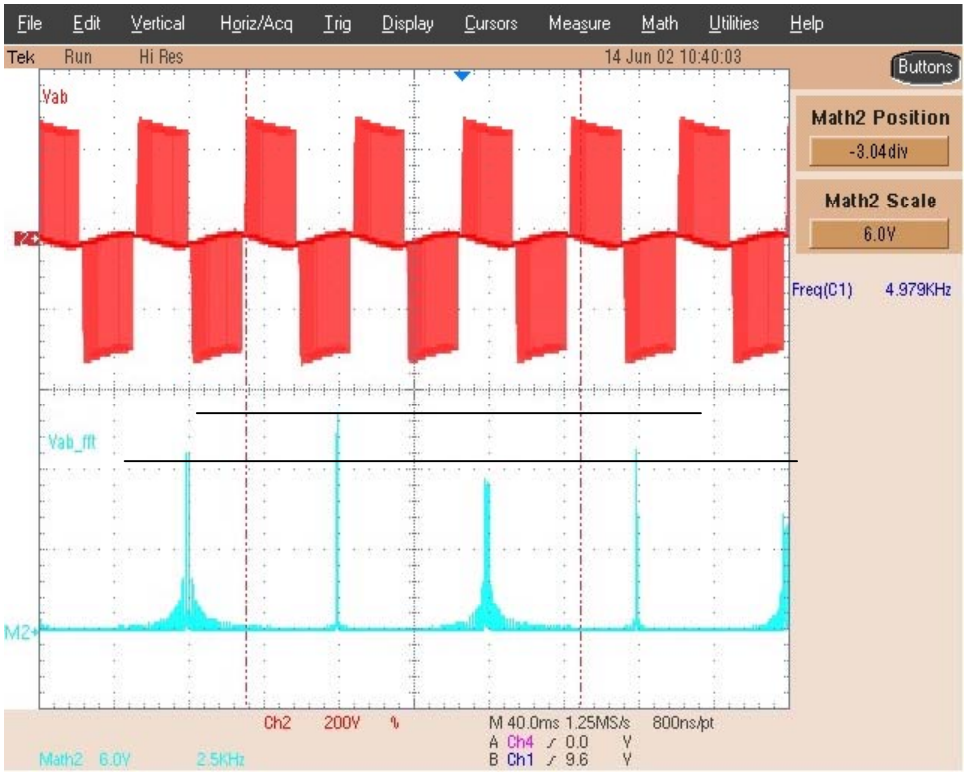

Figure 32 Voltage FFT for 180.0 in-lb, 1000 RPM, and 5 kHz Switching

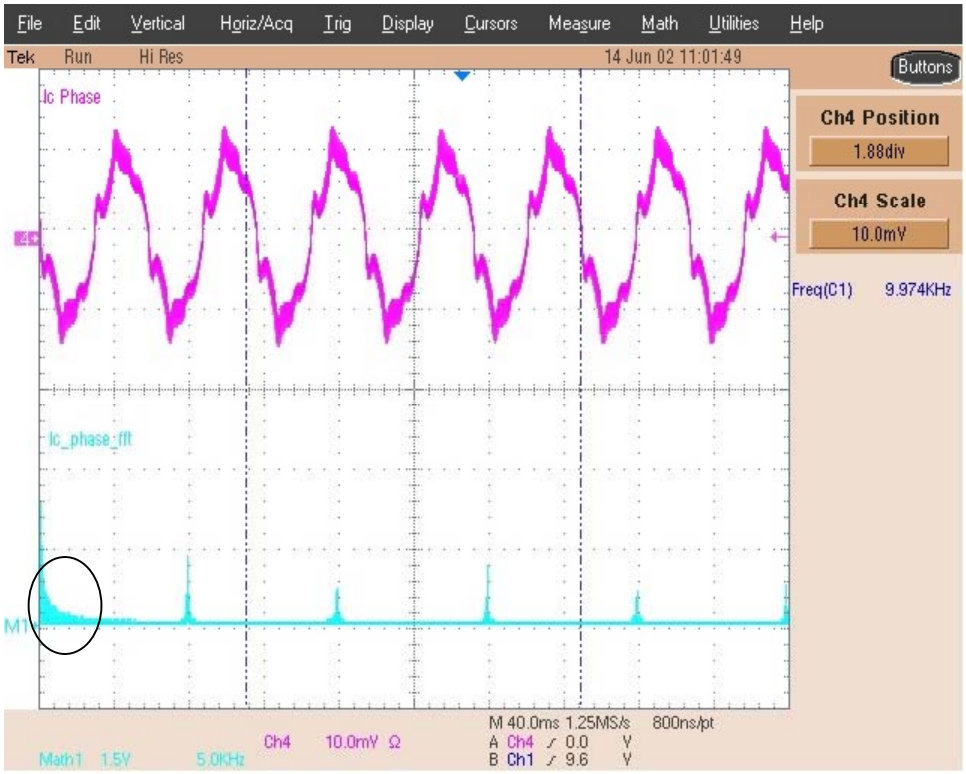

Figure 33 Current FFT for 180.0 in-lb, 1000 RPM, and 10 kHz Switching

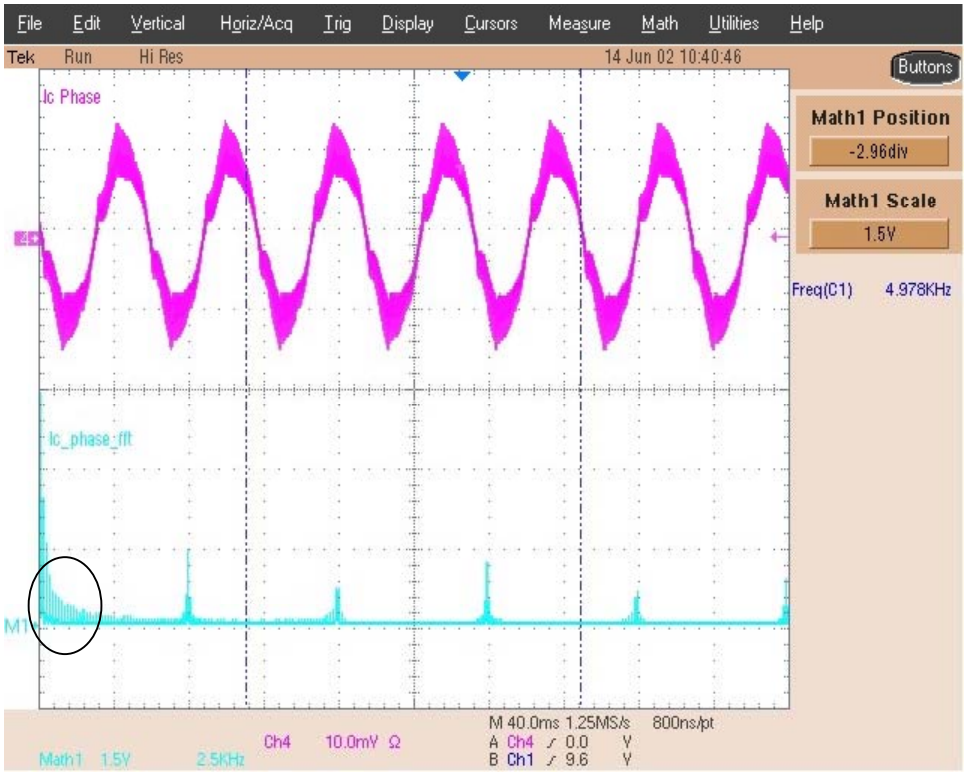

Figure 34 Current FFT for 180.0 in-lb, 1000 RPM, and 5 kHz Switching

The remaining plot of power factor, Figure 35, shows that the power factor increases as the switching frequency decreases. This helps to explain why the improvements occur at lower switching frequencies. For this work, power factor is defined as the displacement power factor, DPF, multiplied by the distortion factors, DF, for voltage and current:

$$PF = DPF \times DF_V \times DF_I \qquad (3.1)$$

Since the harmonic content is directly related to THD, and the harmonic content increases with the lower switching frequency, the distortion factor improves at lower switching frequency.

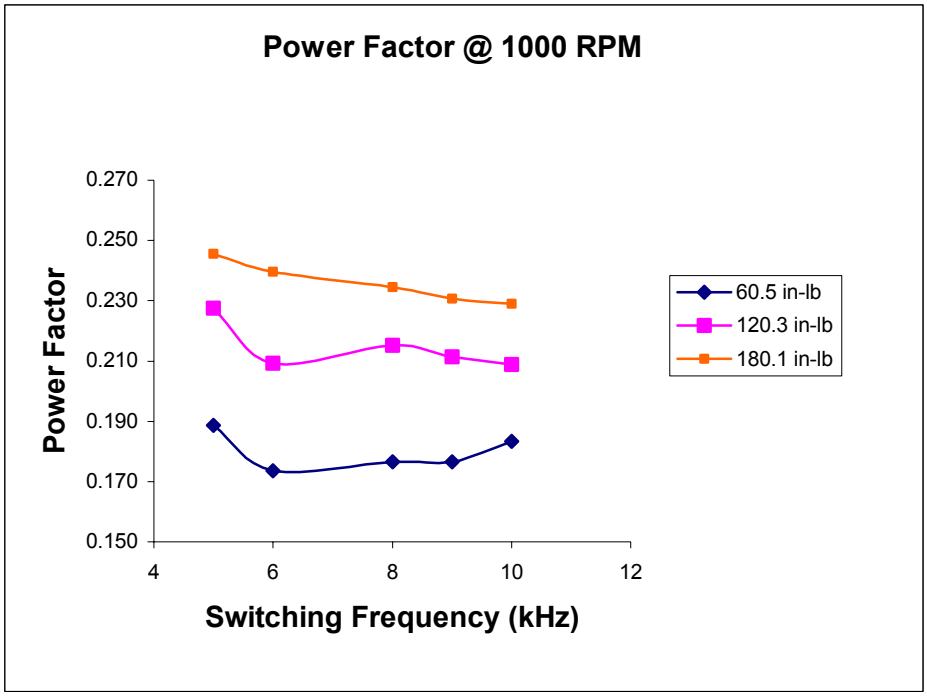

Figure 35 Power Factor at 1000 RPM

3.5.2. 2000 RPM Operation

The second tests were run at 2000 RPM with the same conditions. Below, Figure 36 shows the overall system efficiency for 2000 RPM. The same trends can be seen as in the previous experiments with the exception that at the lightest load, 60.5 in-lb, the overall system efficiency actually decreases with lowered switching frequency.

If you examine the slopes of the trend lines for the data at 1000 RPM and 2000 RPM, they show that the slopes at the same loads in 2000 RPM are less than those in 1000 RPM. For the 60.5 in-lb load this is obvious because of the decrease in efficiency. The heavier loads also show the difference.

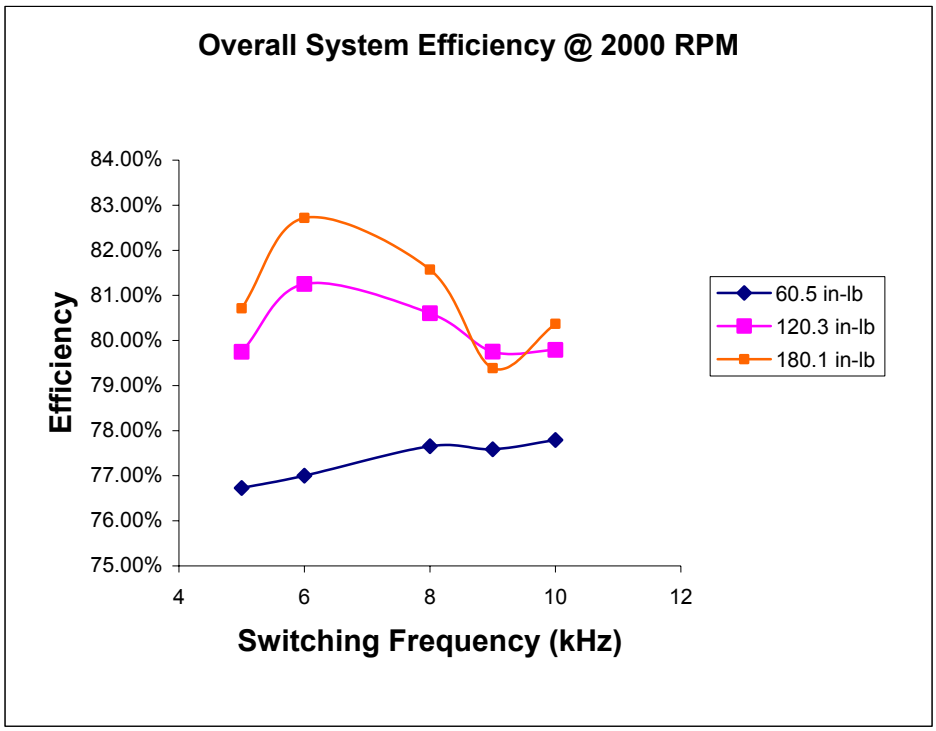

Figure 36 Overall System Efficiency at 2000 RPM

As in previous experiments, the temperature data also shows the same trend. The motor temperature data does not appear to be much different from those at 1000 RPM, but the inverter temperature decreases less than those at 1000 RPM. Figure 37 and Figure 38 show the temperature plots for 2000 RPM operation.

Comparing the motor and inverter temperature graphs again show that the motor temperature increases less than the inverter temperature decreases, but only for the two heavier loads. For the lightest load the inverter temperature is almost constant throughout the frequency range. Therefore, any temperature increase in the motor will give an indication of a decrease of the overall system efficiency.

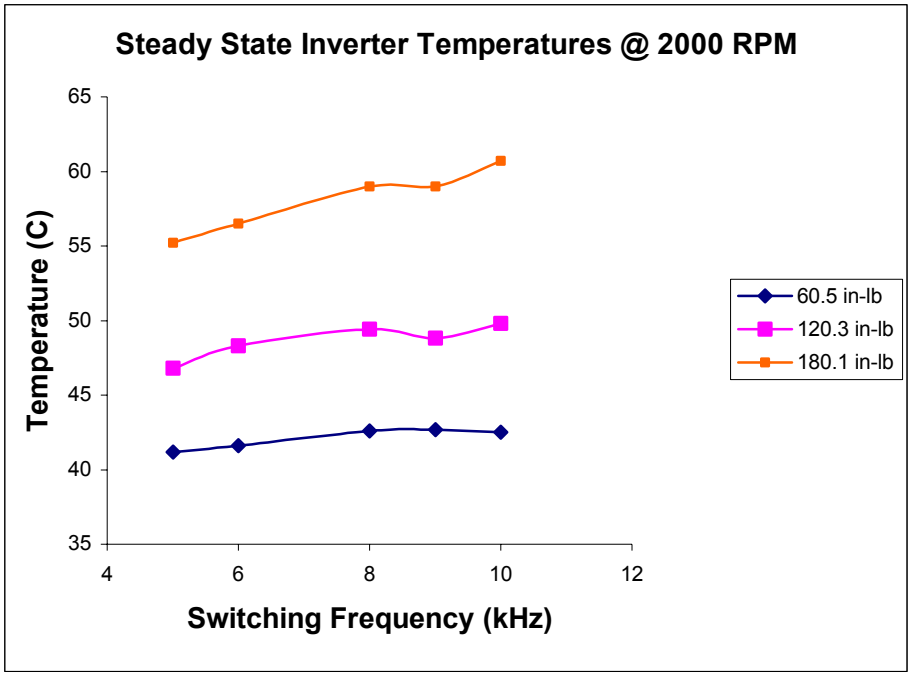

Figure 37 Steady State Inverter Temperatures for 2000 RPM

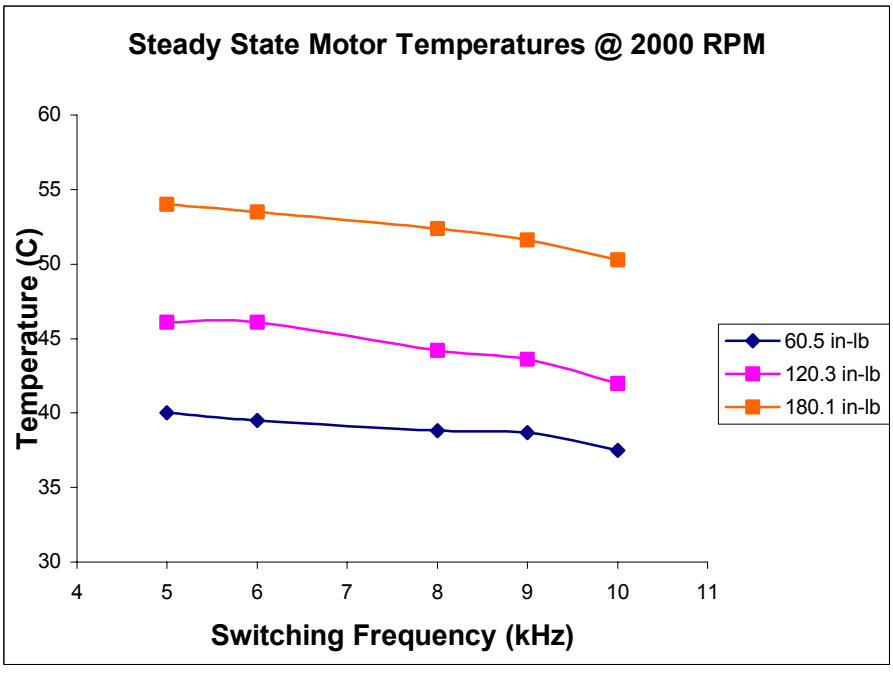

Figure 38 Steady State Motor Temperatures for 2000 RPM

The power loss plots for both motor and inverter are shown in Figure 39 and Figure 40. Analyzing the power loss plots shows the same outcome as the temperature plots. Once again the inverter power loss is essentially constant at the lightest load, and consequently the system power loss increases at the lightest load.

For the two heavier loads, the results are identical to 1000 RPM operation. The inverter power loss still decreases more than the motor power loss increases. Therefore the overall system losses actually decrease with the switching frequency.

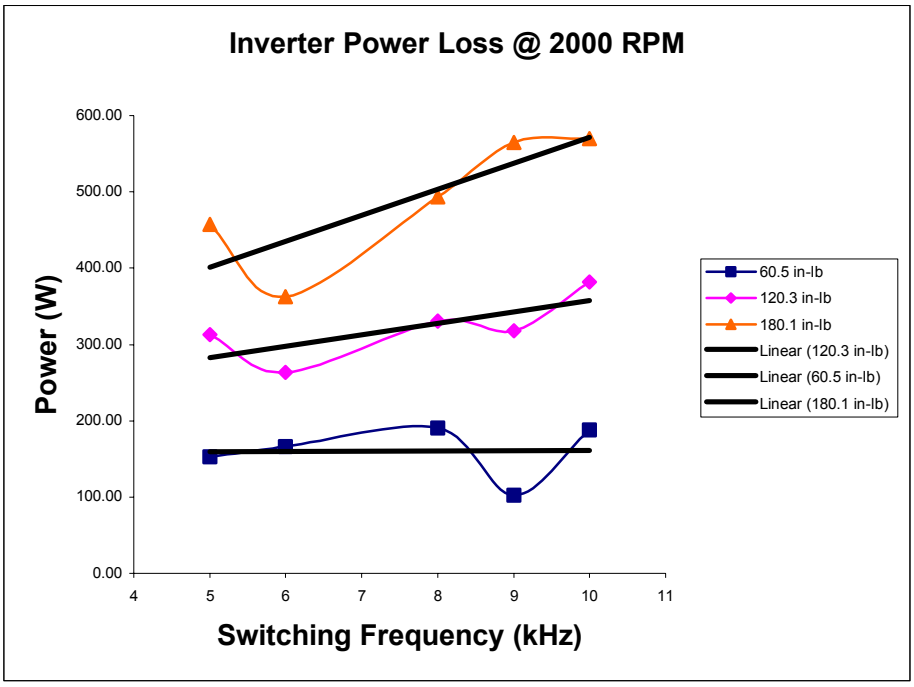

Figure 39 Inverter Power Loss for 2000 RPM

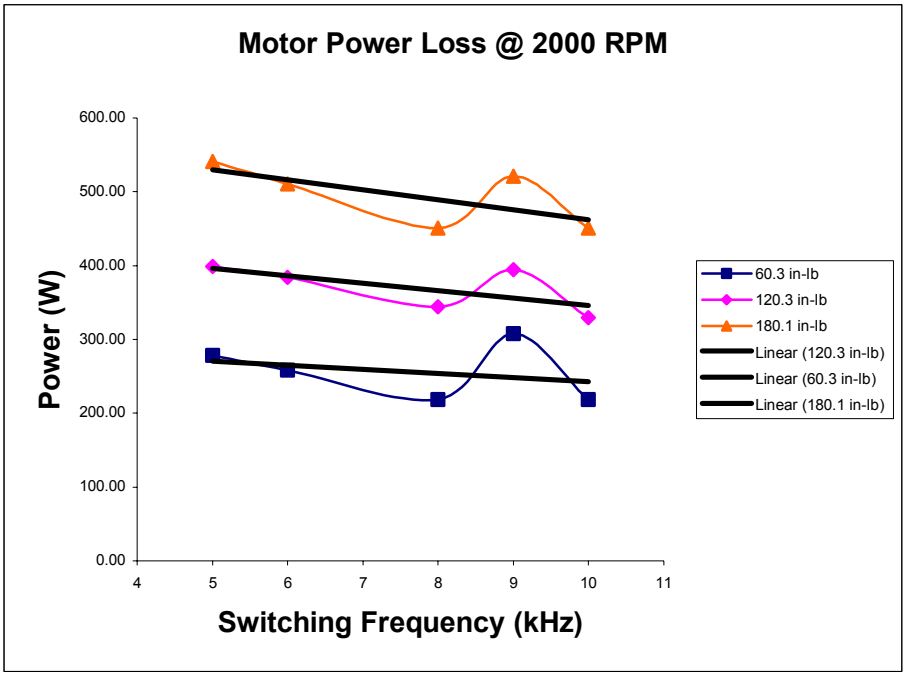

Figure 40 Motor Power Loss for 2000 RPM

3.5.2.1.Harmonic Content

The harmonic content is once again analyzed to show the relationship between the switching frequencies. The same results as in the 1000 RPM test are to be expected with the exception of the lightest load condition. Figure 41 and Figure 42 show the voltage frequency spectrum for the 60.5 in-lb load.

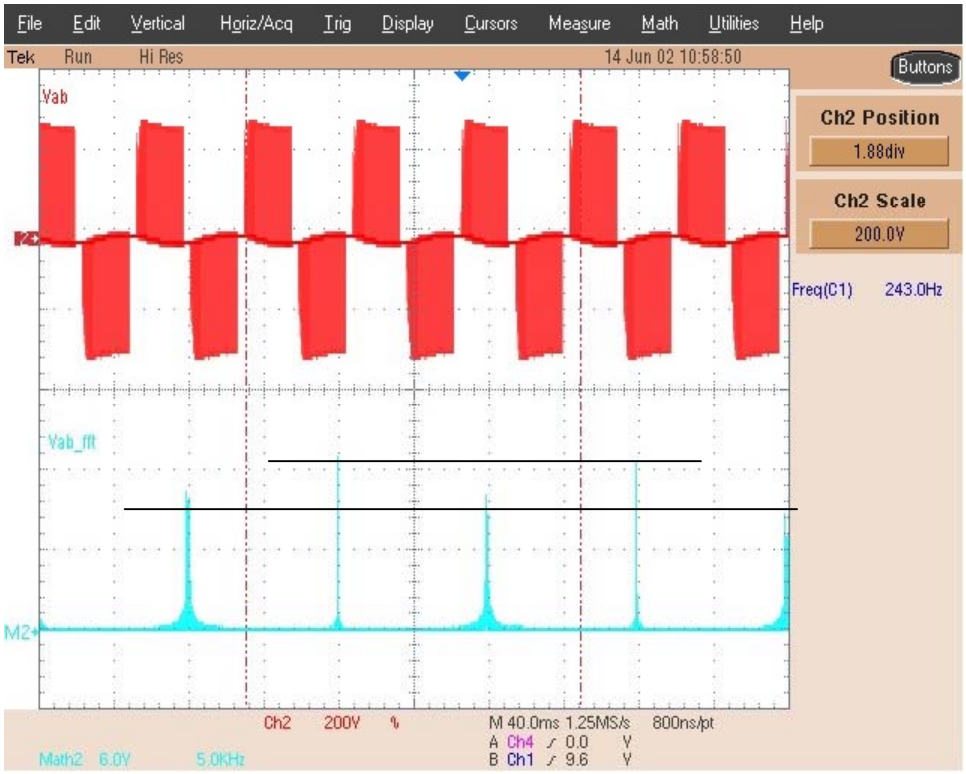

Figure 41 Voltage FFT for 60.5 in-lb, 2000 RPM, and 10 kHz Switching

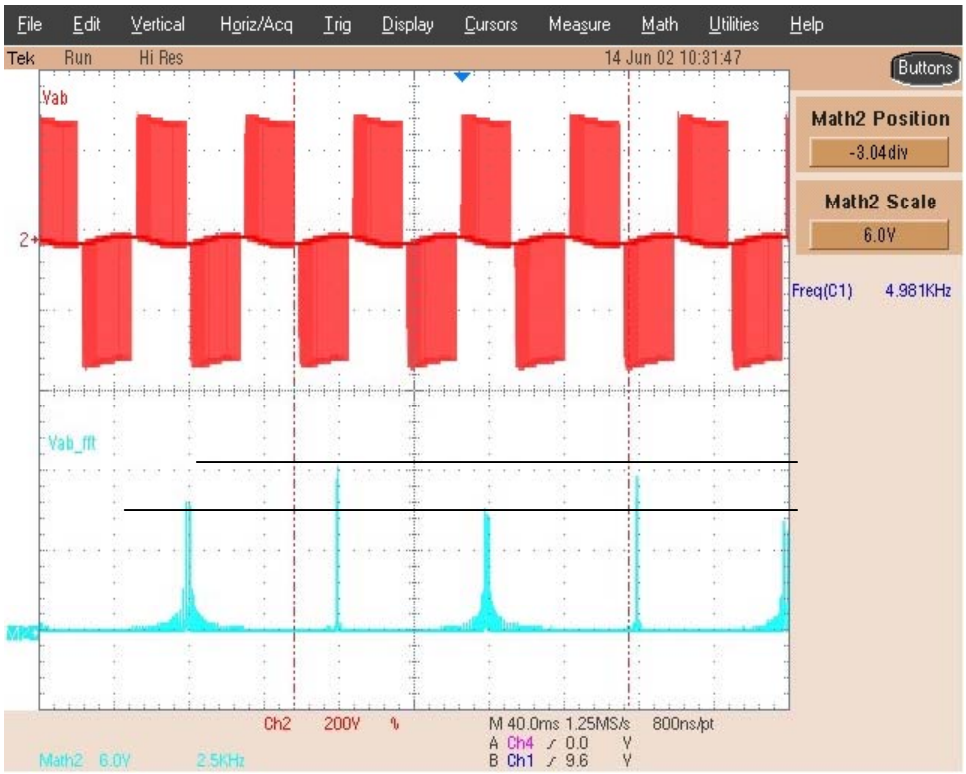

Figure 42 Voltage FFT for 60.5 in-lb, 2000 RPM, and 5 kHz Switching

Once again, the higher 10 kHz FFT shows larger switching frequency harmonics. The difference in the magnitude for both 5 kHz and 10 kHz is approximately the same as before. To explain the decreased efficiency at this load the current frequency spectrum should be analyzed.

Figure 43 and Figure 44 below show the current frequency spectrum. Comparing these results to the 1000 RPM case shows that the current harmonics, the fundamental frequency side bands, are slightly worse than those before. This helps explain the difference in the light load efficiency. Basically, the voltage harmonic improvement no longer offsets the increased current harmonics.

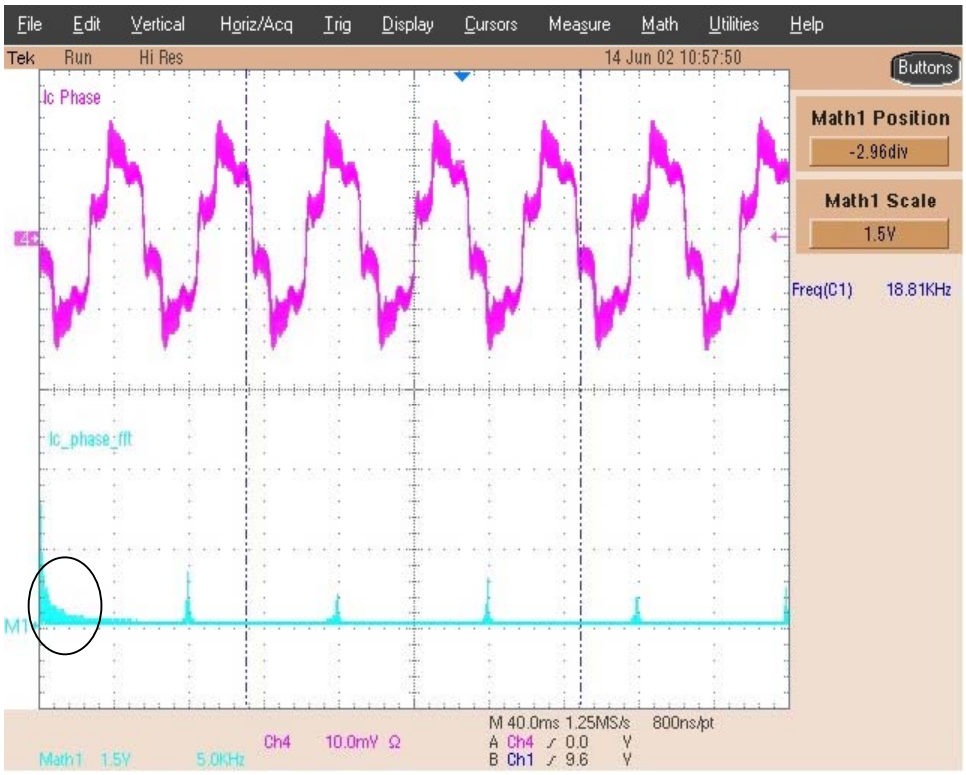

Figure 43 Current FFT for 60.5 in-lb, 2000 RPM, and 10 kHz Switching

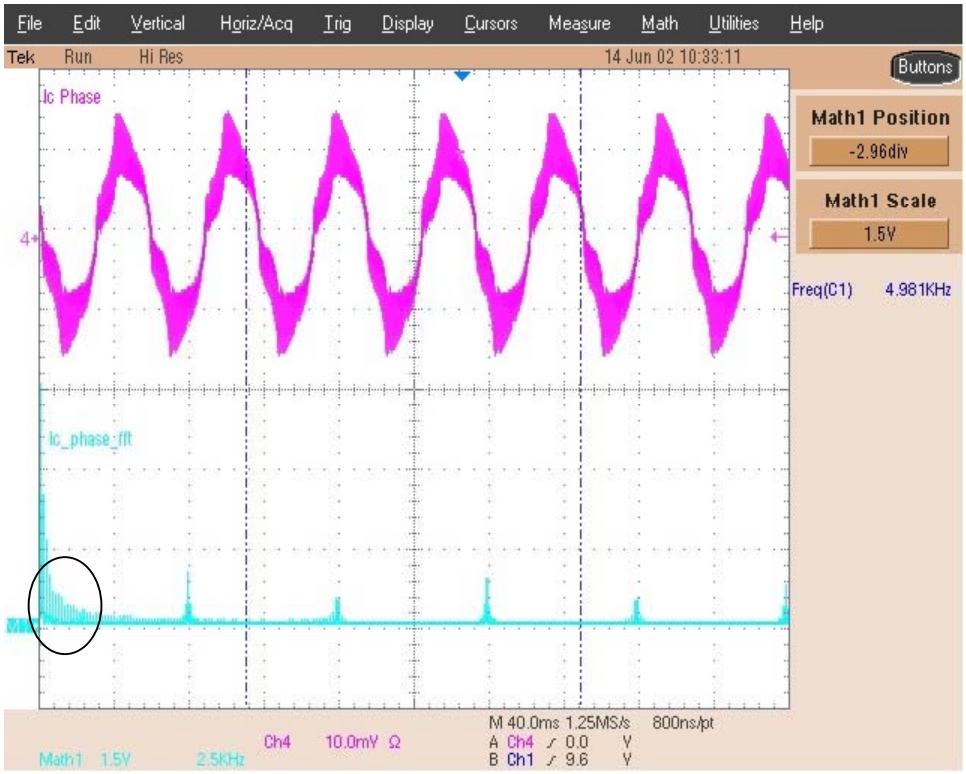

Figure 44 Current FFT for 60.5 in-lb, 2000 RPM, and 5 kHz Switching

For the 120.3 in-lb load, the voltage frequency spectrums are given in Figure 45 and Figure 46. As expected, the harmonic content decreases with the lower switching frequency at 5 kHz. The difference is still very similar to the data from the 1000 RPM test. Once again the current frequency spectrum should be examined to determine any benefits.

The current frequency spectrum scope captures are given in Figure 47 and Figure 48. As with the data from the 1000 RPM testing the fundamental frequency sidebands are worse at 5 kHz. Comparing the content from the 1000 RPM data, the side bands are worse for the 2000 RPM data. Once again the improvement in the voltage harmonics for lower switching frequency offsets the increase in current harmonics at the lower switching frequency.

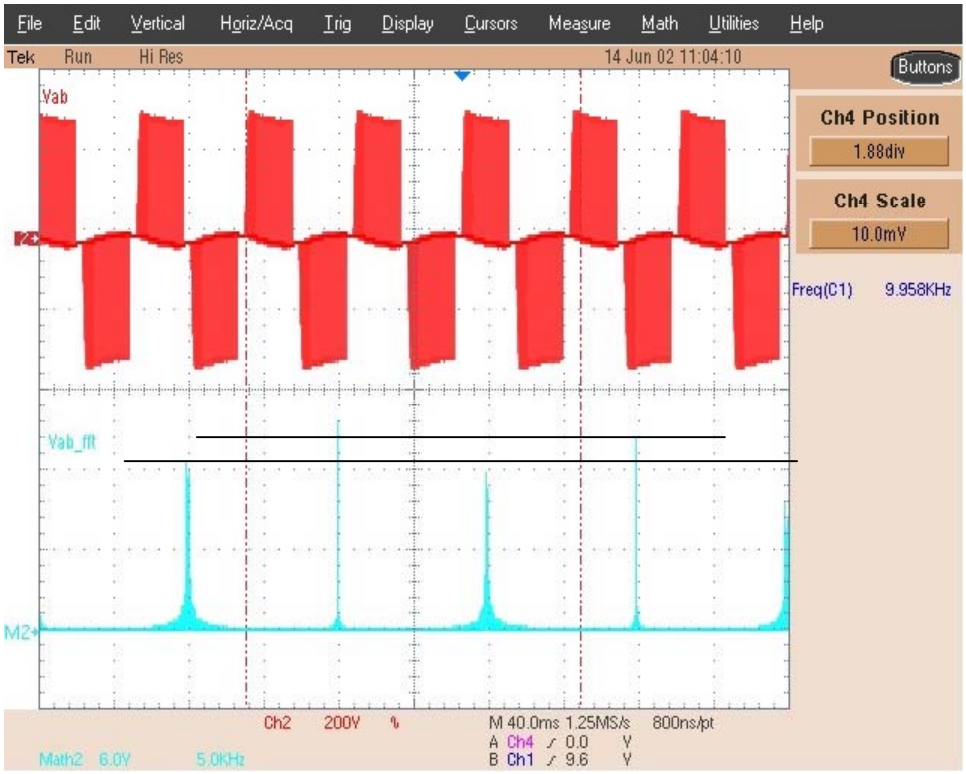

Figure 45 Voltage FFT for 120.3 in-lb, 2000 RPM, and 10 kHz Switching

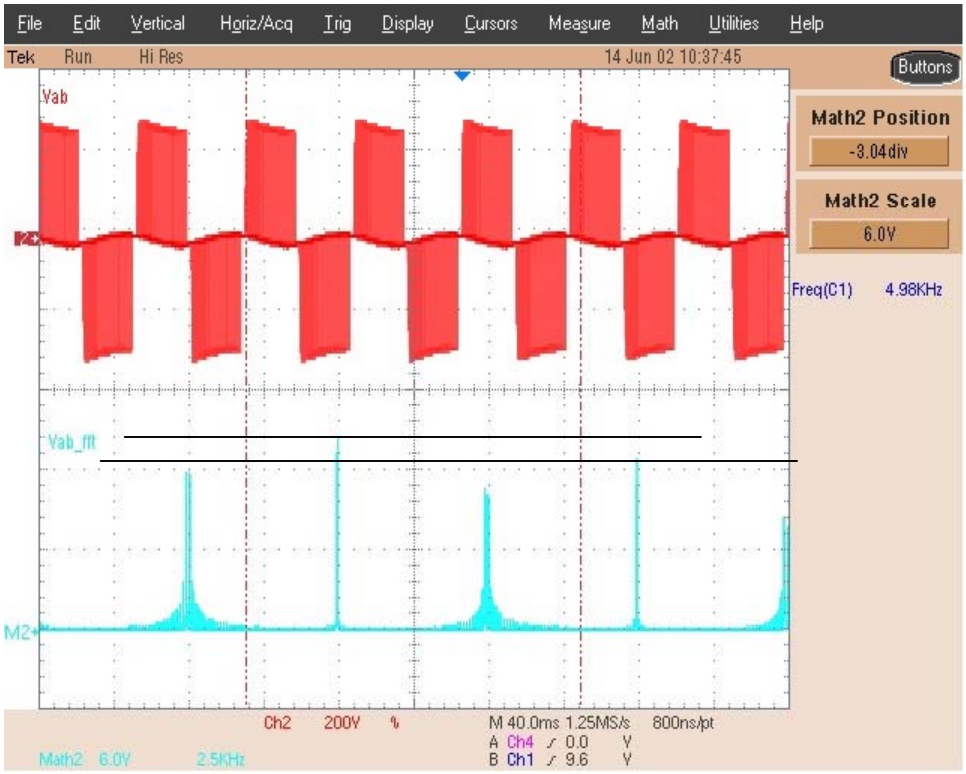

Figure 46 Voltage FFT for 120.3 in-lb, 2000 RPM, and 5 kHz Switching

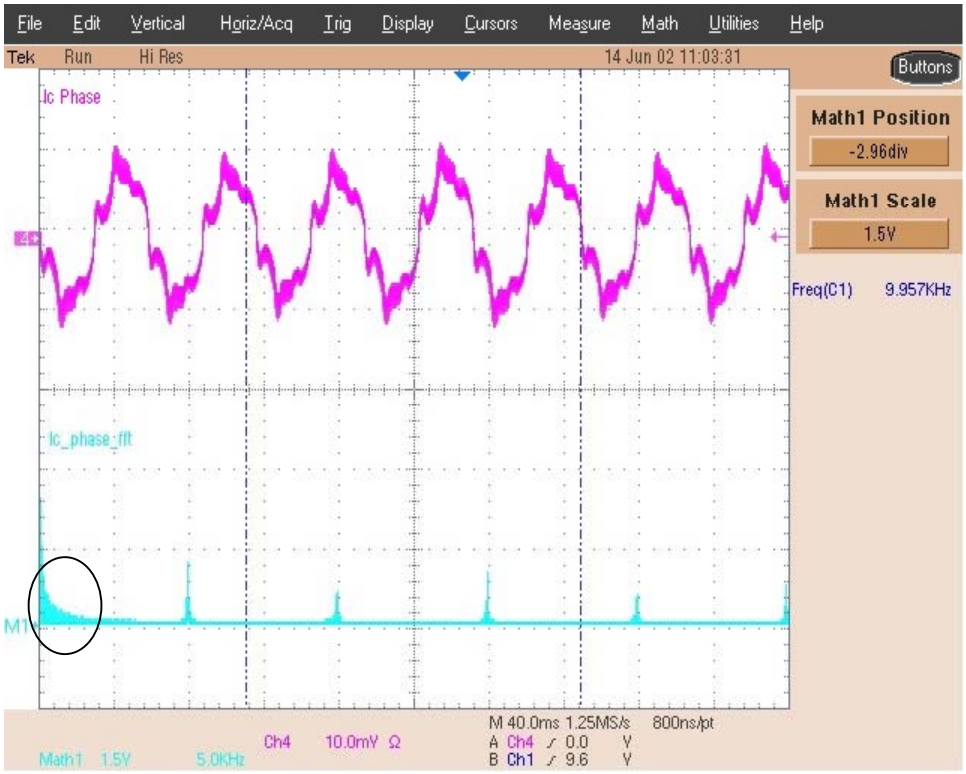

Figure 47 Current FFT for 120.3 in-lb, 2000 RPM, and 10 kHz Switching

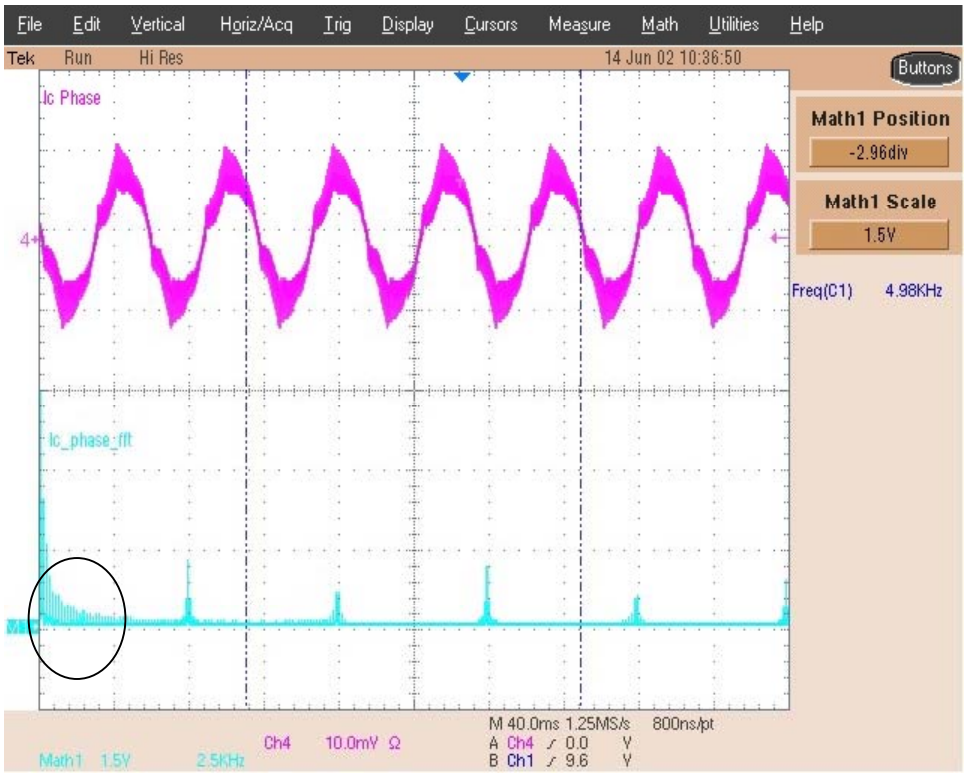

Figure 48 Current FFT for 120.3 in-lb, 2000 RPM, and 5 kHz Switching

Finally, the data for the heaviest load, 180 in-lb., is presented. The voltage frequency spectrums are given in Figure 49 and Figure 50. Examining the data once again shows the same pattern as before. The difference in harmonic content is less noticeable than in the previous experiments at 1000 RPM.

The current frequency spectra are given in Figure 51 and Figure 52. Compared to the data in the 1000 RPM case, the side bands of the fundamental have increased. The improvement in voltage harmonics still offsets the current harmonic increase.

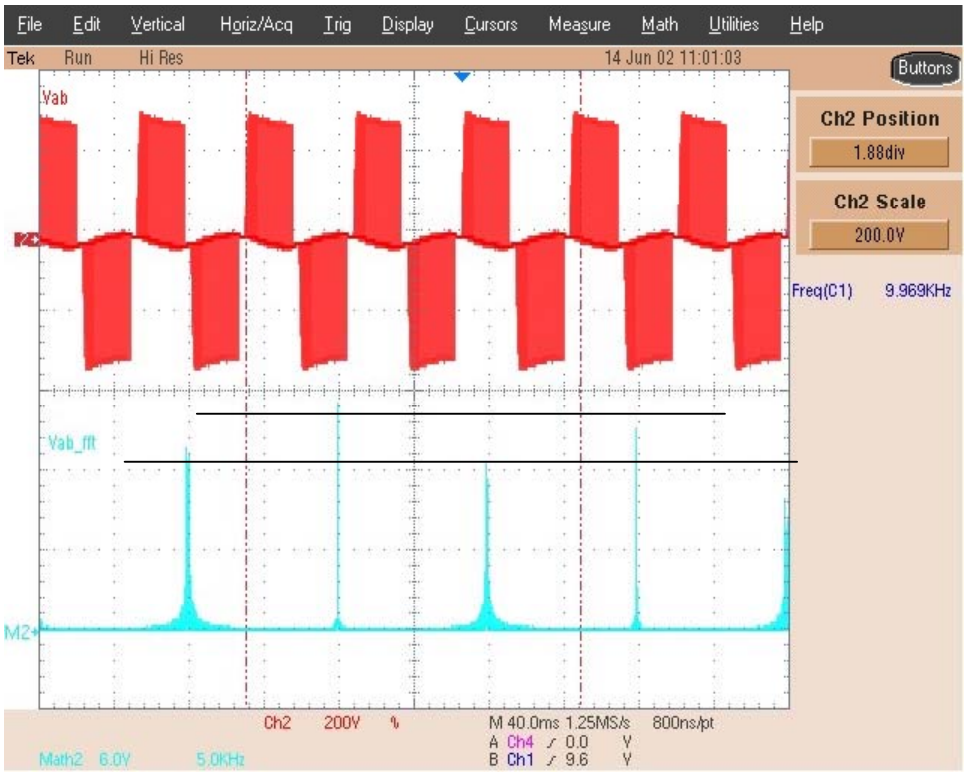

Figure 49 Voltage FFT for 180.0 in-lb, 2000 RPM, and 10 kHz Switching

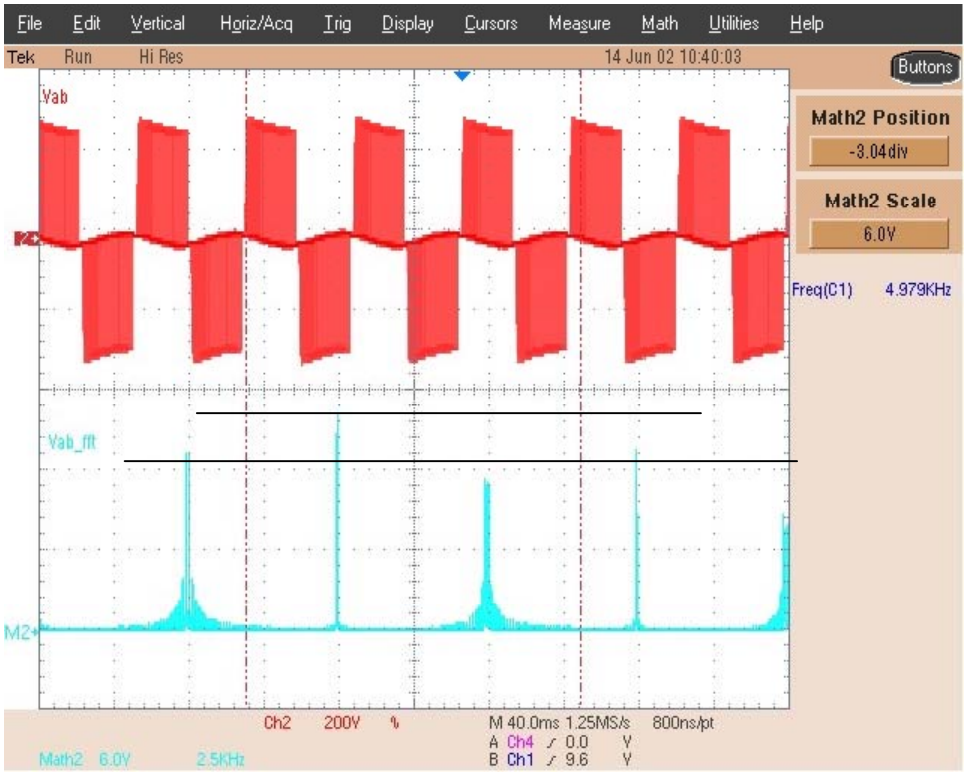

Figure 50 Voltage FFT for 180.0 in-lb, 2000 RPM, and 5 kHz Switching

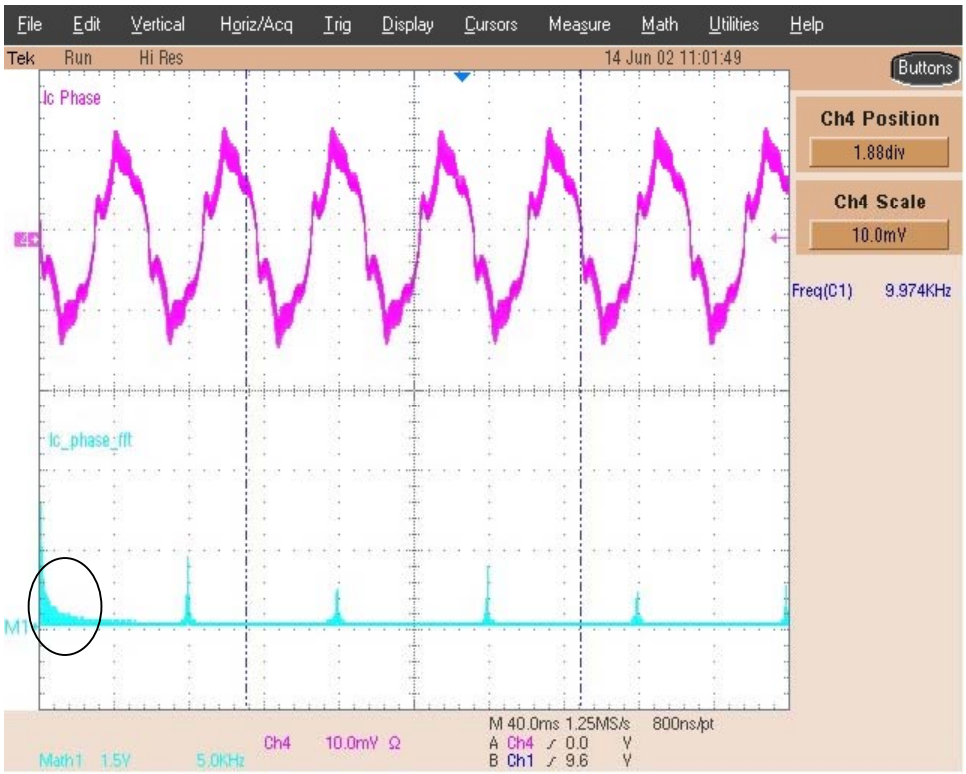

Figure 51 Current FFT for 180.0 in-lb, 2000 RPM, and 10 kHz Switching

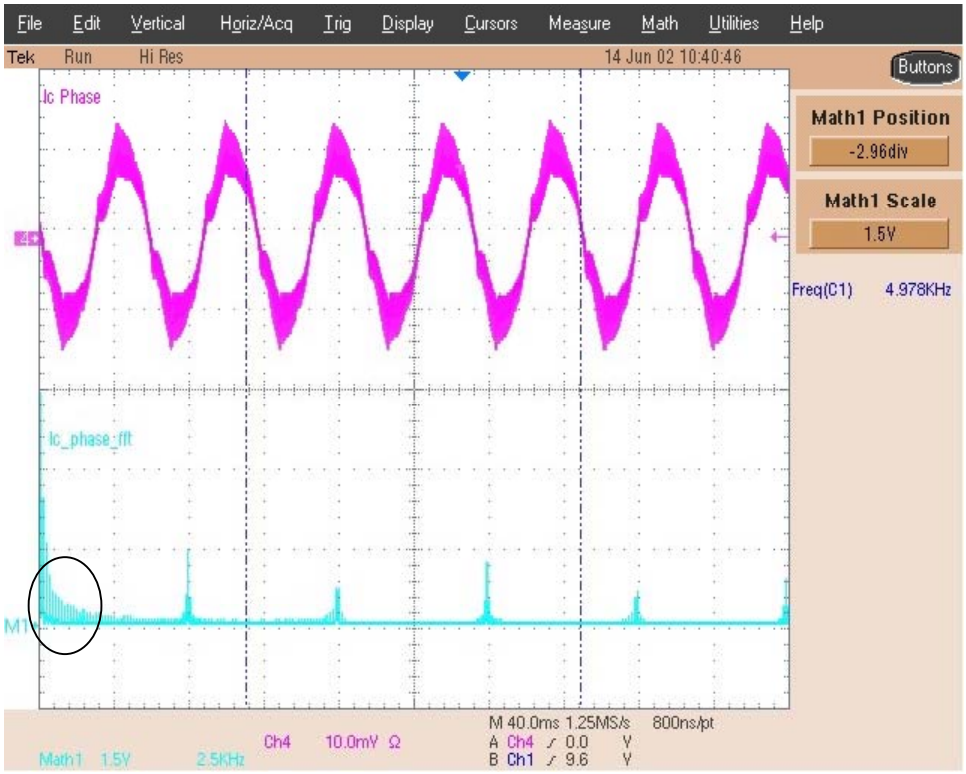

Figure 52 Current FFT for 180.0 in-lb, 2000 RPM, and 5 kHz Switching

The final plot is once again the power factor, Figure 53. The graph again shows an increase in power factor as the switching frequency is lowered with the exception of the lightest load. The trace for the light load shows that it does not increase much at all with switching frequency. This also supports the previous findings for the efficiency, power loss, and temperature. The slopes for the remaining loads also show that the slope of each is not as steep as in the previous 1000 RPM and 2000 RPM sections.

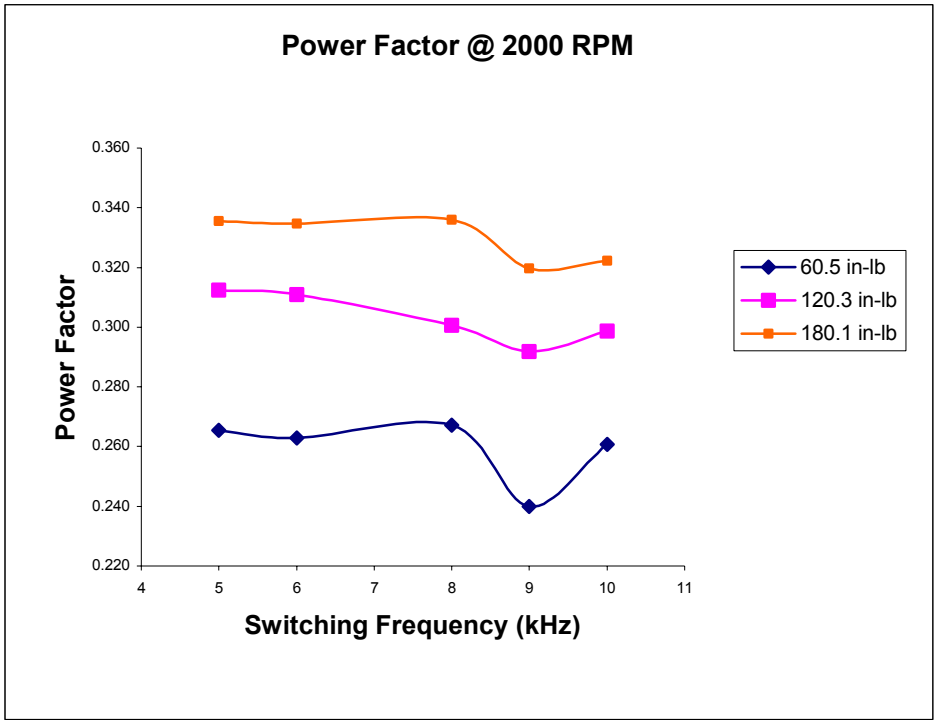

Figure 53 Power Factor at 2000 RPM

3.5.3. 3000 RPM Operation

The third and final tests were run at 3000 RPM again with the same conditions as before. Figure 54 below shows the overall efficiency of the system. Examining this data shows that the improvements are no longer apparent. For this case all three load conditions have a decrease in efficiency as the switching frequency is lowered. The slopes of trend lines once again increase with the load increase, but for this case the load is never high enough.

Therefore, a new trend becomes apparent. As the speed increases the benefit of lowering the switching frequency does not appear at the same loads. It appears that to see the benefit at higher speeds the load must be increased even more. As previously stated this was not possible in this work because of the test setup, but will be included in the future work.

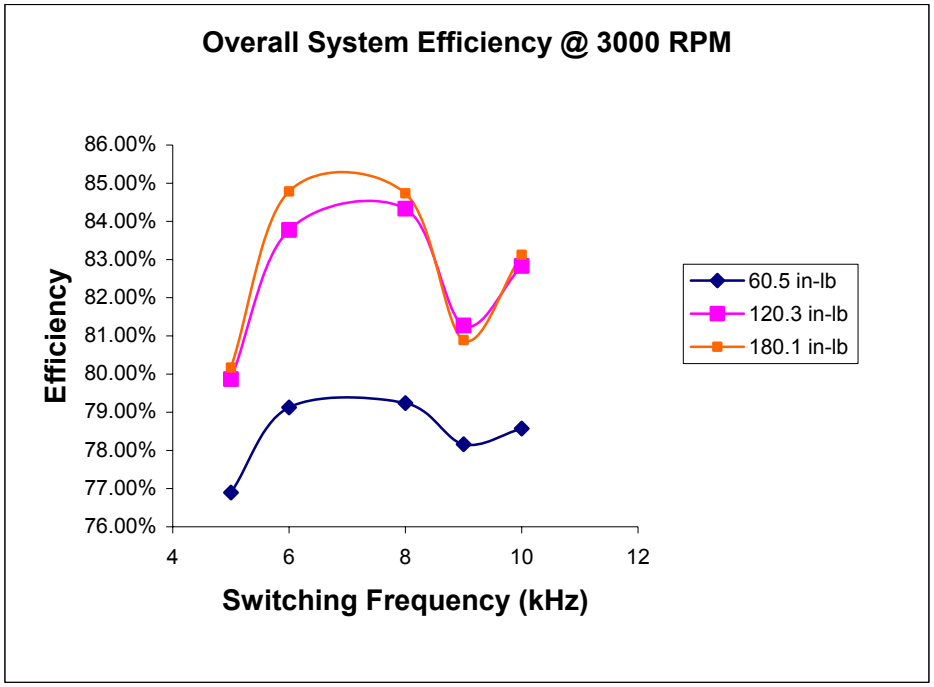

Figure 54 Overall System Efficiency at 3000 RPM

The temperature measurements of both the inverter and induction motor again show a much more stable result. Figure 55 and Figure 56 show the steady state temperatures of both the inverter and motor respectively. The difference when compared to the previous two tests show that the inverter temperature does not noticeably change. The inverter temperature essentially stays constant throughout the range of switching frequency. Compared to before the inverter temperature decreased substantially in the same range.

The motor temperatures are still similar to in the previous sections. They increase at about the same rate as before. Therefore, with all three loads, the overall system heat would increase. This same trend can also be seen in the power loss plots below.

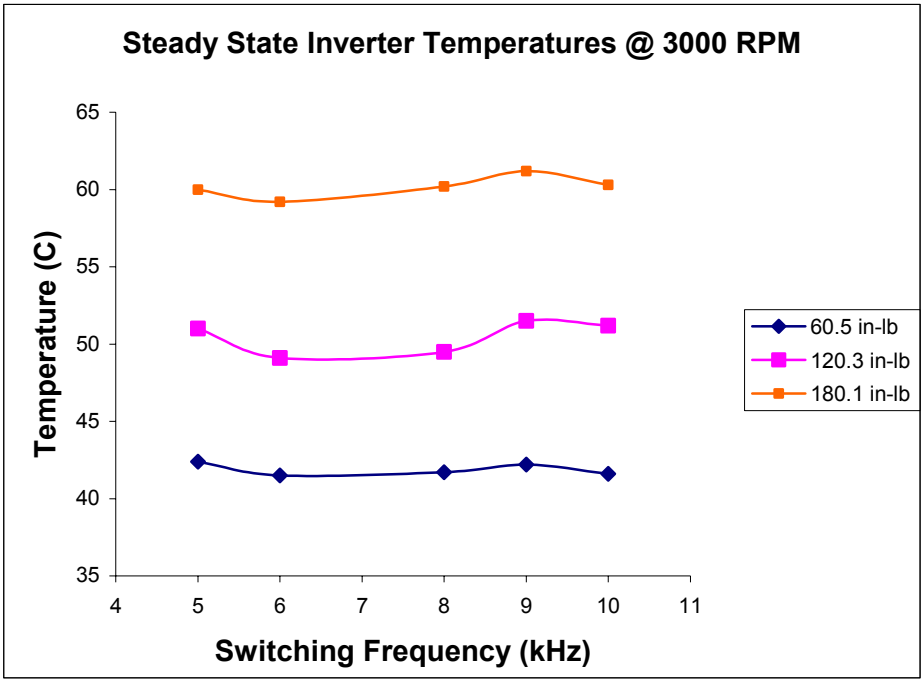

Figure 55 Steady State Inverter Temperatures for 3000 RPM

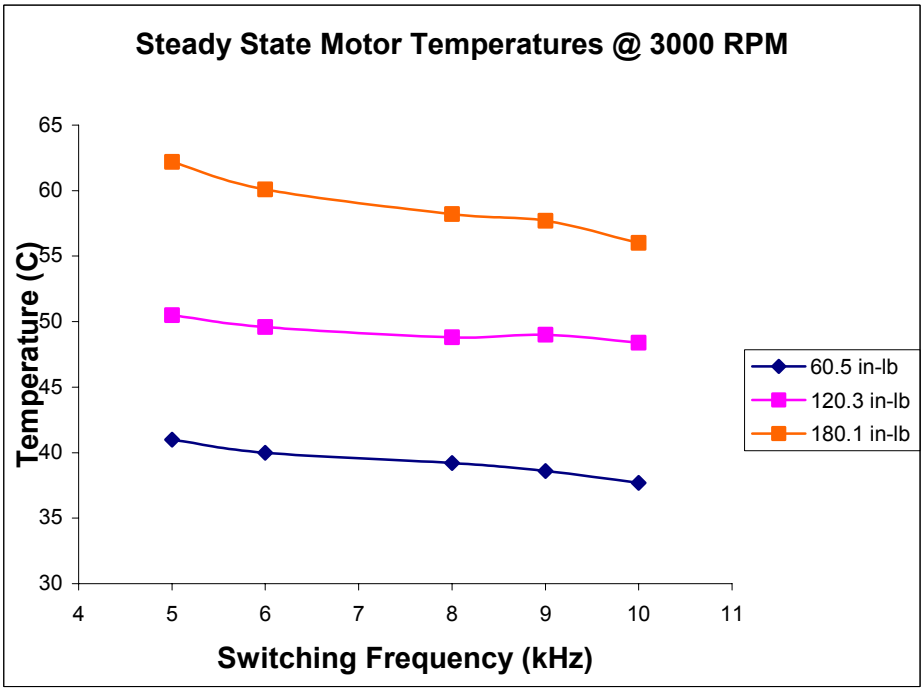

Figure 56 Steady State Motor Temperatures for 3000 RPM

The power loss plots for both the motor and inverter are shown in Figure 57 and Figure 58.

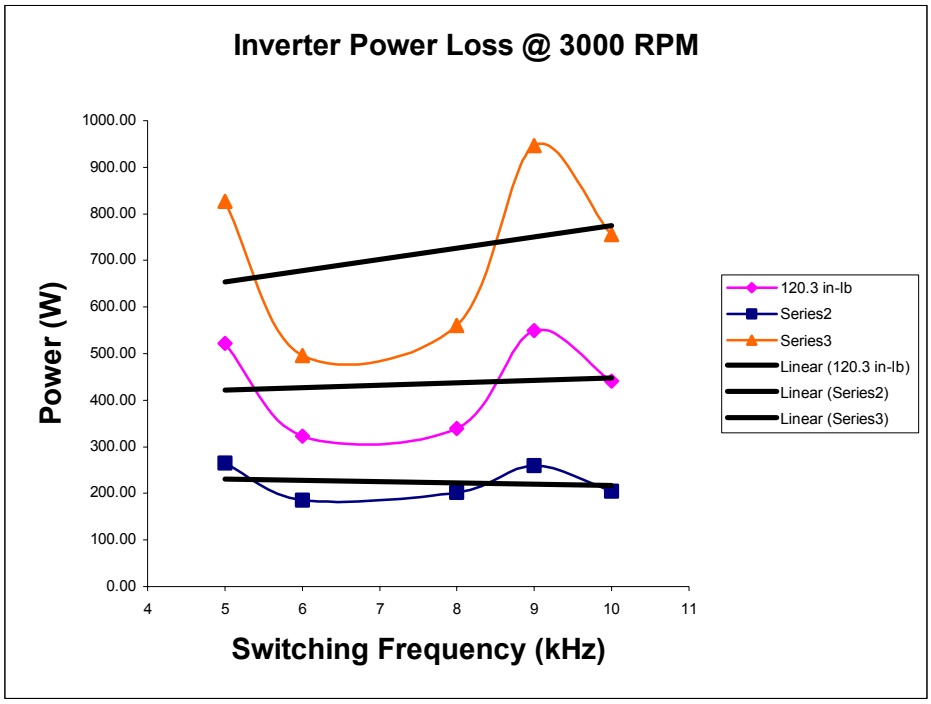

Figure 57 Inverter Power Losses for 3000 RPM

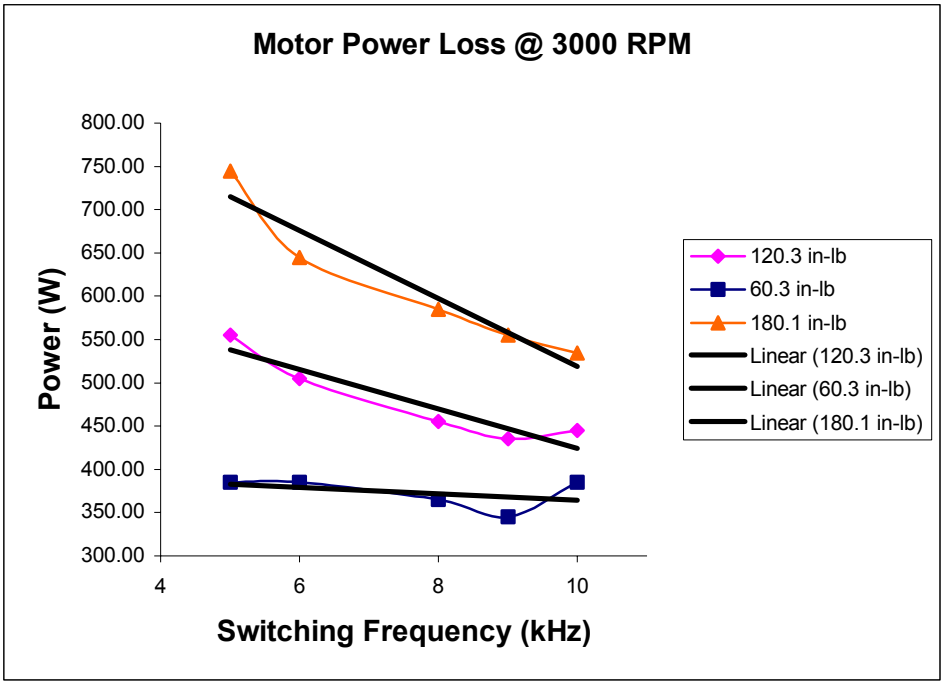

Figure 58 Motor Power Losses for 3000 RPM

3.5.3.1.Harmonic Content

Once again, the harmonic content of both the voltage and current are examined. Figure 59 and Figure 60 show the voltage frequency spectrum 3000 RPM operation. Compared to the previous data the results are very similar. The harmonics decrease with the lower switching frequency. Similar to the 2000 RPM data at the lightest load the current must be examined.

Figure 61 and Figure 62 below show the current frequency spectrum at 5 kHz and 10 kHz. As before the fundamental sidebands increase at the lower switching frequency. Compared to the previous data at 1000 RPM and 2000 RPM, the sidebands have increased slightly. This will explain the decrease in efficiency once again.

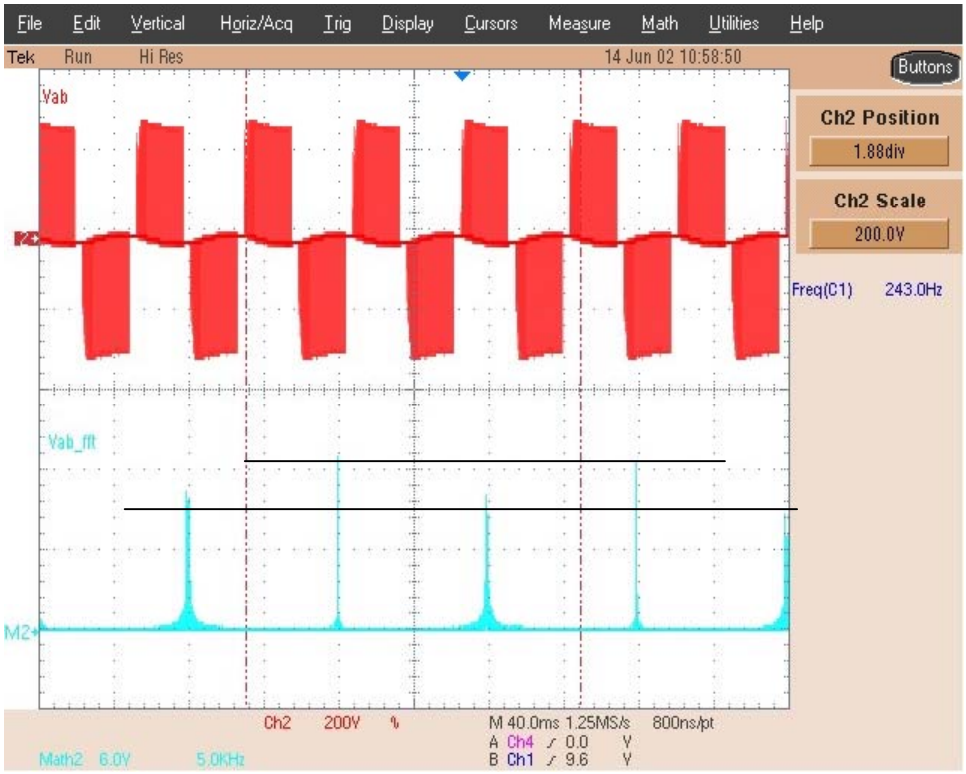

Figure 59 Voltage FFT for 60.5 in-lb, 3000 RPM, and 10 kHz Switching

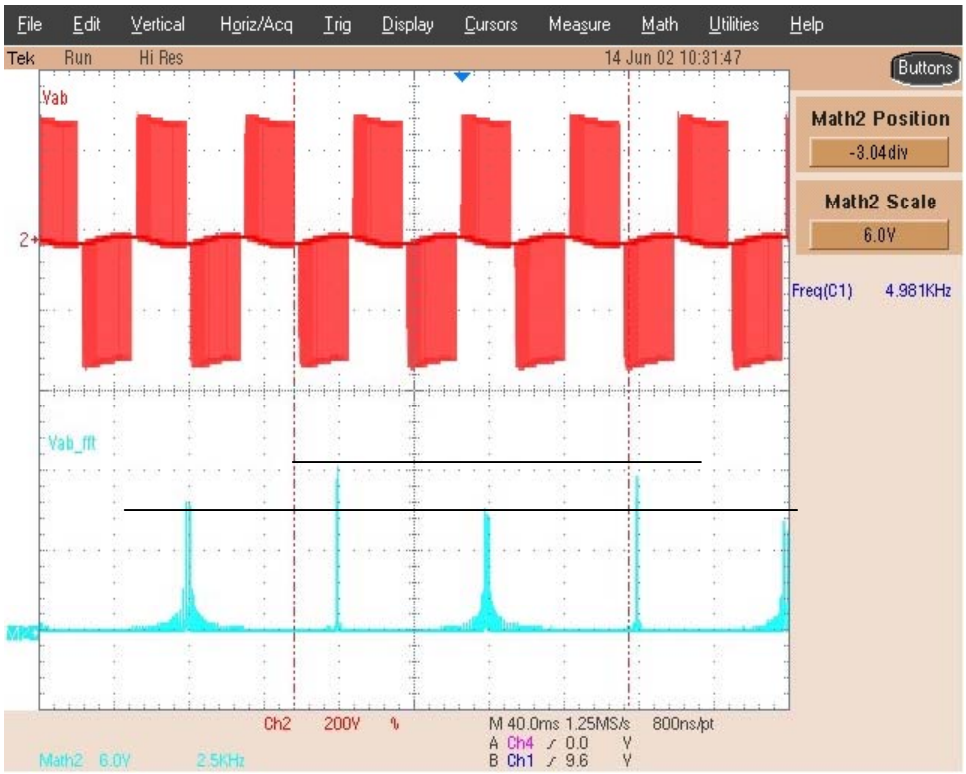

Figure 60 Voltage FFT for 60.5 in-lb, 3000 RPM, and 5 kHz Switching

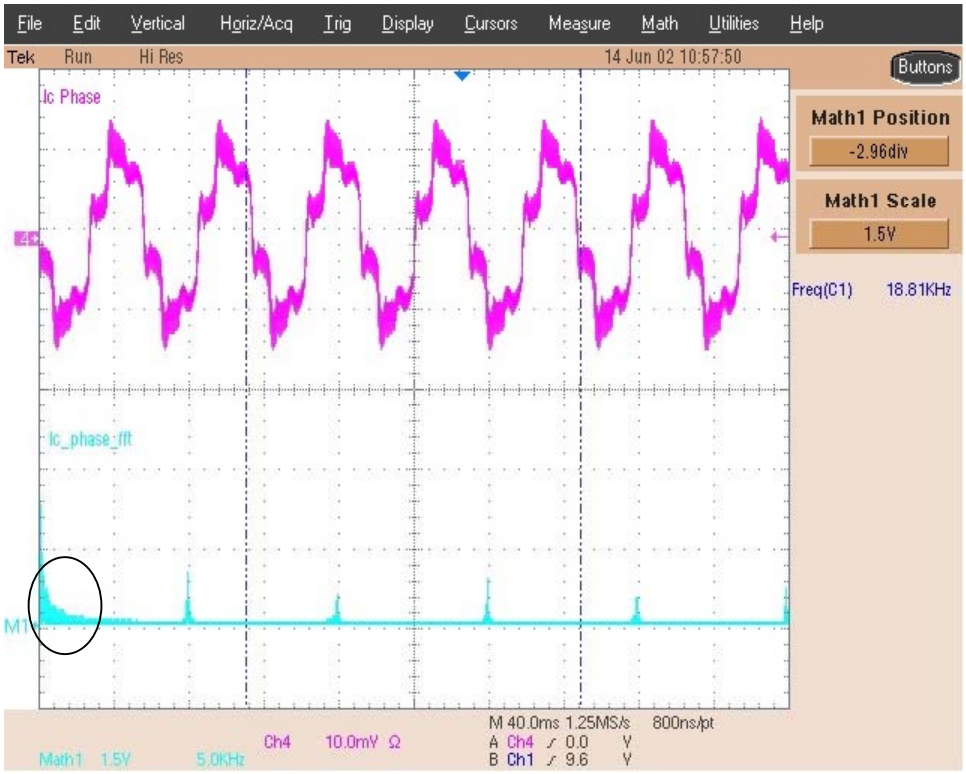

Figure 61 Current FFT for 60.5 in-lb, 3000 RPM, and 10 kHz Switching

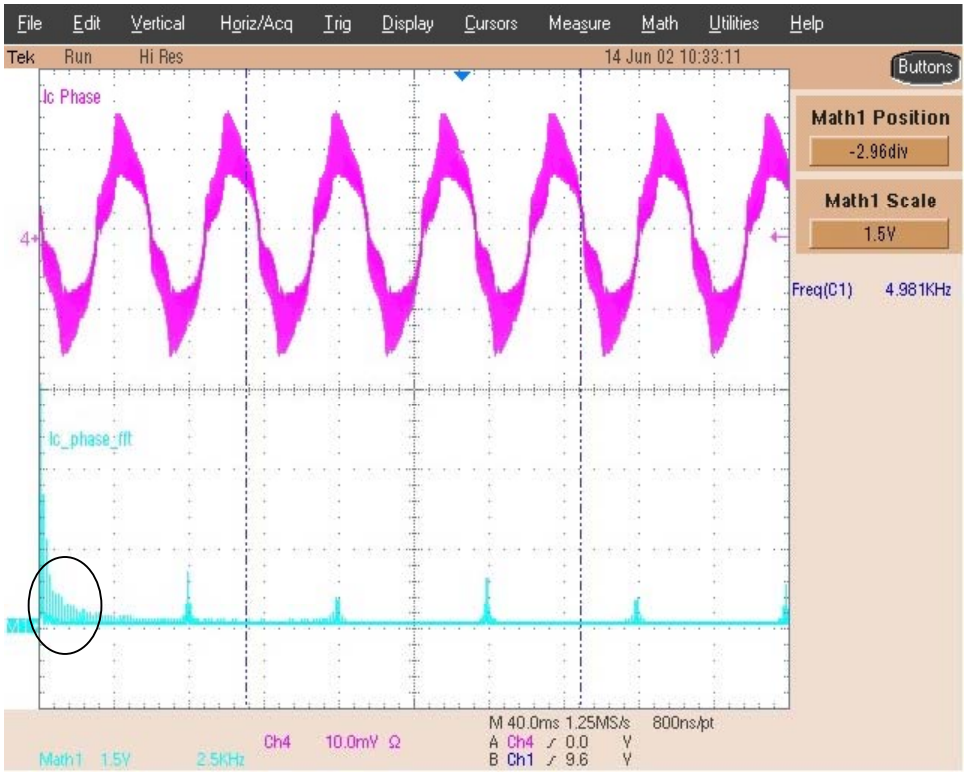

Figure 62 Current FFT for 60.5 in-lb, 3000 RPM, and 5 kHz Switching

Figure 63 and Figure 64 below show the voltage content at 120 in-lb. Following the same trend as before, the harmonics decrease at the lower switching frequency, and also have the approximate same difference as the previous data. Therefore the current spectrums must be examined because in this case the efficiency has decreased where as before it increased.

The current spectrums are given in Figure 65 and Figure 66. The same trend can be seen as in the 1000 RPM and 2000 RPM cases. The fundamental sidebands increase with the decreased switching frequency.

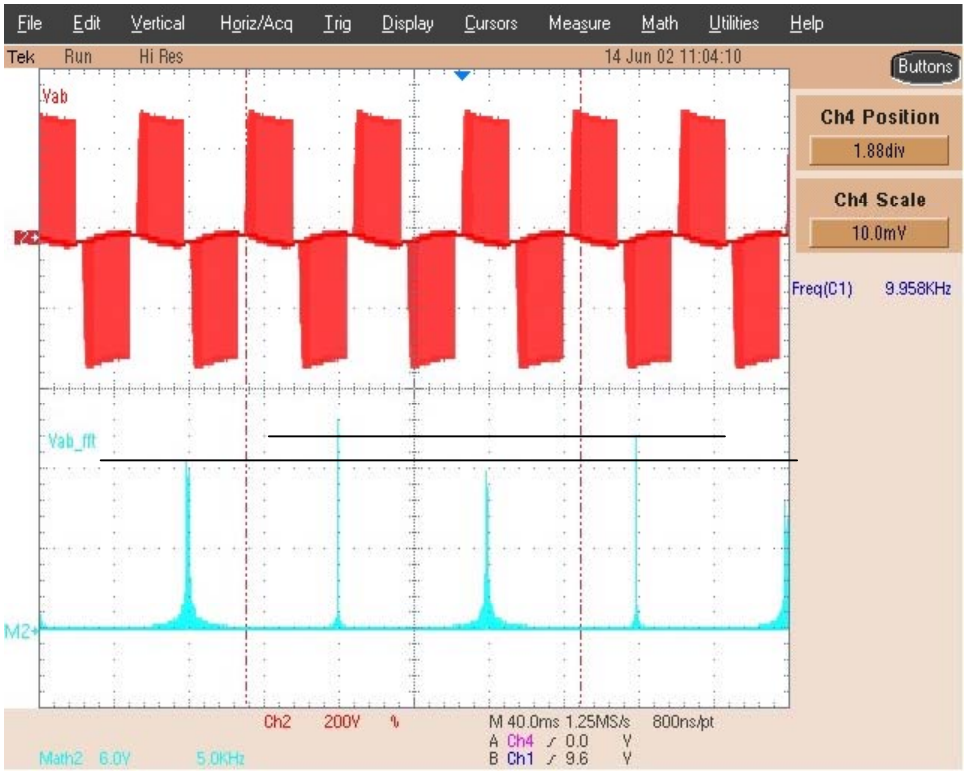

Figure 63 Voltage FFT for 120.3 in-lb, 3000 RPM, and 10 kHz Switching

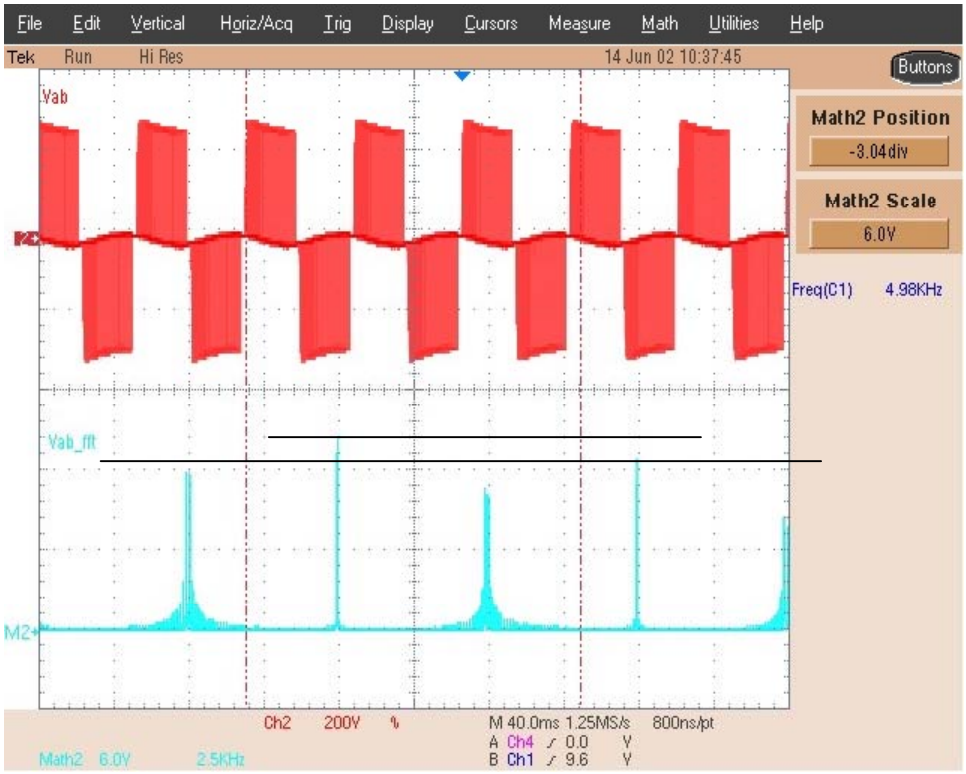

Figure 64 Voltage FFT for 120.3 in-lb, 3000 RPM, and 5 kHz Switching

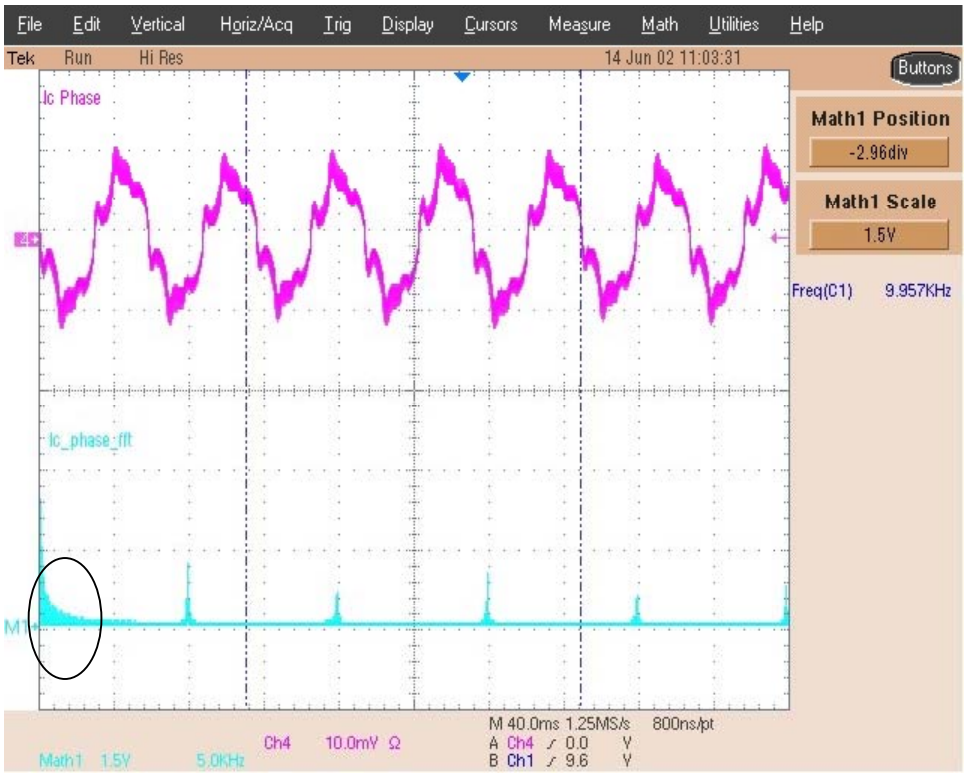

Figure 65 Current FFT for 120.3 in-lb, 3000 RPM, and 10 kHz Switching

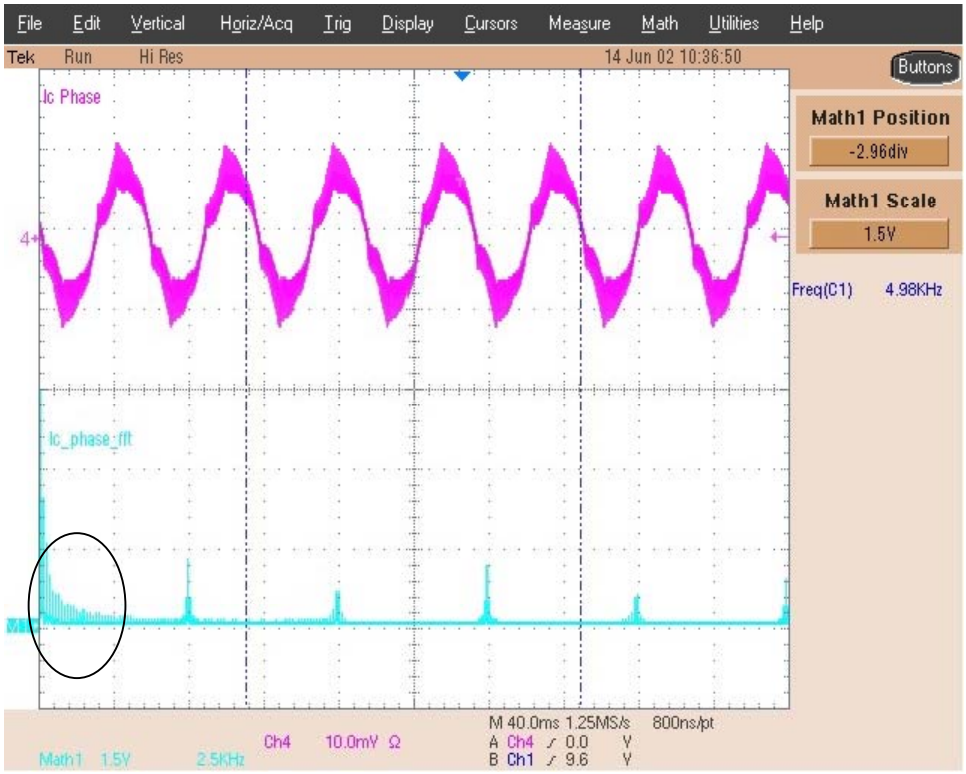

Figure 66 Current FFT for 120.3 in-lb, 3000 RPM, and 5 kHz Switching

The final frequency spectrums are for the 180 in.-lb. load, Figure 67 and Figure 68. As before, the harmonics at 5 kHz are still lower, but in this case the efficiency is worse. The difference is still the same as in the other cases. The current frequency data, Figure 69 and Figure 70, show similar results as previously seen. The sidebands are worse at the lower switching frequency, and are also slightly worse than at the lower speeds.

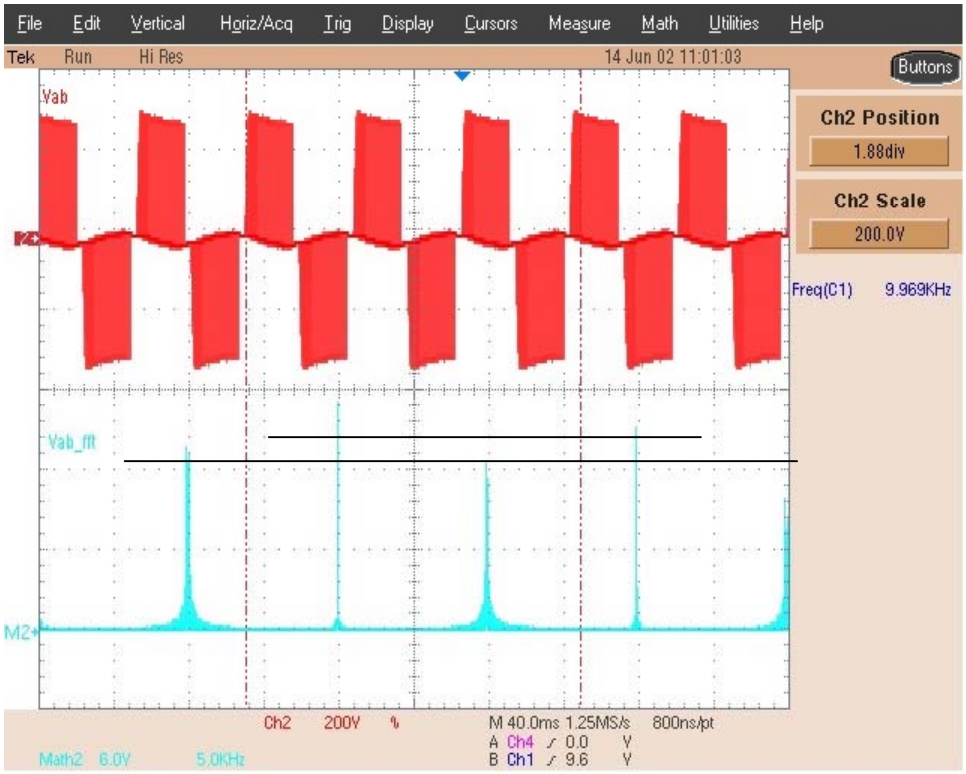

Figure 67 Voltage FFT for 180.0 in-lb, 3000 RPM, and 10 kHz Switching

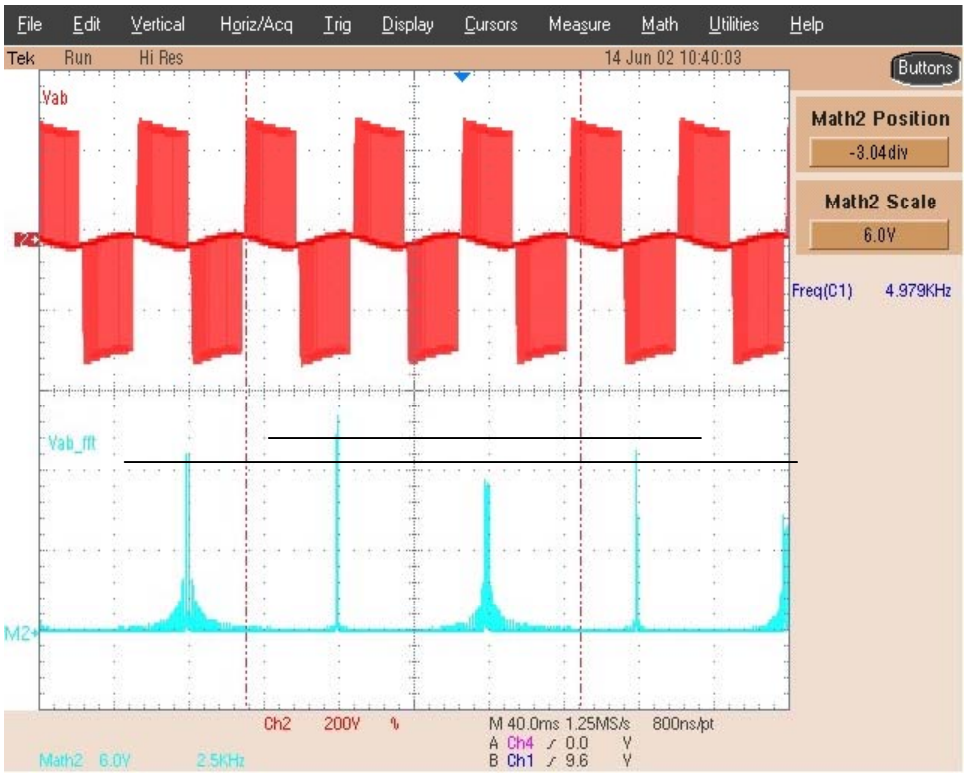

Figure 68 Voltage FFT for 180.0 in-lb, 3000 RPM, and 5 kHz Switching

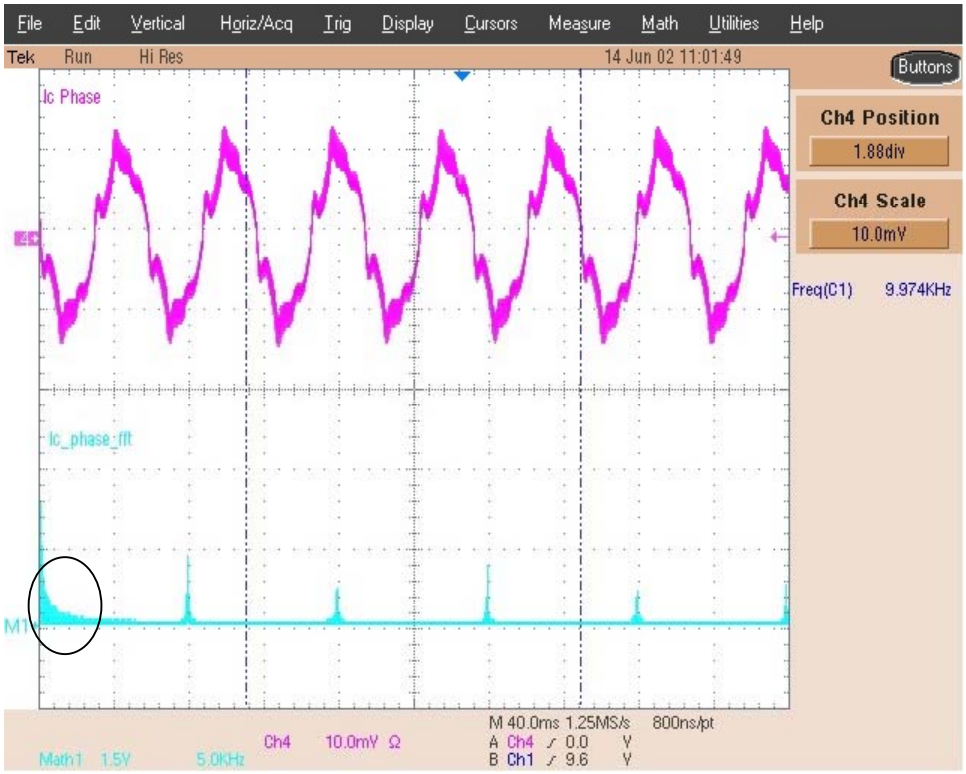

Figure 69 Current FFT for 180.0 in-lb, 3000 RPM, and 10 kHz Switching

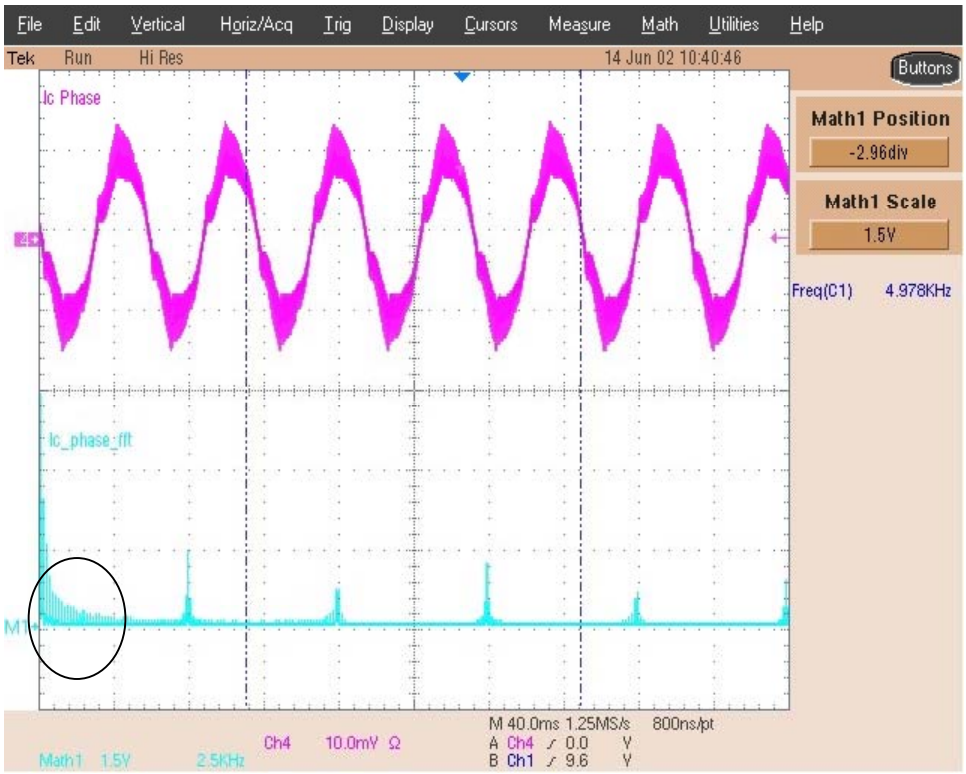

Figure 70 Current FFT for 180.0 in-lb, 3000 RPM, and 5 kHz Switching

The final plot is again that of the power factor. For this data at 3000 RPM the power factors all decrease with the switching frequency. This can be attributed to the increased harmonic content of the current.

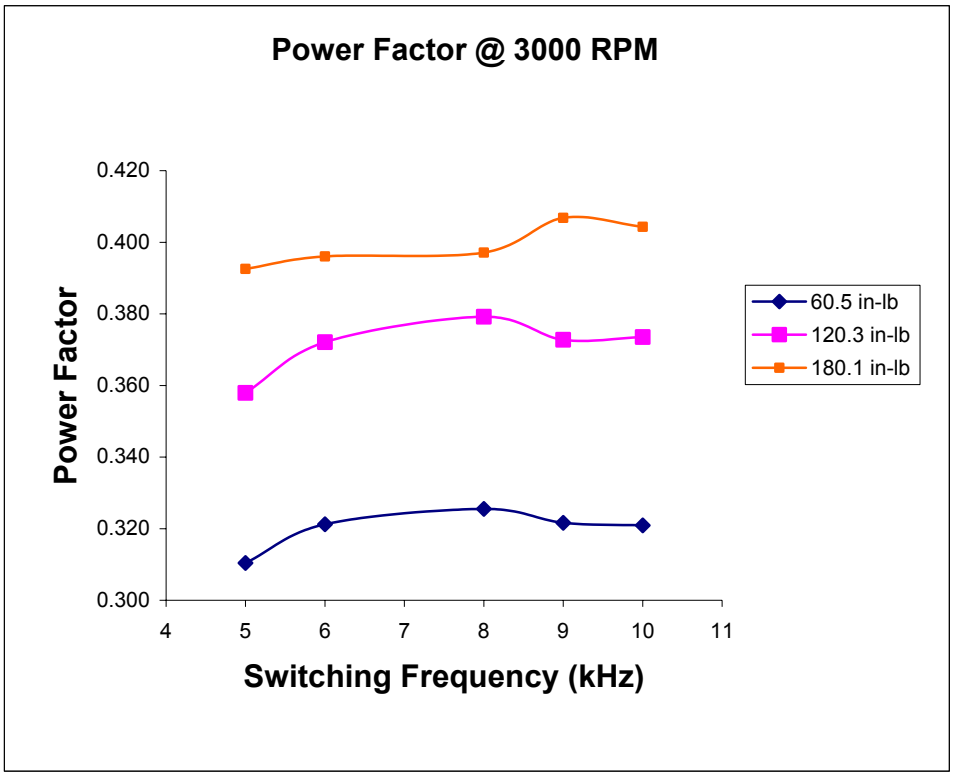

Figure 71 Power Factor at 3000 RPM

4. Analytical and Experimental Comparison

Comparing the analytical results to the experimental results show some agreement and differences. Figure 72 below, shows the efficiency at 1000 RPM for the experimental and analytical trends. The legend is: **ηsys1(fs)** and **η1_ex** are the trend lines for 60 in-lb load, **ηsys2(fs)** and **η2_ex** are the trend lines for 120 in-lb load, and **ηsys3(fs)** and **η3_ex** are the trend lines for 180 in-lb load. The same applies to all three graphs below.

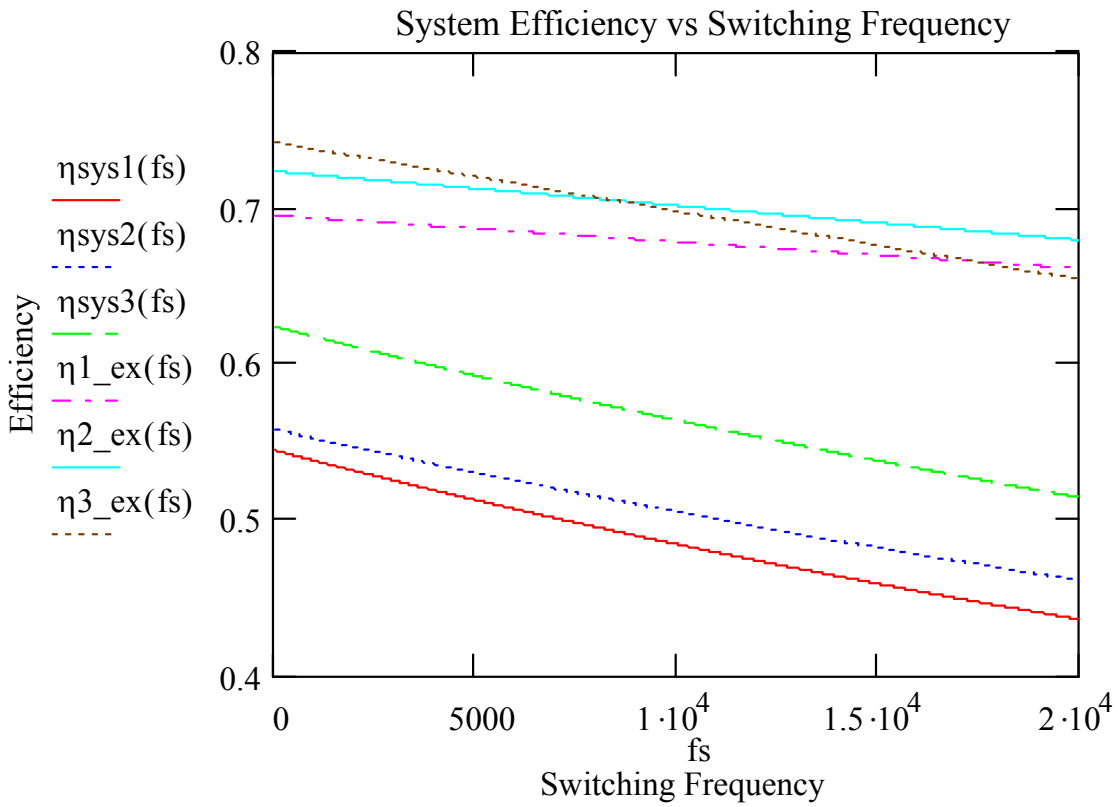

Figure 72 Comparisons of Analytical and Experimental Efficiency Trends, 1000 RPM

Examining the graph shows that the trend for both the analytical and experimental are similar. The major difference is in efficiency value. The magnitude of the experimental

is noticeable higher than the model results. This can be attributed to the inverter modeling. Although the motor model does not take the harmonic losses into account, and would affect the system efficiency, the inverter model is much more intricate, and therefore lends itself to slight changes in model parameters.

Figure 73 below, shows the same results as before except for 2000 RPM. The comparison here shows some of the same trends as 1000 RPM, but now the experimental starts to show the decrease of efficiency with switching frequency. As stated before, the motor model does not account for harmonic losses in this work. For this case, at the lightest load, where the modulation index is extremely low, the motor losses are going to increase with the decreased switching frequency, and offset the benefit produced by improved efficiency from the inverter.

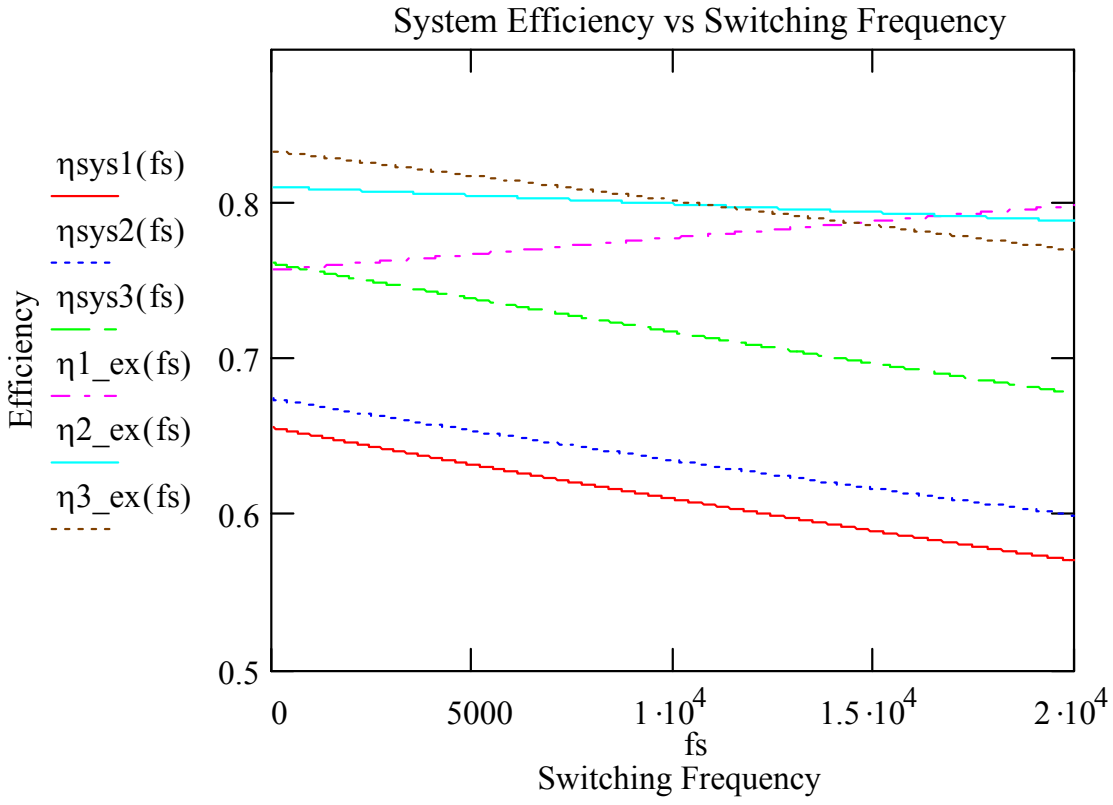

Figure 73 Comparisons of Analytical and Experimental Efficiency Trends, 2000 RPM

The remaining graph for the 3000 RPM case, Figure 74, again shows the overall system efficiency versus switching frequency. Here the experimental efficiency trends are all negative for the reduced switching frequency. For all cases, analytical and experimental, the efficiency can be seen to improve as the load is increased. The rate of change for the improvement in efficiency with lowered switching frequency is also seen to decrease as the speed is increased for both analytical and experimental. For the 3000 RPM case below, the experimental results call for increased switching frequency for all three loads, but as stated before the benefit is reduced as the load is increased.

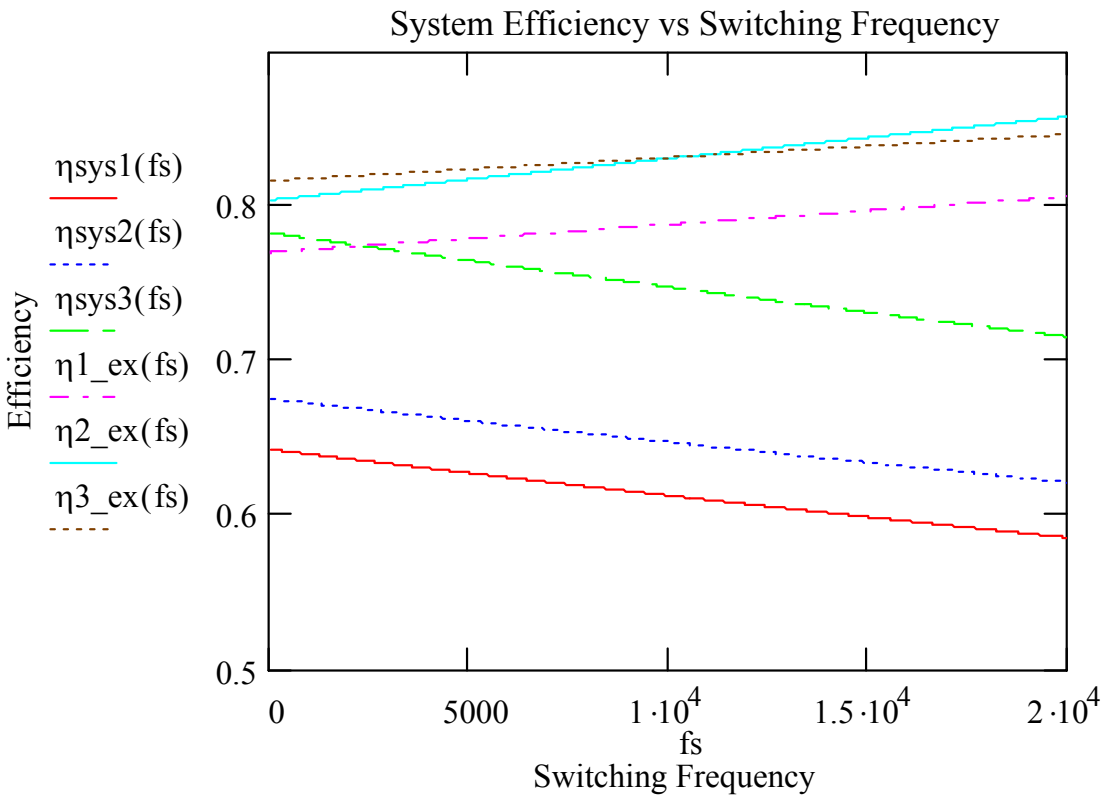

Figure 74 Comparisons of Analytical and Experimental Efficiency Trends, 3000 RPM

5. Conclusion

This work took the analytical model of a traction motor drive and in MathCAD simulated it at the various test conditions. The model was made up of separate inverter and induction motor models. The overall model was used to predict the efficiency trend as the switching frequency is varied.

The same conditions were then tested and the trends shown in the analytical model were verified through experimentation with some differences. The analytical model showed an improvement in efficiency for all test conditions. The experimental section, on the other hand, shows that for higher speeds the trend is for decreased system efficiency at lower switching frequencies. The list below gives the major findings of this work:

- Lowering the switching frequency increases the system efficiency at certain load and speed combinations.
- As the load increases the benefit of lowering the switching frequency also increases.
- As the speed is increased, the benefit of lowering the switching frequency appears to decrease, but increasing the load, as stated before, improves the efficiency

These findings are somewhat anticipated with the improved harmonic distortion with lowering the switching frequency. While the current harmonic distortion increases with the lowered switching frequency, the voltage harmonic distortion decreases at a higher rate. Therefore, conceptually lower switching frequency should generate better efficiency.

Examining the number of switchings per line cycle, the decrease in improvement that occurs at higher speeds is explained counting the number of switchings per line cycle. As the speed increases and the switching frequency stays the same, the number of switchings reduces. With the decreased number of switchings at higher line frequency or speed, the improvement seen in the switching loss is therefore decreased.

Power factor plays a large indirect role in the efficiency of the system. With the lower speeds and loads along with the high DC bus voltage, the modulation index is very low because the motor voltage needed to generate the test load torque is substantially lower than the DC bus voltage. The low modulation index on the whole creates more distortion in the voltage and current. This distortion, along with the switching frequency distortion, is then reflected in the efficiency numbers through the system's total harmonic distortion (THD). The distortion factors of voltage and current, which are functions of THD, are then incorporated into the power factor component. Therefore, for the results presented here, the power factor can be seen to have a large effect on system efficiency.

The data in this work shows that there is the possibility of picking up a couple of efficiency points under certain conditions i.e. switching frequency, speed, and load. With further research, a map of the optimum efficiency conditions throughout the speed and load range could be incorporated into the drive control system to produce these benefits at all possible operating conditions.

5.1. Future Work

The research presented in this thesis is very promising, but there are several areas where the work can be improved and expanded on. While the analytical model used in this work gives an approximate efficiency trend; the motor model portion should be improved to include the harmonic losses introduced with SVM. A better understanding of stray load losses could also improve the analytical results. The inverter model can be expanded to include additional miscellaneous losses.

To expand the results to include higher loading and higher speeds, some improvements in the experimental setup need to occur: thermal and instrumentation/control. Improving these areas will allow for higher load testing verifying the findings that the efficiency improvement increases as the load is increased.

Improving the cooling capacity of both the motor and inverter would benefit greatly. The design called for oil cooling of both the inverter and motor, but for this test both were cooled with forced convection. To improve the thermal capability, the inverter

could be cooled with a larger fan and heat sink or move altogether to water-cooling. The motor, on the other hand, would need some sort of oil cooling setup.

While improving the cooling would increase the load handling of the system, this would also present another problem. The power supply capability would have to be increased. The supply for this work was limited to 100A at 500V. To increase the load and speed the DSP and control would also need upgraded. A more powerful DSP along with better programming should also be used. The code could be written to include closed loop control to better maintain the test load, and include more precision to allow for better modulation index adjustment.

6. References

[1] Department of Energy, "International Energy Outlook", Washington DC, 2002

[2] H. Kouns, Analysis of Performance Characteristics of Electric Vehicle Traction in Low Speed/Low Torque Range", M.S. Thesis, Virginia Polytechnic Institute and State University, 2001

[3] S. Khomfoi, V. Kinnares, P. Viriya, "Influence of PWM Characteristics on the Core Losses due to Harmonic Voltages in PWM Fed Induction Motors", IEEE Power Engineering Society Winter Meeting, Vol. 1, pp. 365-369, 2000

[4] Jae-Young Choi, Marc A, Herwald, Dushan Boroyevich, Fred C. Lee, "Effect of Switching Frequency of Soft Switched Inverter on Electric Vehicle System", IEEE IECON 97, Vol. 2, pp. 658-663, 1997

[5] T. Nergaard, H. Kouns, J.S. Lai, C. Konrad, "Optimal System Efficiency Operation of An Induction Motor Drive", IEEE, 2002

[6] S. Clemente, "A Simple Tool for the Selection of IGBTs for Motor Drives and UPSs", IEEE APEC '95, Vol. 2, pp. 755-764, 1995

[7] J.S.Lai, R. W. Young, G.W. Ott, J.W. McKeever, "Efficiency Modeling and Evaluation of a Resonant Snubber Based Soft-Switching Inverter for Motor Drive Applications" 26th Annual IEEE PESC '95, Vol. 2, pp. 943-949, 1995

[8] Fernand G. De Buck, "Losses and Parasitic Torques in Electric Motors Subjected to PWM Waveforms", IEEE Transactions on Industrial Application, Vol. IA-15, No. 1, Jan/Feb. 1979, pp. 47-53

[9] F. De Buck, P. Gistelinck, and D. De Backer, "A Simple but Reliable Loss Model for Inverter-Supplied Induction Motors", IEEE Transactions on Industry Applications, Vol. IA-20, No. 1, Jan/Feb. 1984, pp. 190-202.

[10] B. K. Bose, "Modern Power Electronics and AC Drives", Pretence Hall, NJ, 2002

[11] Zhengming Zhao, M. Kendig, D. Rogovin, "Modeling, Simulation, ad Analysis of Stator Windings of Induction Machines in High Frequencies", IEEE IAS, Vol. 1, pp. 259-264, 1998

[12] G.C.D. Sousa, B.K. Bose, J. Cleland, R.J. Spiegel, P.J. Chappell, "Loss Modeling of Converter Induction Machine System for Variable Speed Drive", IEEE Power

Electronics and Motion Control, Vol. 1, pp. 114-120, 1992

[13] M. Sokola, V. Vuckovic, E. Levi, “Iron Losses In Current-Controlled PWM Inverter Fed Induction Machines”, MELECON ’96, Vol. 1, pp. 361-364, 1996

[14] S.M. Peeran, C.W.P. Cascadder, “Application, Design, and Specification of Harmonic Filters for Variable Frequency Drives”, IEEE Trans. Industry Applications, Vol. 31, July-Aug, pp. 841-847, 1995

Appendix I

1000RPM

f_s	Torque	N_r	V_{LL} Motor	I_{Line} Motor	P_{In} Motor	V_{dc}	I_{dc} meas R=0.25mOhm	Motor Temp	Inverter Temp
(kHz)	(inlb)	(RPM)	(rms Volts L-L)	(rms A/Phase)	(Watts)	(V)	(mV)	(C)	(C)
Electrical Speed =		**1037.00**							
Line Frequency =		**17.28**							
10	60.5	1006	66.20	41.90	880	296.40	0.90	36.7	41.7
9	60.5	1006	69.50	43.33	920	288.40	0.92	36.7	41.7
8	60.5	1006	69.90	41.71	890	331.30	0.79	36.5	41.9
6	60.5	1006	72.20	43.35	940	311.20	0.87	36.7	41.1
5	60.5	1006	67.50	41.29	910	315.70	0.85	36.6	40.4
		Avg V =	69.06		Avg V =	308.60			
Electrical Speed =		**1037.00**				0.32			
Line Frequency =		**17.28**							
10	120.3	992	74.90	61.73	1670	319.20	1.59	39.4	49.7
9	120.3	992	75.70	61.79	1710	304.80	1.65	40.7	48.8
8	120.3	992	73.50	61.04	1670	308.40	1.60	40.6	48
6	120.3	992	78.00	61.65	1740	321.00	1.54	42	47.1
5	120.3	992	71.20	60.66	1700	297.90	1.68	41.6	46.2
		Avg V =	74.66		Avg V =	310.26			
Electrical Speed =		**1037.00**				0.34			
Line Frequency =		**17.28**							
10	180	980	79.2	79.05	2480	322.2	2.32	43.6	57.2
9	180	980	79.4	79.87	2530	307.6	2.43	46.1	56.6
8	180	980	78.4	78.61	2500	312.8	2.34	46.3	56.1
6	180	980	77.3	79.9	2560	289.7	2.51	47.1	53.5
5	180	980	76	78.03	2520	304.4	2.39	47	52.6
		Avg V =	78.06		Avg V =	307.34			
						0.36			

I_{dc} meas R=0.25mOhm	Slip	Efficiency Inverter	P_{Loss} Inverter	P_{out} Motor	P_{Loss} Motor	Motor Efficiency	Motor Power Factor	Total Efficiency
(A)	(Hz)	(%)	(W)	(W)	(W)	(%)		(%)
3.60	0.52	82.5%	187.04	720.21	159.79	81.8%	0.183	67.50%
3.68	0.52	86.7%	141.31	720.21	199.79	78.3%	0.177	67.86%
3.16	0.52	85.0%	156.91	720.21	169.79	80.9%	0.176	68.79%
3.48	0.52	86.8%	142.98	720.21	219.79	76.6%	0.174	66.50%
3.40	0.52	84.8%	163.38	720.21	189.79	79.1%	0.189	67.10%
6.36	0.75	82.3%	360.11	1412.16	257.84	84.6%	0.209	69.56%
6.60	0.75	85.0%	301.68	1412.16	297.84	82.6%	0.211	70.20%
6.40	0.75	84.6%	303.76	1412.16	257.84	84.6%	0.215	71.55%
6.16	0.75	88.0%	237.36	1412.16	327.84	81.2%	0.209	71.42%
6.72	0.75	84.9%	301.89	1412.16	287.84	83.1%	0.228	70.54%
9.28	0.95	82.9%	510.02	2087.40	392.60	84.2%	0.229	69.81%
9.72	0.95	84.6%	459.87	2087.40	442.60	82.5%	0.231	69.82%
9.36	0.95	85.4%	427.81	2087.40	412.60	83.5%	0.234	71.30%
10.04	0.95	88.0%	348.59	2087.40	472.60	81.5%	0.240	71.77%
9.56	0.95	86.6%	390.06	2087.40	432.60	82.8%	0.246	71.73%

2000RPM

f_s	Torque	N_r	V_{LL} Motor	I_{Line} Motor	P_{in} Motor	V_{dc}	I_{dc} meas R=0.25mOhm	Motor Temp	Inverter Temp
(kHz)	(inlb)	(RPM)	(rms Volts L-L)	(rms A/Phase)	(Watts)	(V)	(mV)	(C)	(C)
Electrical Speed =		**2023.00**							
Line Frequency =		**33.72**							
10	60.5	1986	85.60	42.46	1640	296.70	1.54	37.5	42.5
9	60.5	1986	95.60	43.59	1730	303.40	1.51	38.7	42.7
8	60.5	1986	80.80	43.93	1640	289.70	1.58	38.8	42.6
6	60.5	1986	86.40	42.74	1680	305.70	1.51	39.5	41.6
5	60.5	1986	86.20	42.95	1700	306.80	1.51	40	41.2
		Avg V =	86.92		Avg V =	300.46			
Electrical Speed =		**2023.00**				0.41			
Line Frequency =		**33.72**							
10	120.3	1971	96.30	63.02	3135	315.10	2.79	42	49.8
9	120.3	1971	101.80	62.26	3200	311.90	2.82	43.6	48.8
8	120.3	1971	92.90	65.22	3150	310.80	2.80	44.2	49.4
6	120.3	1971	94.30	62.89	3190	300.80	2.87	46.1	48.3
5	120.3	1971	94.00	63.07	3205	303.30	2.90	46.1	46.8
		Avg V =	95.86		Avg V =	308.38			
Electrical Speed =		**2023.00**				0.44			
Line Frequency =		**33.72**							
10	180.1	1961	103.2	80.49	4630	320.2	4.06	50.3	60.7
9	180.1	1961	104.2	81.54	4700	299.8	4.39	51.6	59
8	180.1	1961	96.8	82.29	4630	295.8	4.33	52.4	59
6	180.1	1961	100.8	80.36	4690	302.9	4.17	53.5	56.5
5	180.1	1961	100.9	80.57	4720	308.2	4.2	54	55.2
		Avg V =	101.18		Avg V =	305.38			
						0.47			

I_{dc} meas R=0.25mOhm	Slip	Efficiency Inverter	P_{Loss} Inverter	P_{Out} Motor	P_{Loss} Motor	Motor Efficiency	Motor Power Factor	Total Efficiency
(A)	(Hz)	(%)	(W)	(W)	(W)	(%)		(%)
6.16	0.62	89.7%	187.67	1421.81	218.19	86.7%	0.261	77.79%
6.04	0.62	94.4%	102.54	1421.81	308.19	82.2%	0.240	77.59%
6.32	0.62	89.6%	190.90	1421.81	218.19	86.7%	0.267	77.66%
6.04	0.62	91.0%	166.43	1421.81	258.19	84.6%	0.263	77.00%
6.04	0.62	91.7%	153.07	1421.81	278.19	83.6%	0.265	76.73%
11.16	0.87	89.2%	381.52	2805.82	329.18	89.5%	0.299	79.79%
11.28	0.87	91.0%	318.23	2805.82	394.18	87.7%	0.292	79.75%
11.20	0.87	90.5%	330.96	2805.82	344.18	89.1%	0.301	80.60%
11.48	0.87	92.4%	263.18	2805.82	384.18	88.0%	0.311	81.25%
11.60	0.87	91.1%	313.28	2805.82	399.18	87.5%	0.312	79.75%
16.24	1.03	89.0%	570.05	4179.25	450.75	90.3%	0.322	80.37%
17.56	1.03	89.3%	564.49	4179.25	520.75	88.9%	0.320	79.39%
17.32	1.03	90.4%	493.26	4179.25	450.75	90.3%	0.336	81.57%
16.68	1.03	92.8%	362.37	4179.25	510.75	89.1%	0.335	82.72%
16.80	1.03	91.2%	457.76	4179.25	540.75	88.5%	0.336	80.72%

3000RPM

f_s	Torque	N_r	V_{LL} Motor	I_{Line} Motor	P_{in} Motor	V_{dc}	I_{dc} meas R=0.25mOhm	Motor Temp	Inverter Temp
(kHz)	(inlb)	(RPM)	(rms Volts L-L)	(rms A/Phase)	(Watts)	(V)	(mV)	(C)	(C)
Electrical Speed =		**3061.00**							
Line Frequency =		**51.02**							
10	60.5	3024	105.90	43.37	2550	300.80	2.29	37.7	41.6
9	60.5	3024	96.20	46.89	2510	303.70	2.28	38.6	42.2
8	60.5	3024	100.60	44.66	2530	300.90	2.27	39.2	41.7
6	60.5	3024	97.50	47.06	2550	309.50	2.21	40	41.5
5	60.5	3024	88.90	53.41	2550	308.7	2.28	41	42.4
		Avg V =	97.82		Avg V =	304.72			
Electrical Speed =		**3061.00**				0.45			
Line Frequency =		**51.02**							
10	120.3	3003	113.70	64.24	4720	307.20	4.20	48.4	51.2
9	120.3	3003	105.10	69.49	4710	303.70	4.33	49	51.5
8	120.3	3003	108.30	66.58	4730	295.40	4.29	48.8	49.5
6	120.3	3003	106.60	69.66	4780	302.30	4.22	49.6	49.1
5	120.3	3003	99.60	78.32	4830	306.20	4.37	50.5	51
		Avg V =	106.66		Avg V =	302.96			
Electrical Speed =		**3061.00**				0.50			
Line Frequency =		**51.02**							
10	180.1	2982	116.7	84.41	6890	306.8	6.23	56	60.3
9	180.1	2982	108.8	90.24	6910	298.5	6.58	57.7	61.2
8	180.1	2982	116.4	86.78	6940	312.5	6.00	58.2	60.2
6	180.1	2982	113.5	90.01	7000	307.2	6.10	60.1	59.2
5	180.1	2982	105.8	98.82	7100	302.1	6.56	62.2	60
		Avg V =	112.24		Avg V =	305.42			
						0.52			

I_{dc} meas R=0.25mOhm	Slip	Efficiency Inverter	P_{Loss} Inverter	P_{out} Motor	P_{Loss} Motor	Motor Efficiency	Motor Power Factor	Total Efficiency
(A)	(Hz)	(%)	(W)	(W)	(W)	(%)		(%)
9.16	0.62	92.5%	205.33	2164.93	385.07	84.9%	0.321	78.57%
9.12	0.62	90.6%	259.74	2164.93	345.07	86.3%	0.322	78.16%
9.08	0.62	92.6%	202.17	2164.93	365.07	85.6%	0.326	79.24%
8.84	0.62	93.2%	185.98	2164.93	385.07	84.9%	0.321	79.13%
9.12	0.62	90.6%	265.34	2164.93	385.07	84.9%	0.310	76.90%
16.80	0.97	91.5%	440.96	4274.92	445.08	90.6%	0.374	82.83%
17.32	0.97	89.5%	550.08	4274.92	435.08	90.8%	0.373	81.27%
17.16	0.97	93.3%	339.06	4274.92	455.08	90.4%	0.379	84.33%
16.88	0.97	93.7%	322.82	4274.92	505.08	89.4%	0.372	83.78%
17.48	0.97	90.2%	522.38	4274.92	555.08	88.5%	0.358	79.87%
24.92	1.32	90.1%	755.46	6355.19	534.81	92.2%	0.404	83.12%
26.32	1.32	88.0%	946.52	6355.19	554.81	92.0%	0.407	80.89%
24.00	1.32	92.5%	560.00	6355.19	584.81	91.6%	0.397	84.74%
24.40	1.32	93.4%	495.68	6355.19	644.81	90.8%	0.396	84.78%
26.24	1.32	89.6%	827.10	6355.19	744.81	89.5%	0.393	80.17%

Appendix II

System Calculation for 1000RPM

1) Motor Efficiency

Machine Parameters at 60Hz:

$rs := 0.012$ $Lls := 39.5 \cdot 10^{-6}$ $rc := 14.4$ $p := 2$ $Ns := 1037$

$rr := 0.0125$ $Llr := 41 \cdot 10^{-6}$ $Lm := 2.7 \cdot 10^{-3}$ $Vdc := 300$

Operating Conditions:

(5 ftlbs)

$Te1 := 6.78$

$Nr1 := 1006$

$\omega r1 := Nr1 \cdot \frac{2 \cdot \pi}{60}$

$sl1 := \frac{\omega e - \omega r1}{\omega e}$

(10 ftlbs)

$Te2 := 13.56$

$Nr2 := 992$

$\omega r2 := Nr2 \cdot \frac{2 \cdot \pi}{60}$

$\omega e := Ns \cdot \frac{2\pi}{60}$

$sl2 := \frac{\omega e - \omega r2}{\omega e}$

(15 ftlbs)

$Te3 := 20.34$

$Nr3 := 980$

$\omega r3 := Nr3 \cdot \frac{2 \cdot \pi}{60}$

$sl3 := \frac{\omega e - \omega r3}{\omega e}$

Displacment Factor:

$$Zm := \frac{rc \cdot \omega e \cdot Lmi}{rc + \omega e \cdot Lmi} \qquad Zs := rs + \omega e \cdot Llsi$$

$Zr3 := \frac{rr}{sl3} + \omega e \cdot Llri$

$Zeq3 := Zs + \frac{Zm \cdot Zr1}{Zm + Zr3}$

$\theta 3 := \arg(Zeq3)$

$DF3 := \cos(\theta 3)$

$Zr2 := \frac{rr}{sl2} + \omega e \cdot Llri$

$Zeq2 := Zs + \frac{Zm \cdot Zr1}{Zm + Zr2}$

$\theta 2 := \arg(Zeq2)$

$DF2 := \cos(\theta 2)$

$Zr1 := \frac{rr}{sl1} + \omega e \cdot Llri$

$Zeq1 := Zs + \frac{Zm \cdot Zr1}{Zm + Zr1}$

$\theta 1 := \arg(Zeq1)$

$DF1 := \cos(\theta 1)$

Motor Calculations Te1 :

$$Vs1 := \sqrt{\frac{2}{3 \cdot p} \cdot Te1 \cdot \omega e \cdot \frac{sl1}{rr} \cdot \left[\left(rs + \frac{rr}{sl1} \right)^2 + \omega e^2 \cdot (Lls + Llr)^2 \right]}$$

$$Ir1 := \sqrt{\frac{2}{3 \cdot p} \cdot Te1 \cdot \omega e \cdot \frac{sl1}{rr}}$$

$$Im1(fs) := \frac{Vs1 \cdot \sqrt{rc^2 + (\omega e \cdot Lm)^2}}{\omega e \cdot rc \cdot Lm}$$

$$Is1 := \frac{Ir1 \cdot \sqrt{\left(\frac{rc \cdot rr}{sl1} - \omega e^2 \cdot Llr \cdot Lm\right)^2 + \left[\omega e \cdot \left(Lm \cdot rc + \frac{rr}{sl1} \cdot Lm + rc \cdot Llr\right)\right]^2}}{rc \cdot \omega e \cdot Lm}$$

$$Vc1(fs) := Vs1 - Is1 \cdot rs$$

Efficiency Calculations:

$$Pout1 := 3 \cdot Ir1^2 \cdot \frac{rr \cdot (1 - sl1)}{sl1}$$

$$Pin1 := 3Vs1 \cdot Is1 \cdot DF1$$

$$\eta mot1 := \frac{Pout1}{Pin1}$$

Motor Calculations Te2:

$$Vs2 := \sqrt{\frac{2}{3 \cdot p} \cdot Te2 \cdot \omega e \cdot \frac{sl2}{rr} \cdot \left[\left(rs + \frac{rr}{sl2}\right)^2 + \omega e^2 \cdot (Lls + Llr)^2\right]}$$

$$Ir2 := \sqrt{\frac{2}{3 \cdot p} \cdot Te2 \cdot \omega e \cdot \frac{sl2}{rr}}$$

$$Im2(fs) := \frac{Vs2 \cdot \sqrt{rc^2 + (\omega e \cdot Lm)^2}}{\omega e \cdot rc \cdot Lm}$$

$$Is2 := \frac{Ir2 \cdot \sqrt{\left(\frac{rc \cdot rr}{sl1} - \omega e^2 \cdot Llr \cdot Lm\right)^2 + \left[\omega e \cdot \left(Lm \cdot rc + \frac{rr}{sl1} \cdot Lm + rc \cdot Llr\right)\right]^2}}{rc \cdot \omega e \cdot Lm}$$

$$Vc2(fs) := Vs2 - Is2 \cdot rs$$

Efficiency Calculations:

$$Pout2 := 3 \cdot Ir2^2 \cdot \frac{rr \cdot (1 - sl2)}{sl2}$$

$$Pin2 := 3Vs2 \cdot Is2 \cdot DF2$$

$$\eta mot2 := \frac{Pout2}{Pin2}$$

Motor Calculations Te3:

$$Vs3 := \sqrt{\frac{2}{3 \cdot p} \cdot Te3 \cdot \omega e \cdot \frac{sl3}{rr} \cdot \left[\left(rs + \frac{rr}{sl3} \right)^2 + \omega e^2 \cdot (Lls + Llr)^2 \right]}$$

$$Ir3 := \sqrt{\frac{2}{3 \cdot p} \cdot Te3 \cdot \omega e \cdot \frac{sl3}{rr}}$$

$$Im3(fs) := \frac{Vs3 \cdot \sqrt{rc^2 + (\omega e \cdot Lm)^2}}{\omega e \cdot rc \cdot Lm}$$

$$Is3 := \frac{Ir3 \cdot \sqrt{\left(\frac{rc \cdot rr}{sl1} - \omega e^2 \cdot Llr \cdot Lm \right)^2 + \left[\omega e \cdot \left(Lm \cdot rc + \frac{rr}{sl1} \cdot Lm + rc \cdot Llr \right) \right]^2}}{rc \cdot \omega e \cdot Lm}$$

$$Vc3(fs) := Vs3 - Is3 \cdot rs$$

Efficiency Calculations:

$$Pout3 := 3 \cdot Ir3^2 \cdot \frac{rr \cdot (1 - sl3)}{sl3}$$

$$Pin3 := 3Vs3 \cdot Is3 \cdot DF3$$

$$\eta mot3 := \frac{Pout3}{Pin3}$$

$$Pin1 = 1.071 \times 10^3$$

$$Pin2 = 1.98 \times 10^3$$

$$Pin3 = 2.491 \times 10^3$$

2) Inverter Efficiency

Parameters w/ SKM300GB063D IGBT:

$Rce := 0.0033$	$Vtest := 300$	$kgon := 2$	$k := 1.109 \cdot 10^{-4}$
$Vcesat := 1$		$kgoff := 1$	$h := 1.0506$
$Rak := 0.00125$	$Resr := 0.01$	$trr := 50 \cdot 10^{-9}$	$m := 6.175 \cdot 10^{-4}$
$Vf := 1.1$	$ripple := 0.10$	$tr := 80 \cdot 10^{-9}$	$n := .7198$

Modulation Index

$$M1 := \frac{Vs1\cdot\sqrt{2}}{Vdc} \qquad M2 := \frac{Vs2\cdot\sqrt{2}}{Vdc} \qquad M3 := \frac{Vs3\cdot\sqrt{2}}{Vdc}$$

Inverter Losses - Te1

Conduction Losses - SVM

$$Pcsw3a1 := \frac{1}{2\cdot\pi}\cdot\int_{0}^{\frac{\pi}{3}}\left[0.427+\sqrt{2}\cdot Is1\cdot\sin(x)\cdot 0.0237-7.3\cdot 10^{-5}\cdot\left(\sqrt{2}\cdot Is1\cdot\sin(x)\right)^{2}\right]\cdot\sqrt{2}\cdot Is1\cdot\sin(x)\cdot\left(\frac{1}{2}+\frac{1}{2}\cdot M1\cdot\sin(x+\theta 1)\right)dx$$

$$Pcsw3b1 := \frac{1}{2\cdot\pi}\cdot\int_{\frac{\pi}{3}}^{\frac{2\cdot\pi}{3}}\left[0.427+\sqrt{2}\cdot Is1\cdot\sin(x)\cdot 0.0237-7.3\cdot 10^{-5}\cdot\left(\sqrt{2}\cdot Is1\cdot\sin(x)\right)^{2}\right]\cdot\sqrt{2}\cdot Is1\cdot\sin(x)\,dx$$

$$Pcsw3c1 := \frac{1}{2\cdot\pi}\cdot\int_{\frac{2\cdot\pi}{3}}^{\pi}\left[0.427+\sqrt{2}\cdot Is1\cdot\sin(x)\cdot 0.0237-7.3\cdot 10^{-5}\cdot\left(\sqrt{2}\cdot Is1\cdot\sin(x)\right)^{2}\right]\cdot\sqrt{2}\cdot Is1\cdot\sin(x)\cdot\left(\frac{1}{2}+\frac{1}{2}\cdot M1\cdot\sin(x+\theta 1)\right)dx$$

$$Pcswsvm1 := Pcsw3a1 + Pcsw3b1 + Pcsw3c1$$

$$Pcd3a1 := \frac{1}{2\cdot\pi}\cdot\int_{0}^{\frac{\pi}{3}}\left[0.4256+\sqrt{2}\cdot Is1\cdot\sin(x)\cdot .0212-.000062\cdot\left(\sqrt{2}\cdot Is1\cdot\sin(x)\right)^{2}\right]\cdot\sqrt{2}\cdot Is1\cdot\sin(x)\cdot\left(\frac{1}{2}-\frac{1}{2}\cdot M1\cdot\sin(x+\theta 1)\right)dx$$

$$Pcd3b1 := \frac{1}{2\cdot\pi}\cdot\int_{\frac{\pi}{3}}^{\frac{2\cdot\pi}{3}}\left[0.4256+\sqrt{2}\cdot Is1\cdot\sin(x)\cdot .0212-.000062\cdot\left(\sqrt{2}\cdot Is1\cdot\sin(x)\right)^{2}\right]\cdot\sqrt{2}\cdot Is1\cdot\sin(x)\,dx$$

$$Pcd3c1 := \frac{1}{2\cdot\pi}\cdot\int_{\frac{2\cdot\pi}{3}}^{\pi}\left[0.4256+\sqrt{2}\cdot Is1\cdot\sin(x)\cdot .0212-.000062\cdot\left(\sqrt{2}\cdot Is1\cdot\sin(x)\right)^{2}\right]\cdot\sqrt{2}\cdot Is1\cdot\sin(x)\cdot\left(\frac{1}{2}-\frac{1}{2}\cdot M1\cdot\sin(x+\theta 1)\right)dx$$

$$Pcdsvm1 := Pcd3a1 + Pcd3b1 + Pcd3c1$$

$$Pcsvm1 := 6\cdot(Pcswsvm1 + Pcdsvm1)$$

Switching Losses:

$$Pswon1(fs) := \frac{1}{2\cdot\sqrt{\pi}}\cdot fs\cdot\frac{k}{\sqrt{3}}\cdot\left(Is1\cdot\sqrt{2}\right)^{h}\cdot kgon\cdot\frac{Vdc}{Vtest}\cdot\frac{\Gamma\left(\frac{h+1}{2}\right)}{\Gamma\left(\frac{h}{2}+1\right)}$$

$$Pswoff1(fs) := \frac{1}{2\cdot\sqrt{\pi}}\cdot fs\cdot\frac{m}{\sqrt{3}}\cdot\left(Is1\cdot\sqrt{2}\right)^{n}\cdot kgoff\cdot\frac{Vdc}{Vtest}\cdot\frac{\Gamma\left(\frac{n+1}{2}\right)}{\Gamma\left(\frac{n}{2}+1\right)}$$

$$Prr1(fs) := \frac{Is1\cdot\sqrt{2}\cdot Vdc}{8\cdot\pi}\cdot\frac{trr^{2}}{tr - trr}\cdot fs$$

$$Psw1(fs) := 6\cdot(Pswon1(fs) + Pswoff1(fs) + Prr1(fs))$$

Miscellaneous Losses:

$$Pcap1(fs) := (Is1\cdot ripple)^{2}\cdot(Resr)$$

Total Losses:

$$Plossinv1(fs) := Pcsvm1 + \frac{Psw1(fs)}{2} + Pcap1(fs)$$

Divide Psw by 2 for SVM.

$$\eta inv1(fs) := \frac{Pin1}{Pin1 + Plossinv1(fs)}$$

Inverter Losses - Te2

Conduction Losses - SVM

$$Pcsw3a2 := \frac{1}{2\cdot\pi}\cdot\int_{0}^{\frac{\pi}{3}}\left[0.427 + \sqrt{2}\cdot Is2\cdot\sin(x)\cdot 0.0237 - 7.3\cdot 10^{-5}\cdot\left(\sqrt{2}\cdot Is2\cdot\sin(x)\right)^{2}\right]\cdot\sqrt{2}\cdot Is2\cdot\sin(x)\cdot\left(\frac{1}{2} + \frac{1}{2}\cdot M2\cdot\sin(x + \theta 2)\right)dx$$

$$Pcsw3b2 := \frac{1}{2\cdot\pi}\cdot\int_{\frac{\pi}{3}}^{\frac{2\cdot\pi}{3}} \left[0.427 + \sqrt{2}\cdot Is2\cdot\sin(x)\cdot 0.0237 - 7.3\cdot 10^{-5}\cdot\left(\sqrt{2}\cdot Is2\cdot\sin(x)\right)^2\right]\cdot\sqrt{2}\cdot Is2\cdot\sin(x)\,dx$$

$$Pcsw3c2 := \frac{1}{2\cdot\pi}\cdot\int_{\frac{2\cdot\pi}{3}}^{\pi} \left[0.427 + \sqrt{2}\cdot Is2\cdot\sin(x)\cdot 0.0237 - 7.3\cdot 10^{-5}\cdot\left(\sqrt{2}\cdot Is2\cdot\sin(x)\right)^2\right]\cdot\sqrt{2}\cdot Is2\cdot\sin(x)\cdot\left(\frac{1}{2} + \frac{1}{2}\cdot M2\cdot\sin(x + \theta 2)\right)dx$$

$$Pcswsvm2 := Pcsw3a2 + Pcsw3b2 + Pcsw3c2$$

$$Pcd3a2 := \frac{1}{2\cdot\pi}\cdot\int_{0}^{\frac{\pi}{3}} \left[0.4256 + \sqrt{2}\cdot Is2\cdot\sin(x)\cdot .0212 - .000062\cdot\left(\sqrt{2}\cdot Is2\cdot\sin(x)\right)^2\right]\cdot\sqrt{2}\cdot Is2\cdot\sin(x)\cdot\left(\frac{1}{2} - \frac{1}{2}\cdot M2\cdot\sin(x + \theta 2)\right)dx$$

$$Pcd3b2 := \frac{1}{2\cdot\pi}\cdot\int_{\frac{\pi}{3}}^{\frac{2\cdot\pi}{3}} \left[0.4256 + \sqrt{2}\cdot Is2\cdot\sin(x)\cdot .0212 - .000062\cdot\left(\sqrt{2}\cdot Is2\cdot\sin(x)\right)^2\right]\cdot\sqrt{2}\cdot Is2\cdot\sin(x)\,dx$$

$$Pcd3c2 := \frac{1}{2\cdot\pi}\cdot\int_{\frac{2\cdot\pi}{3}}^{\pi} \left[0.4256 + \sqrt{2}\cdot Is2\cdot\sin(x)\cdot .0212 - .000062\cdot\left(\sqrt{2}\cdot Is2\cdot\sin(x)\right)^2\right]\cdot\sqrt{2}\cdot Is2\cdot\sin(x)\cdot\left(\frac{1}{2} - \frac{1}{2}\cdot M2\cdot\sin(x + \theta 2)\right)dx$$

$$Pcdsvm2 := Pcd3a2 + Pcd3b2 + Pcd3c2$$

$$Pcsvm2 := 6\cdot(Pcswsvm2 + Pcdsvm2)$$

Switching Losses:

$$Pswon2(fs) := \frac{1}{2\cdot\sqrt{\pi}}\cdot fs\cdot\frac{k}{\sqrt{3}}\cdot\left(Is2\cdot\sqrt{2}\right)^h\cdot kgon\cdot\frac{Vdc}{Vtest}\cdot\frac{\Gamma\left(\frac{h+1}{2}\right)}{\Gamma\left(\frac{h}{2}+1\right)}$$

$$Pswoff2(fs) := \frac{1}{2\cdot\sqrt{\pi}}\cdot fs\cdot\frac{m}{\sqrt{3}}\cdot\left(Is2\cdot\sqrt{2}\right)^{n}\cdot kgoff\cdot\frac{Vdc}{Vtest}\cdot\frac{\Gamma\left(\frac{n+1}{2}\right)}{\Gamma\left(\frac{n}{2}+1\right)}$$

$$Prr2(fs) := \frac{Is2\cdot\sqrt{2}\cdot Vdc}{8\cdot\pi}\cdot\frac{trr^{2}}{tr-trr}\cdot fs$$

$$Psw2(fs) := 6\cdot(Pswon2(fs) + Pswoff2(fs) + Prr2(fs))$$

Miscellaneous Losses:

$$Pcap2(fs) := (Is2\cdot ripple)^{2}\cdot(Resr)$$

Total Losses:

$$Plossinv2(fs) := Pcsvm2 + \frac{Psw2(fs)}{2} + Pcap2(fs)$$

$$\eta inv2(fs) := \frac{Pin2}{Pin2 + Plossinv2(fs)}$$

Inverter Losses - Te3

Conduction Losses - SVM

$$Pcsw3a3 := \frac{1}{2\cdot\pi}\cdot\int_{0}^{\frac{\pi}{3}}\left[0.427 + \sqrt{2}\cdot Is3\cdot\sin(x)\cdot 0.0237 - 7.3\cdot 10^{-5}\cdot\left(\sqrt{2}\cdot Is3\cdot\sin(x)\right)^{2}\right]\cdot\sqrt{2}\cdot Is3\cdot\sin(x)\cdot\left(\frac{1}{2}+\frac{1}{2}\cdot M3\cdot\sin\left(x+\theta 3\right)\right)dx$$

$$Pcsw3b3 := \frac{1}{2\cdot\pi}\cdot\int_{\frac{\pi}{3}}^{\frac{2\cdot\pi}{3}}\left[0.427 + \sqrt{2}\cdot Is3\cdot\sin(x)\cdot 0.0237 - 7.3\cdot 10^{-5}\cdot\left(\sqrt{2}\cdot Is3\cdot\sin(x)\right)^{2}\right]\cdot\sqrt{2}\cdot Is3\cdot\sin(x)\,dx$$

$$Pcsw3c3 := \frac{1}{2\cdot\pi}\cdot\int_{\frac{2\cdot\pi}{3}}^{\pi}\left[0.427 + \sqrt{2}\cdot Is3\cdot\sin(x)\cdot 0.0237 - 7.3\cdot 10^{-5}\cdot\left(\sqrt{2}\cdot Is3\cdot\sin(x)\right)^{2}\right]\cdot\sqrt{2}\cdot Is3\cdot\sin(x)\cdot\left(\frac{1}{2}+\frac{1}{2}\cdot M3\cdot\sin\left(x+\theta 3\right)\right)dx$$

$$Pcswsvm3 := Pcsw3a3 + Pcsw3b3 + Pcsw3c3$$

$$Pcd3a3 := \frac{1}{2\cdot\pi}\cdot\int_{0}^{\frac{\pi}{3}}\left[0.4256+\sqrt{2}\cdot Is3\cdot\sin(x)\cdot.0212-.000062\cdot\left(\sqrt{2}\cdot Is3\cdot\sin(x)\right)^{2}\right]\cdot\sqrt{2}\cdot Is3\cdot\sin(x)\cdot\left(\frac{1}{2}-\frac{1}{2}\cdot M3\cdot\sin(x+\theta 3)\right)dx$$

$$Pcd3b3 := \frac{1}{2\cdot\pi}\cdot\int_{\frac{\pi}{3}}^{\frac{2\cdot\pi}{3}}\left[0.4256+\sqrt{2}\cdot Is3\cdot\sin(x)\cdot.0212-.000062\cdot\left(\sqrt{2}\cdot Is3\cdot\sin(x)\right)^{2}\right]\cdot\sqrt{2}\cdot Is3\cdot\sin(x)\,dx$$

$$Pcd3c3 := \frac{1}{2\cdot\pi}\cdot\int_{\frac{2\cdot\pi}{3}}^{\pi}\left[0.4256+\sqrt{2}\cdot Is3\cdot\sin(x)\cdot.0212-.000062\cdot\left(\sqrt{2}\cdot Is3\cdot\sin(x)\right)^{2}\right]\cdot\sqrt{2}\cdot Is3\cdot\sin(x)\cdot\left(\frac{1}{2}-\frac{1}{2}\cdot M3\cdot\sin(x+\theta 3)\right)dx$$

$$Pcdsvm3 := Pcd3a3 + Pcd3b3 + Pcd3c3$$

$$Pcsvm3 := 6\cdot(Pcswsvm3 + Pcdsvm3)$$

Switching Losses:

$$Pswon3(fs) := \frac{1}{2\cdot\sqrt{\pi}}\cdot fs\cdot\frac{k}{\sqrt{3}}\cdot\left(Is3\cdot\sqrt{2}\right)^{h}\cdot kgon\cdot\frac{Vdc}{Vtest}\cdot\frac{\Gamma\left(\frac{h+1}{2}\right)}{\Gamma\left(\frac{h}{2}+1\right)}$$

$$Pswoff3(fs) := \frac{1}{2\cdot\sqrt{\pi}}\cdot fs\cdot\frac{m}{\sqrt{3}}\cdot\left(Is3\cdot\sqrt{2}\right)^{n}\cdot kgoff\cdot\frac{Vdc}{Vtest}\cdot\frac{\Gamma\left(\frac{n+1}{2}\right)}{\Gamma\left(\frac{n}{2}+1\right)}$$

$$Prr3(fs) := \frac{Is3\cdot\sqrt{2}\cdot Vdc}{8\cdot\pi}\cdot\frac{trr^{2}}{tr-trr}\cdot fs$$

$$Psw3(fs) := 6\cdot(Pswon3(fs) + Pswoff3(fs) + Prr3(fs))$$

Miscellaneous Losses:

$$Pcap3(fs) := (Is3\cdot ripple)^{2}\cdot(Resr)$$

$$Plossinv3(fs) := Pcsvm3 + \frac{Psw3(fs)}{2} + Pcap3(fs)$$

$$\eta inv3(fs) := \frac{Pin3}{Pin3 + Plossinv3(fs)}$$

3) System Efficiency

Total Losses:

$\eta sys1(fs) := \eta mot1 \cdot \eta inv1(fs)$

$\eta sys2(fs) := \eta mot2 \cdot \eta inv2(fs)$

$\eta sys3(fs) := \eta mot3 \cdot \eta inv3(fs)$

System Calculation for 2000RPM

1) Motor Efficiency

Machine Parameters at 60Hz:

$rs := 0.012$ $Lls := 39.5 \cdot 10^{-6}$ $rc := 14.4$ $p := 2$ $Ns := 2023$

$rr := 0.0125$ $Llr := 41 \cdot 10^{-6}$ $Lm := 2.7 \cdot 10^{-3}$ $Vdc := 300$

Operating Conditions:

(5 ftlbs)

$Te1 := 6.78$

$Nr1 := 1986$

$\omega r1 := Nr1 \cdot \frac{2 \cdot \pi}{60}$

$sl1 := \frac{\omega e - \omega r1}{\omega e}$

(10 ftlbs)

$Te2 := 13.56$

$Nr2 := 1971$

$\omega r2 := Nr2 \cdot \frac{2 \cdot \pi}{60}$

$\omega e := Ns \cdot \frac{2\pi}{60}$

$sl2 := \frac{\omega e - \omega r2}{\omega e}$

(15 ftlbs)

$Te3 := 20.34$

$Nr3 := 1961$

$\omega r3 := Nr3 \cdot \frac{2 \cdot \pi}{60}$

$sl3 := \frac{\omega e - \omega r3}{\omega e}$

Displacment Factor:

$$Zm := \frac{rc \cdot \omega e \cdot Lmi}{rc + \omega e \cdot Lmi} \qquad Zs := rs + \omega e \cdot Llsi$$

$Zr3 := \frac{rr}{sl3} + \omega e \cdot Llri$

$Zeq3 := Zs + \frac{Zm \cdot Zr1}{Zm + Zr3}$

$\theta 3 := \arg(Zeq3)$

$DF3 := \cos(\theta 3)$

$Zr2 := \frac{rr}{sl2} + \omega e \cdot Llri$

$Zeq2 := Zs + \frac{Zm \cdot Zr1}{Zm + Zr2}$

$\theta 2 := \arg(Zeq2)$

$DF2 := \cos(\theta 2)$

$Zr1 := \frac{rr}{sl1} + \omega e \cdot Llri$

$Zeq1 := Zs + \frac{Zm \cdot Zr1}{Zm + Zr1}$

$\theta 1 := \arg(Zeq1)$

$DF1 := \cos(\theta 1)$

Motor Calculations Te1:

$$Vs1 := \sqrt{\frac{2}{3 \cdot p} \cdot Te1 \cdot \omega e \cdot \frac{sl1}{rr} \cdot \left[\left(rs + \frac{rr}{sl1} \right)^2 + \omega e^2 \cdot (Lls + Llr)^2 \right]}$$

$$Ir1 := \sqrt{\frac{2}{3 \cdot p} \cdot Te1 \cdot \omega e \cdot \frac{sl1}{rr}}$$

$$Im1(fs) := \frac{Vs1 \cdot \sqrt{rc^2 + (\omega e \cdot Lm)^2}}{\omega e \cdot rc \cdot Lm}$$

$$Is1 := \frac{Ir1 \cdot \sqrt{\left(\frac{rc \cdot rr}{sl1} - \omega e^2 \cdot Llr \cdot Lm\right)^2 + \left[\omega e \cdot \left(Lm \cdot rc + \frac{rr}{sl1} \cdot Lm + rc \cdot Llr\right)\right]^2}}{rc \cdot \omega e \cdot Lm}$$

$$Vc1(fs) := Vs1 - Is1 \cdot rs$$

Efficiency Calculations:

$$Pout1 := 3 \cdot Ir1^2 \cdot \frac{rr \cdot (1 - sl1)}{sl1}$$

$$Pin1 := 3Vs1 \cdot Is1 \cdot DF1$$

$$\eta mot1 := \frac{Pout1}{Pin1}$$

Motor Calculations Te2:

$$Vs2 := \sqrt{\frac{2}{3 \cdot p} \cdot Te2 \cdot \omega e \cdot \frac{sl2}{rr} \cdot \left[\left(rs + \frac{rr}{sl2}\right)^2 + \omega e^2 \cdot (Lls + Llr)^2\right]}$$

$$Ir2 := \sqrt{\frac{2}{3 \cdot p} \cdot Te2 \cdot \omega e \cdot \frac{sl2}{rr}}$$

$$Im2(fs) := \frac{Vs2 \cdot \sqrt{rc^2 + (\omega e \cdot Lm)^2}}{\omega e \cdot rc \cdot Lm}$$

$$Is2 := \frac{Ir2 \cdot \sqrt{\left(\frac{rc \cdot rr}{sl1} - \omega e^2 \cdot Llr \cdot Lm\right)^2 + \left[\omega e \cdot \left(Lm \cdot rc + \frac{rr}{sl1} \cdot Lm + rc \cdot Llr\right)\right]^2}}{rc \cdot \omega e \cdot Lm}$$

$$Vc2(fs) := Vs2 - Is2 \cdot rs$$

Efficiency Calculations:

$$Pout2 := 3 \cdot Ir2^2 \cdot \frac{rr \cdot (1 - sl2)}{sl2}$$

$$Pin2 := 3Vs2 \cdot Is2 \cdot DF2$$

$$\eta mot2 := \frac{Pout2}{Pin2}$$

Motor Calculations Te3:

$$Vs3 := \sqrt{\frac{2}{3 \cdot p} \cdot Te3 \cdot \omega e \cdot \frac{sl3}{rr} \cdot \left[\left(rs + \frac{rr}{sl3} \right)^2 + \omega e^2 \cdot (Lls + Llr)^2 \right]}$$

$$Ir3 := \sqrt{\frac{2}{3 \cdot p} \cdot Te3 \cdot \omega e \cdot \frac{sl3}{rr}}$$

$$Im3(fs) := \frac{Vs3 \cdot \sqrt{rc^2 + (\omega e \cdot Lm)^2}}{\omega e \cdot rc \cdot Lm}$$

$$Is3 := \frac{Ir3 \cdot \sqrt{\left(\frac{rc \cdot rr}{sl1} - \omega e^2 \cdot Llr \cdot Lm \right)^2 + \left[\omega e \cdot \left(Lm \cdot rc + \frac{rr}{sl1} \cdot Lm + rc \cdot Llr \right) \right]^2}}{rc \cdot \omega e \cdot Lm}$$

$$Vc3(fs) := Vs3 - Is3 \cdot rs$$

Efficiency Calculations:

$$Pout3 := 3 \cdot Ir3^2 \cdot \frac{rr \cdot (1 - sl3)}{sl3}$$

$$Pin3 := 3Vs3 \cdot Is3 \cdot DF3$$

$$\eta mot3 := \frac{Pout3}{Pin3}$$

$$Pin1 = 1.913 \times 10^3$$

$$Pin2 = 3.628 \times 10^3$$

$$Pin3 = 4.693 \times 10^3$$

2) Inverter Efficiency

Parameters w/ SKM300GB063D IGBT:

$Rce := 0.0033$	$Vtest := 300$	$kgon := 2$	$k := 1.109 \cdot 10^{-4}$
$Vcesat := 1$		$kgoff := 1$	$h := 1.0506$
$Rak := 0.00125$	$Resr := 0.01$	$trr := 50 \cdot 10^{-9}$	$m := 6.175 \cdot 10^{-4}$
$Vf := 1.1$	$ripple := 0.10$	$tr := 80 \cdot 10^{-9}$	$n := .7198$

Modulation Index

$$M1 := \frac{Vs1\cdot\sqrt{2}}{Vdc} \qquad M2 := \frac{Vs2\cdot\sqrt{2}}{Vdc} \qquad M3 := \frac{Vs3\cdot\sqrt{2}}{Vdc}$$

Inverter Losses - Te1

Conduction Losses - SVM

$$Pcsw3a1 := \frac{1}{2\cdot\pi}\cdot\int_{0}^{\frac{\pi}{3}}\left[0.427+\sqrt{2}\cdot Is1\cdot\sin(x)\cdot 0.0237-7.3\cdot 10^{-5}\cdot\left(\sqrt{2}\cdot Is1\cdot\sin(x)\right)^{2}\right]\cdot\sqrt{2}\cdot Is1\cdot\sin(x)\cdot\left(\frac{1}{2}+\frac{1}{2}\cdot M1\cdot\sin(x+\theta 1)\right)dx$$

$$Pcsw3b1 := \frac{1}{2\cdot\pi}\cdot\int_{\frac{\pi}{3}}^{\frac{2\cdot\pi}{3}}\left[0.427+\sqrt{2}\cdot Is1\cdot\sin(x)\cdot 0.0237-7.3\cdot 10^{-5}\cdot\left(\sqrt{2}\cdot Is1\cdot\sin(x)\right)^{2}\right]\cdot\sqrt{2}\cdot Is1\cdot\sin(x)\,dx$$

$$Pcsw3c1 := \frac{1}{2\cdot\pi}\cdot\int_{\frac{2\cdot\pi}{3}}^{\pi}\left[0.427+\sqrt{2}\cdot Is1\cdot\sin(x)\cdot 0.0237-7.3\cdot 10^{-5}\cdot\left(\sqrt{2}\cdot Is1\cdot\sin(x)\right)^{2}\right]\cdot\sqrt{2}\cdot Is1\cdot\sin(x)\cdot\left(\frac{1}{2}+\frac{1}{2}\cdot M1\cdot\sin(x+\theta 1)\right)dx$$

$$Pcswsvm1 := Pcsw3a1 + Pcsw3b1 + Pcsw3c1$$

$$Pcd3a1 := \frac{1}{2\cdot\pi}\cdot\int_{0}^{\frac{\pi}{3}}\left[0.4256+\sqrt{2}\cdot Is1\cdot\sin(x)\cdot .0212-.000062\cdot\left(\sqrt{2}\cdot Is1\cdot\sin(x)\right)^{2}\right]\cdot\sqrt{2}\cdot Is1\cdot\sin(x)\cdot\left(\frac{1}{2}-\frac{1}{2}\cdot M1\cdot\sin(x+\theta 1)\right)dx$$

$$Pcd3b1 := \frac{1}{2\cdot\pi}\cdot\int_{\frac{\pi}{3}}^{\frac{2\cdot\pi}{3}}\left[0.4256+\sqrt{2}\cdot Is1\cdot\sin(x)\cdot .0212-.000062\cdot\left(\sqrt{2}\cdot Is1\cdot\sin(x)\right)^{2}\right]\cdot\sqrt{2}\cdot Is1\cdot\sin(x)\,dx$$

$$Pcd3c1 := \frac{1}{2\cdot\pi}\cdot\int_{\frac{2\cdot\pi}{3}}^{\pi}\left[0.4256+\sqrt{2}\cdot Is1\cdot\sin(x)\cdot .0212-.000062\cdot\left(\sqrt{2}\cdot Is1\cdot\sin(x)\right)^{2}\right]\cdot\sqrt{2}\cdot Is1\cdot\sin(x)\cdot\left(\frac{1}{2}-\frac{1}{2}\cdot M1\cdot\sin(x+\theta 1)\right)dx$$

$$Pcdsvm1 := Pcd3a1 + Pcd3b1 + Pcd3c1$$

$$Pcsvm1 := 6\cdot(Pcswsvm1 + Pcdsvm1)$$

Switching Losses:

$$Pswon1(fs) := \frac{1}{2\cdot\sqrt{\pi}}\cdot fs\cdot\frac{k}{\sqrt{3}}\cdot\left(Is1\cdot\sqrt{2}\right)^{h}\cdot kgon\cdot\frac{Vdc}{Vtest}\cdot\frac{\Gamma\left(\frac{h+1}{2}\right)}{\Gamma\left(\frac{h}{2}+1\right)}$$

$$Pswoff1(fs) := \frac{1}{2\cdot\sqrt{\pi}}\cdot fs\cdot\frac{m}{\sqrt{3}}\cdot\left(Is1\cdot\sqrt{2}\right)^{n}\cdot kgoff\cdot\frac{Vdc}{Vtest}\cdot\frac{\Gamma\left(\frac{n+1}{2}\right)}{\Gamma\left(\frac{n}{2}+1\right)}$$

$$Prr1(fs) := \frac{Is1\cdot\sqrt{2}\cdot Vdc}{8\cdot\pi}\cdot\frac{trr^{2}}{tr-trr}\cdot fs$$

$$Psw1(fs) := 6\cdot(Pswon1(fs) + Pswoff1(fs) + Prr1(fs))$$

Miscellaneous Losses:

$$Pcap1(fs) := (Is1\cdot ripple)^{2}\cdot(Resr)$$

Total Losses:

$$Plossinv1(fs) := Pcsvm1 + \frac{Psw1(fs)}{2} + Pcap1(fs)$$

Divide Psw by 2 for SVM.

$$\eta inv1(fs) := \frac{Pin1}{Pin1 + Plossinv1(fs)}$$

Inverter Losses - Te2

Conduction Losses - SVM

$$Pcsw3a2 := \frac{1}{2\cdot\pi}\cdot\int_{0}^{\frac{\pi}{3}}\left[0.427 + \sqrt{2}\cdot Is2\cdot\sin(x)\cdot 0.0237 - 7.3\cdot10^{-5}\cdot\left(\sqrt{2}\cdot Is2\cdot\sin(x)\right)^{2}\right]\cdot\sqrt{2}\cdot Is2\cdot\sin(x)\cdot\left(\frac{1}{2}+\frac{1}{2}\cdot M2\cdot\sin(x+\theta2)\right)dx$$

$$Pcsw3b2 := \frac{1}{2\cdot\pi}\cdot\int_{\frac{\pi}{3}}^{\frac{2\cdot\pi}{3}}\left[0.427 + \sqrt{2}\cdot Is2\cdot\sin(x)\cdot 0.0237 - 7.3\cdot10^{-5}\cdot\left(\sqrt{2}\cdot Is2\cdot\sin(x)\right)^{2}\right]\cdot\sqrt{2}\cdot Is2\cdot\sin(x)\,dx$$

$$Pcsw3c2 := \frac{1}{2\cdot\pi}\cdot\int_{\frac{2\cdot\pi}{3}}^{\pi}\left[0.427 + \sqrt{2}\cdot Is2\cdot\sin(x)\cdot 0.0237 - 7.3\cdot10^{-5}\cdot\left(\sqrt{2}\cdot Is2\cdot\sin(x)\right)^{2}\right]\cdot\sqrt{2}\cdot Is2\cdot\sin(x)\cdot\left(\frac{1}{2}+\frac{1}{2}\cdot M2\cdot\sin(x+\theta2)\right)dx$$

$$Pcswsvm2 := Pcsw3a2 + Pcsw3b2 + Pcsw3c2$$

$$Pcd3a2 := \frac{1}{2\cdot\pi}\cdot\int_{0}^{\frac{\pi}{3}}\left[0.4256 + \sqrt{2}\cdot Is2\cdot\sin(x)\cdot.0212 - .000062\cdot\left(\sqrt{2}\cdot Is2\cdot\sin(x)\right)^2\right]\cdot\sqrt{2}\cdot Is2\cdot\sin(x)\cdot\left(\frac{1}{2} - \frac{1}{2}\cdot M2\cdot\sin\left(x + \theta 2\right)\right)dx$$

$$Pcd3b2 := \frac{1}{2\cdot\pi}\cdot\int_{\frac{\pi}{3}}^{\frac{2\cdot\pi}{3}}\left[0.4256 + \sqrt{2}\cdot Is2\cdot\sin(x)\cdot.0212 - .000062\cdot\left(\sqrt{2}\cdot Is2\cdot\sin(x)\right)^2\right]\cdot\sqrt{2}\cdot Is2\cdot\sin(x)\,dx$$

$$Pcd3c2 := \frac{1}{2\cdot\pi}\cdot\int_{\frac{2\cdot\pi}{3}}^{\pi}\left[0.4256 + \sqrt{2}\cdot Is2\cdot\sin(x)\cdot.0212 - .000062\cdot\left(\sqrt{2}\cdot Is2\cdot\sin(x)\right)^2\right]\cdot\sqrt{2}\cdot Is2\cdot\sin(x)\cdot\left(\frac{1}{2} - \frac{1}{2}\cdot M2\cdot\sin\left(x + \theta 2\right)\right)dx$$

$$Pcdsvm2 := Pcd3a2 + Pcd3b2 + Pcd3c2$$

$$Pcsvm2 := 6\cdot(Pcswsvm2 + Pcdsvm2)$$

Switching Losses:

$$Pswon2(fs) := \frac{1}{2\cdot\sqrt{\pi}}\cdot fs\cdot\frac{k}{\sqrt{3}}\cdot\left(Is2\cdot\sqrt{2}\right)^h\cdot kgon\cdot\frac{Vdc}{Vtest}\cdot\frac{\Gamma\left(\frac{h+1}{2}\right)}{\Gamma\left(\frac{h}{2}+1\right)}$$

$$Pswoff2(fs) := \frac{1}{2\cdot\sqrt{\pi}}\cdot fs\cdot\frac{m}{\sqrt{3}}\cdot\left(Is2\cdot\sqrt{2}\right)^n\cdot kgoff\cdot\frac{Vdc}{Vtest}\cdot\frac{\Gamma\left(\frac{n+1}{2}\right)}{\Gamma\left(\frac{n}{2}+1\right)}$$

$$Prr2(fs) := \frac{Is2\cdot\sqrt{2}\cdot Vdc}{8\cdot\pi}\cdot\frac{trr^2}{tr - trr}\cdot fs$$

$$Psw2(fs) := 6\cdot(Pswon2(fs) + Pswoff2(fs) + Prr2(fs))$$

Miscellaneous Losses:

$$Pcap2(fs) := (Is2 \cdot ripple)^2 \cdot (Resr)$$

Total Losses:

$$Plossinv2(fs) := Pcsvm2 + \frac{Psw2(fs)}{2} + Pcap2(fs)$$

$$\eta inv2(fs) := \frac{Pin2}{Pin2 + Plossinv2(fs)}$$

Inverter Losses - Te3

Conduction Losses - SVM

$$Pcsw3a3 := \frac{1}{2\cdot\pi}\cdot\int_{0}^{\frac{\pi}{3}}\left[0.427 + \sqrt{2}\cdot Is3\cdot\sin(x)\cdot 0.0237 - 7.3\cdot 10^{-5}\cdot\left(\sqrt{2}\cdot Is3\cdot\sin(x)\right)^2\right]\cdot\sqrt{2}\cdot Is3\cdot\sin(x)\cdot\left(\frac{1}{2} + \frac{1}{2}\cdot M3\cdot\sin\left(x + \theta 3\right)\right)dx$$

$$Pcsw3b3 := \frac{1}{2\cdot\pi}\cdot\int_{\frac{\pi}{3}}^{\frac{2\cdot\pi}{3}}\left[0.427 + \sqrt{2}\cdot Is3\cdot\sin(x)\cdot 0.0237 - 7.3\cdot 10^{-5}\cdot\left(\sqrt{2}\cdot Is3\cdot\sin(x)\right)^2\right]\cdot\sqrt{2}\cdot Is3\cdot\sin(x)\,dx$$

$$Pcsw3c3 := \frac{1}{2\cdot\pi}\cdot\int_{\frac{2\cdot\pi}{3}}^{\pi}\left[0.427 + \sqrt{2}\cdot Is3\cdot\sin(x)\cdot 0.0237 - 7.3\cdot 10^{-5}\cdot\left(\sqrt{2}\cdot Is3\cdot\sin(x)\right)^2\right]\cdot\sqrt{2}\cdot Is3\cdot\sin(x)\cdot\left(\frac{1}{2} + \frac{1}{2}\cdot M3\cdot\sin\left(x + \theta 3\right)\right)dx$$

$$Pcswsvm3 := Pcsw3a3 + Pcsw3b3 + Pcsw3c3$$

$$Pcd3a3 := \frac{1}{2\cdot\pi}\cdot\int_{0}^{\frac{\pi}{3}}\left[0.4256 + \sqrt{2}\cdot Is3\cdot\sin(x)\cdot .0212 - .000062\cdot\left(\sqrt{2}\cdot Is3\cdot\sin(x)\right)^2\right]\cdot\sqrt{2}\cdot Is3\cdot\sin(x)\cdot\left(\frac{1}{2} - \frac{1}{2}\cdot M3\cdot\sin\left(x + \theta 3\right)\right)dx$$

$$Pcd3b3 := \frac{1}{2\cdot\pi}\cdot\int_{\frac{\pi}{3}}^{\frac{2\cdot\pi}{3}}\left[0.4256 + \sqrt{2}\cdot Is3\cdot\sin(x)\cdot .0212 - .000062\cdot\left(\sqrt{2}\cdot Is3\cdot\sin(x)\right)^2\right]\cdot\sqrt{2}\cdot Is3\cdot\sin(x)\,dx$$

$$Pcd3c3 := \frac{1}{2\cdot\pi}\cdot\int_{\frac{2\cdot\pi}{3}}^{\pi}\left[0.4256 + \sqrt{2}\cdot Is3\cdot\sin(x)\cdot .0212 - .000062\cdot\left(\sqrt{2}\cdot Is3\cdot\sin(x)\right)^2\right]\cdot\sqrt{2}\cdot Is3\cdot\sin(x)\cdot\left(\frac{1}{2} - \frac{1}{2}\cdot M3\cdot\sin\left(x + \theta 3\right)\right)dx$$

$$Pcdsvm3 := Pcd3a3 + Pcd3b3 + Pcd3c3$$

$$Pcsvm3 := 6\cdot(Pcswsvm3 + Pcdsvm3)$$

Switching Losses:

$$Pswon3(fs) := \frac{1}{2\cdot\sqrt{\pi}}\cdot fs\cdot\frac{k}{\sqrt{3}}\cdot\left(Is3\cdot\sqrt{2}\right)^{h}\cdot kgon\cdot\frac{Vdc}{Vtest}\cdot\frac{\Gamma\left(\frac{h+1}{2}\right)}{\Gamma\left(\frac{h}{2}+1\right)}$$

$$Pswoff3(fs) := \frac{1}{2\cdot\sqrt{\pi}}\cdot fs\cdot\frac{m}{\sqrt{3}}\cdot\left(Is3\cdot\sqrt{2}\right)^{n}\cdot kgoff\cdot\frac{Vdc}{Vtest}\cdot\frac{\Gamma\left(\frac{n+1}{2}\right)}{\Gamma\left(\frac{n}{2}+1\right)}$$

$$Prr3(fs) := \frac{Is3\cdot\sqrt{2}\cdot Vdc}{8\cdot\pi}\cdot\frac{trr^{2}}{tr - trr}\cdot fs$$

$$Psw3(fs) := 6\cdot(Pswon3(fs) + Pswoff3(fs) + Prr3(fs))$$

Miscellaneous Losses:

$$Pcap3(fs) := (Is3\cdot ripple)^{2}\cdot(Resr)$$

$$Plossinv3(fs) := Pcsvm3 + \frac{Psw3(fs)}{2} + Pcap3(fs)$$

$$\eta inv3(fs) := \frac{Pin3}{Pin3 + Plossinv3(fs)}$$

3) System Efficiency

Total Losses:

$$\eta sys1(fs) := \eta mot1\cdot\eta inv1(fs)$$

$$\eta sys2(fs) := \eta mot2\cdot\eta inv2(fs)$$

$$\eta sys3(fs) := \eta mot3\cdot\eta inv3(fs)$$

System Calculation for 3000RPM

1) Motor Efficiency

Machine Parameters at 60Hz:

$rs := 0.012$ $Lls := 39.5 \cdot 10^{-6}$ $rc := 14.4$ $p := 2$ $Ns := 3061$

$rr := 0.0125$ $Llr := 41 \cdot 10^{-6}$ $Lm := 2.7 \cdot 10^{-3}$ $Vdc := 300$

Operating Conditions:

(5 ftlbs)

$Te1 := 6.78$

$Nr1 := 3024$

$\omega r1 := Nr1 \cdot \frac{2 \cdot \pi}{60}$

(10 ftlbs)

$Te2 := 13.56$

$Nr2 := 3003$

$\omega r2 := Nr2 \cdot \frac{2 \cdot \pi}{60}$

$\omega e := Ns \cdot \frac{2\pi}{60}$

(15 ftlbs)

$Te3 := 20.34$

$Nr3 := 2982$

$\omega r3 := Nr3 \cdot \frac{2 \cdot \pi}{60}$

$sl1 := \frac{\omega e - \omega r1}{\omega e}$ $sl2 := \frac{\omega e - \omega r2}{\omega e}$ $sl3 := \frac{\omega e - \omega r3}{\omega e}$

Displacment Factor:

$Zm := \frac{rc \cdot \omega e \cdot Lmi}{rc + \omega e \cdot Lmi}$ $Zs := rs + \omega e \cdot Lsi$

$Zr3 := \frac{rr}{sl3} + \omega e \cdot Lri$ $Zr2 := \frac{rr}{sl2} + \omega e \cdot Lri$ $Zr1 := \frac{rr}{sl1} + \omega e \cdot Lri$

$Zeq3 := Zs + \frac{Zm \cdot Zr1}{Zm + Zr3}$ $Zeq2 := Zs + \frac{Zm \cdot Zr1}{Zm + Zr2}$ $Zeq1 := Zs + \frac{Zm \cdot Zr1}{Zm + Zr1}$

$\theta 3 := \arg(Zeq3)$ $\theta 2 := \arg(Zeq2)$ $\theta 1 := \arg(Zeq1)$

$DF3 := \cos(\theta 3)$ $DF2 := \cos(\theta 2)$ $DF1 := \cos(\theta 1)$

Motor Calculations Te1:

$$Vs1 := \sqrt{\frac{2}{3 \cdot p} \cdot Te1 \cdot \omega e \cdot \frac{sl1}{rr} \cdot \left[\left(rs + \frac{rr}{sl1} \right)^2 + \omega e^2 \cdot (Lls + Lm)^2 \right]}$$

$$Ir1 := \sqrt{\frac{2}{3 \cdot p} \cdot Te1 \cdot \omega e \cdot \frac{sl1}{rr}}$$

$$Im1(fs) := \frac{Vs1 \cdot \sqrt{rc^2 + (\omega e \cdot Lm)^2}}{\omega e \cdot rc \cdot Lm}$$

$$Is1 := \frac{Ir1 \cdot \sqrt{\left(\frac{rc \cdot rr}{sl1} - \omega e^2 \cdot Llr \cdot Lm\right)^2 + \left[\omega e \cdot \left(Lm \cdot rc + \frac{rr}{sl1} \cdot Lm + rc \cdot Llr\right)\right]^2}}{rc \cdot \omega e \cdot Lm}$$

$$Vc1(fs) := Vs1 - Is1 \cdot rs$$

Efficiency Calculations:

$$Pout1 := 3 \cdot Ir1^2 \cdot \frac{rr \cdot (1 - sl1)}{sl1}$$

$$Pin1 := 3Vs1 \cdot Is1 \cdot DF1$$

$$\eta mot1 := \frac{Pout1}{Pin1}$$

Motor Calculations Te2:

$$Vs2 := \sqrt{\frac{2}{3 \cdot p} \cdot Te2 \cdot \omega e \cdot \frac{sl2}{rr} \cdot \left[\left(rs + \frac{rr}{sl2}\right)^2 + \omega e^2 \cdot (Lls + Llr)^2\right]}$$

$$Ir2 := \sqrt{\frac{2}{3 \cdot p} \cdot Te2 \cdot \omega e \cdot \frac{sl2}{rr}}$$

$$Im2(fs) := \frac{Vs2 \cdot \sqrt{rc^2 + (\omega e \cdot Lm)^2}}{\omega e \cdot rc \cdot Lm}$$

$$Is2 := \frac{Ir2 \cdot \sqrt{\left(\frac{rc \cdot rr}{sl1} - \omega e^2 \cdot Llr \cdot Lm\right)^2 + \left[\omega e \cdot \left(Lm \cdot rc + \frac{rr}{sl1} \cdot Lm + rc \cdot Llr\right)\right]^2}}{rc \cdot \omega e \cdot Lm}$$

$$Vc2(fs) := Vs2 - Is2 \cdot rs$$

Efficiency Calculations:

$$Pout2 := 3 \cdot Ir2^2 \cdot \frac{rr \cdot (1 - sl2)}{sl2}$$

$$Pin2 := 3Vs2 \cdot Is2 \cdot DF2$$

$$\eta mot2 := \frac{Pout2}{Pin2}$$

Motor Calculations Te3:

$$Vs3 := \sqrt{\frac{2}{3 \cdot p} \cdot Te3 \cdot \omega e \cdot \frac{sl3}{rr} \cdot \left[\left(rs + \frac{rr}{sl3} \right)^2 + \omega e^2 \cdot (Lls + Llr)^2 \right]}$$

$$Ir3 := \sqrt{\frac{2}{3 \cdot p} \cdot Te3 \cdot \omega e \cdot \frac{sl3}{rr}}$$

$$Im3(fs) := \frac{Vs3 \cdot \sqrt{rc^2 + (\omega e \cdot Lm)^2}}{\omega e \cdot rc \cdot Lm}$$

$$Is3 := \frac{Ir3 \cdot \sqrt{\left(\frac{rc \cdot rr}{sl1} - \omega e^2 \cdot Llr \cdot Lm \right)^2 + \left[\omega e \cdot \left(Lm \cdot rc + \frac{rr}{sl1} \cdot Lm + rc \cdot Llr \right) \right]^2}}{rc \cdot \omega e \cdot Lm}$$

$$Vc3(fs) := Vs3 - Is3 \cdot rs$$

Efficiency Calculations:

$$Pout3 := 3 \cdot Ir3^2 \cdot \frac{rr \cdot (1 - sl3)}{sl3}$$

$$Pin3 := 3Vs3 \cdot Is3 \cdot DF3$$

$$\eta mot3 := \frac{Pout3}{Pin3}$$

$$Pin1 = 3.102 \times 10^3$$

$$Pin2 = 5.741 \times 10^3$$

$$Pin3 = 7.177 \times 10^3$$

2) Inverter Efficiency

Parameters w/ SKM300GB063D IGBT:

$Rce := 0.0033$	$Vtest := 300$	$kgon := 2$	$k := 1.109 \cdot 10^{-4}$
$Vcesat := 1$		$kgoff := 1$	$h := 1.0506$
$Rak := 0.00125$	$Resr := 0.01$	$trr := 50 \cdot 10^{-9}$	$m := 6.175 \cdot 10^{-4}$
$Vf := 1.1$	$ripple := 0.10$	$tr := 80 \cdot 10^{-9}$	$n := .7198$

Modulation Index

$$M1 := \frac{Vs1\cdot\sqrt{2}}{Vdc} \qquad M2 := \frac{Vs2\cdot\sqrt{2}}{Vdc} \qquad M3 := \frac{Vs3\cdot\sqrt{2}}{Vdc}$$

Inverter Losses - Te1

Conduction Losses - SVM

$$Pcsw3a1 := \frac{1}{2\cdot\pi}\cdot\int_{0}^{\frac{\pi}{3}}\left[0.427+\sqrt{2}\cdot Is1\cdot\sin(x)\cdot 0.0237-7.3\cdot 10^{-5}\cdot\left(\sqrt{2}\cdot Is1\cdot\sin(x)\right)^{2}\right]\cdot\sqrt{2}\cdot Is1\cdot\sin(x)\cdot\left(\frac{1}{2}+\frac{1}{2}\cdot M1\cdot\sin(x+\theta 1)\right)dx$$

$$Pcsw3b1 := \frac{1}{2\cdot\pi}\cdot\int_{\frac{\pi}{3}}^{\frac{2\cdot\pi}{3}}\left[0.427+\sqrt{2}\cdot Is1\cdot\sin(x)\cdot 0.0237-7.3\cdot 10^{-5}\cdot\left(\sqrt{2}\cdot Is1\cdot\sin(x)\right)^{2}\right]\cdot\sqrt{2}\cdot Is1\cdot\sin(x)\,dx$$

$$Pcsw3c1 := \frac{1}{2\cdot\pi}\cdot\int_{\frac{2\cdot\pi}{3}}^{\pi}\left[0.427+\sqrt{2}\cdot Is1\cdot\sin(x)\cdot 0.0237-7.3\cdot 10^{-5}\cdot\left(\sqrt{2}\cdot Is1\cdot\sin(x)\right)^{2}\right]\cdot\sqrt{2}\cdot Is1\cdot\sin(x)\cdot\left(\frac{1}{2}+\frac{1}{2}\cdot M1\cdot\sin(x+\theta 1)\right)dx$$

$$Pcswsvm1 := Pcsw3a1 + Pcsw3b1 + Pcsw3c1$$

$$Pcd3a1 := \frac{1}{2\cdot\pi}\cdot\int_{0}^{\frac{\pi}{3}}\left[0.4256+\sqrt{2}\cdot Is1\cdot\sin(x)\cdot .0212-.000062\cdot\left(\sqrt{2}\cdot Is1\cdot\sin(x)\right)^{2}\right]\cdot\sqrt{2}\cdot Is1\cdot\sin(x)\cdot\left(\frac{1}{2}-\frac{1}{2}\cdot M1\cdot\sin(x+\theta 1)\right)dx$$

$$Pcd3b1 := \frac{1}{2\cdot\pi}\cdot\int_{\frac{\pi}{3}}^{\frac{2\cdot\pi}{3}}\left[0.4256+\sqrt{2}\cdot Is1\cdot\sin(x)\cdot .0212-.000062\cdot\left(\sqrt{2}\cdot Is1\cdot\sin(x)\right)^{2}\right]\cdot\sqrt{2}\cdot Is1\cdot\sin(x)\,dx$$

$$Pcd3c1 := \frac{1}{2\cdot\pi}\cdot\int_{\frac{2\cdot\pi}{3}}^{\pi}\left[0.4256+\sqrt{2}\cdot Is1\cdot\sin(x)\cdot .0212-.000062\cdot\left(\sqrt{2}\cdot Is1\cdot\sin(x)\right)^{2}\right]\cdot\sqrt{2}\cdot Is1\cdot\sin(x)\cdot\left(\frac{1}{2}-\frac{1}{2}\cdot M1\cdot\sin(x+\theta 1)\right)dx$$

$$Pcdsvm1 := Pcd3a1 + Pcd3b1 + Pcd3c1$$

$$Pcsvm1 := 6\cdot(Pcswsvm1 + Pcdsvm1)$$

Switching Losses:

$$Pswon1(fs) := \frac{1}{2\cdot\sqrt{\pi}}\cdot fs\cdot\frac{k}{\sqrt{3}}\cdot\left(Is1\cdot\sqrt{2}\right)^{h}\cdot kgon\cdot\frac{Vdc}{Vtest}\cdot\frac{\Gamma\left(\frac{h+1}{2}\right)}{\Gamma\left(\frac{h}{2}+1\right)}$$

$$Pswoff1(fs) := \frac{1}{2\cdot\sqrt{\pi}}\cdot fs\cdot\frac{m}{\sqrt{3}}\cdot\left(Is1\cdot\sqrt{2}\right)^{n}\cdot kgoff\cdot\frac{Vdc}{Vtest}\cdot\frac{\Gamma\left(\frac{n+1}{2}\right)}{\Gamma\left(\frac{n}{2}+1\right)}$$

$$Prr1(fs) := \frac{Is1\cdot\sqrt{2}\cdot Vdc}{8\cdot\pi}\cdot\frac{trr^{2}}{tr - trr}\cdot fs$$

$$Psw1(fs) := 6\cdot(Pswon1(fs) + Pswoff1(fs) + Prr1(fs))$$

Miscellaneous Losses:

$$Pcap1(fs) := (Is1\cdot ripple)^{2}\cdot(Resr)$$

Total Losses:

$$Plossinv1(fs) := Pcsvm1 + \frac{Psw1(fs)}{2} + Pcap1(fs)$$

Divide Psw by 2 for SVM.

$$\eta inv1(fs) := \frac{Pin1}{Pin1 + Plossinv1(fs)}$$

Inverter Losses - Te2

Conduction Losses - SVM

$$Pcsw3a2 := \frac{1}{2\cdot\pi}\cdot\int_{0}^{\frac{\pi}{3}}\left[0.427 + \sqrt{2}\cdot Is2\cdot\sin(x)\cdot 0.0237 - 7.3\cdot 10^{-5}\cdot\left(\sqrt{2}\cdot Is2\cdot\sin(x)\right)^{2}\right]\cdot\sqrt{2}\cdot Is2\cdot\sin(x)\cdot\left(\frac{1}{2} + \frac{1}{2}\cdot M2\cdot\sin(x + \theta 2)\right)dx$$

$$Pcsw3b2 := \frac{1}{2\cdot\pi}\cdot\int_{\frac{\pi}{3}}^{\frac{2\cdot\pi}{3}} \left[0.427 + \sqrt{2}\cdot Is2\cdot\sin(x)\cdot 0.0237 - 7.3\cdot 10^{-5}\cdot\left(\sqrt{2}\cdot Is2\cdot\sin(x)\right)^2\right]\cdot\sqrt{2}\cdot Is2\cdot\sin(x)\,dx$$

$$Pcsw3c2 := \frac{1}{2\cdot\pi}\cdot\int_{\frac{2\cdot\pi}{3}}^{\pi} \left[0.427 + \sqrt{2}\cdot Is2\cdot\sin(x)\cdot 0.0237 - 7.3\cdot 10^{-5}\cdot\left(\sqrt{2}\cdot Is2\cdot\sin(x)\right)^2\right]\cdot\sqrt{2}\cdot Is2\cdot\sin(x)\cdot\left(\frac{1}{2} + \frac{1}{2}\cdot M2\cdot\sin(x + \theta 2)\right)dx$$

$$Pcswsvm2 := Pcsw3a2 + Pcsw3b2 + Pcsw3c2$$

$$Pcd3a2 := \frac{1}{2\cdot\pi}\cdot\int_{0}^{\frac{\pi}{3}} \left[0.4256 + \sqrt{2}\cdot Is2\cdot\sin(x)\cdot .0212 - .000062\cdot\left(\sqrt{2}\cdot Is2\cdot\sin(x)\right)^2\right]\cdot\sqrt{2}\cdot Is2\cdot\sin(x)\cdot\left(\frac{1}{2} - \frac{1}{2}\cdot M2\cdot\sin(x + \theta 2)\right)dx$$

$$Pcd3b2 := \frac{1}{2\cdot\pi}\cdot\int_{\frac{\pi}{3}}^{\frac{2\cdot\pi}{3}} \left[0.4256 + \sqrt{2}\cdot Is2\cdot\sin(x)\cdot .0212 - .000062\cdot\left(\sqrt{2}\cdot Is2\cdot\sin(x)\right)^2\right]\cdot\sqrt{2}\cdot Is2\cdot\sin(x)\,dx$$

$$Pcd3c2 := \frac{1}{2\cdot\pi}\cdot\int_{\frac{2\cdot\pi}{3}}^{\pi} \left[0.4256 + \sqrt{2}\cdot Is2\cdot\sin(x)\cdot .0212 - .000062\cdot\left(\sqrt{2}\cdot Is2\cdot\sin(x)\right)^2\right]\cdot\sqrt{2}\cdot Is2\cdot\sin(x)\cdot\left(\frac{1}{2} - \frac{1}{2}\cdot M2\cdot\sin(x + \theta 2)\right)dx$$

$$Pcdsvm2 := Pcd3a2 + Pcd3b2 + Pcd3c2$$

$$Pcsvm2 := 6\cdot(Pcswsvm2 + Pcdsvm2)$$

Switching Losses:

$$Pswon2(fs) := \frac{1}{2\cdot\sqrt{\pi}}\cdot fs\cdot\frac{k}{\sqrt{3}}\cdot\left(Is2\cdot\sqrt{2}\right)^{h}\cdot kgon\cdot\frac{Vdc}{Vtest}\cdot\frac{\Gamma\left(\frac{h+1}{2}\right)}{\Gamma\left(\frac{h}{2}+1\right)}$$

$$Pswoff2(fs) := \frac{1}{2\cdot\sqrt{\pi}}\cdot fs\cdot\frac{m}{\sqrt{3}}\cdot\left(Is2\cdot\sqrt{2}\right)^{n}\cdot kgoff\cdot\frac{Vdc}{Vtest}\cdot\frac{\Gamma\left(\frac{n+1}{2}\right)}{\Gamma\left(\frac{n}{2}+1\right)}$$

$$Prr2(fs) := \frac{Is2\cdot\sqrt{2}\cdot Vdc}{8\cdot\pi}\cdot\frac{trr^{2}}{tr-trr}\cdot fs$$

$$Psw2(fs) := 6\cdot(Pswon2(fs) + Pswoff2(fs) + Prr2(fs))$$

Miscellaneous Losses:

$$Pcap2(fs) := (Is2\cdot ripple)^{2}\cdot(Resr)$$

Total Losses:

$$Plossinv2(fs) := Pcsvm2 + \frac{Psw2(fs)}{2} + Pcap2(fs)$$

$$\eta inv2(fs) := \frac{Pin2}{Pin2 + Plossinv2(fs)}$$

Inverter Losses - Te3

Conduction Losses - SVM

$$Pcsw3a3 := \frac{1}{2\cdot\pi}\cdot\int_{0}^{\frac{\pi}{3}}\left[0.427+\sqrt{2}\cdot Is3\cdot\sin(x)\cdot 0.0237-7.3\cdot10^{-5}\cdot\left(\sqrt{2}\cdot Is3\cdot\sin(x)\right)^{2}\right]\cdot\sqrt{2}\cdot Is3\cdot\sin(x)\cdot\left(\frac{1}{2}+\frac{1}{2}\cdot M3\cdot\sin\left(x+\theta3\right)\right)dx$$

$$Pcsw3b3 := \frac{1}{2\cdot\pi}\cdot\int_{\frac{\pi}{3}}^{\frac{2\cdot\pi}{3}}\left[0.427+\sqrt{2}\cdot Is3\cdot\sin(x)\cdot 0.0237-7.3\cdot10^{-5}\cdot\left(\sqrt{2}\cdot Is3\cdot\sin(x)\right)^{2}\right]\cdot\sqrt{2}\cdot Is3\cdot\sin(x)\,dx$$

$$Pcsw3c3 := \frac{1}{2\cdot\pi}\cdot\int_{\frac{2\cdot\pi}{3}}^{\pi}\left[0.427+\sqrt{2}\cdot Is3\cdot\sin(x)\cdot 0.0237-7.3\cdot10^{-5}\cdot\left(\sqrt{2}\cdot Is3\cdot\sin(x)\right)^{2}\right]\cdot\sqrt{2}\cdot Is3\cdot\sin(x)\cdot\left(\frac{1}{2}+\frac{1}{2}\cdot M3\cdot\sin\left(x+\theta3\right)\right)dx$$

$$Pcswsvm3 := Pcsw3a3 + Pcsw3b3 + Pcsw3c3$$

$$Pcd3a3 := \frac{1}{2\cdot\pi}\cdot\int_{0}^{\frac{\pi}{3}} \left[0.4256 + \sqrt{2}\cdot Is3\cdot\sin(x)\cdot.0212 - .000062\cdot\left(\sqrt{2}\cdot Is3\cdot\sin(x)\right)^2\right]\cdot\sqrt{2}\cdot Is3\cdot\sin(x)\cdot\left(\frac{1}{2} - \frac{1}{2}\cdot M3\cdot\sin\left(x + \theta 3\right)\right) dx$$

$$Pcd3b3 := \frac{1}{2\cdot\pi}\cdot\int_{\frac{\pi}{3}}^{\frac{2\cdot\pi}{3}} \left[0.4256 + \sqrt{2}\cdot Is3\cdot\sin(x)\cdot.0212 - .000062\cdot\left(\sqrt{2}\cdot Is3\cdot\sin(x)\right)^2\right]\cdot\sqrt{2}\cdot Is3\cdot\sin(x)\, dx$$

$$Pcd3c3 := \frac{1}{2\cdot\pi}\cdot\int_{\frac{2\cdot\pi}{3}}^{\pi} \left[0.4256 + \sqrt{2}\cdot Is3\cdot\sin(x)\cdot.0212 - .000062\cdot\left(\sqrt{2}\cdot Is3\cdot\sin(x)\right)^2\right]\cdot\sqrt{2}\cdot Is3\cdot\sin(x)\cdot\left(\frac{1}{2} - \frac{1}{2}\cdot M3\cdot\sin\left(x + \theta 3\right)\right) dx$$

$$Pcdsvm3 := Pcd3a3 + Pcd3b3 + Pcd3c3$$

$$Pcsvm3 := 6\cdot(Pcswsvm3 + Pcdsvm3)$$

Switching Losses:

$$Pswon3(fs) := \frac{1}{2\cdot\sqrt{\pi}}\cdot fs\cdot\frac{k}{\sqrt{3}}\cdot\left(Is3\cdot\sqrt{2}\right)^h\cdot kgon\cdot\frac{Vdc}{Vtest}\cdot\frac{\Gamma\left(\frac{h+1}{2}\right)}{\Gamma\left(\frac{h}{2}+1\right)}$$

$$Pswoff3(fs) := \frac{1}{2\cdot\sqrt{\pi}}\cdot fs\cdot\frac{m}{\sqrt{3}}\cdot\left(Is3\cdot\sqrt{2}\right)^n\cdot kgoff\cdot\frac{Vdc}{Vtest}\cdot\frac{\Gamma\left(\frac{n+1}{2}\right)}{\Gamma\left(\frac{n}{2}+1\right)}$$

$$Prr3(fs) := \frac{Is3\cdot\sqrt{2}\cdot Vdc}{8\cdot\pi}\cdot\frac{trr^2}{tr - trr}\cdot fs$$

$$Psw3(fs) := 6\cdot(Pswon3(fs) + Pswoff3(fs) + Prr3(fs))$$

Miscellaneous Losses:

$$Pcap3(fs) := (Is3\cdot ripple)^2\cdot(Resr)$$

$$Plossinv3(fs) := Pcsvm3 + \frac{Psw3(fs)}{2} + Pcap3(fs)$$

$$\eta inv3(fs) := \frac{Pin3}{Pin3 + Plossinv3(fs)}$$

3) System Efficiency

Total Losses:

$\eta sys1(fs) := \eta mot1 \cdot \eta inv1(fs)$

$\eta sys2(fs) := \eta mot2 \cdot \eta inv2(fs)$

$\eta sys3(fs) := \eta mot3 \cdot \eta inv3(fs)$

Vita

William L Cornwell

William Cornwell received his Bachelor of Science degree in Electrical Engineering from Virginia Tech in 1998. After joining Black & Decker Corporation in 1998 he worked in the Motor Technology group for two years. His primary assignments were the design of small PM and Brushless DC motors using FEA. After leaving in the summer of 2000, he returned to Virginia Tech and finished his Master of Science in Electrical Engineering in 2002. His research interests include power electronics and automotive technology. Currently William works for Airak, Inc. in Manassas, VA doing research and development in the areas of high power electronics.